Photoproduction of the J/ψ meson at HERA at next-to-leading order within the framework of nonrelativistic QCD

Dissertation zur Erlangung des Doktorgrades
des Departments Physik der Universität Hamburg

vorgelegt von
Mathias Butenschön
aus Hamburg

Hamburg
2009

Erstgutachter der Dissertation:	Prof. Dr. B. A. Kniehl
Zweitgutachter der Dissertation:	Prof. Dr. J. Bartels
Erstgutachter der Disputation:	Prof. Dr. B. A. Kniehl
Zweitgutachter der Disputation:	Prof. Dr. G. Kramer
Datum der Disputation:	23. Juni 2009
Vorsitzender des Prüfungsausschusses:	Prof. Dr. G. Sigl
Vorsitzender des Promotionsausschusses:	Prof. Dr. R. Klanner
Dekan der MIN-Fakultät:	Prof. Dr. H. Graener

Abstract

Nonrelativistic QCD (NRQCD) provides a rigorous factorization scheme which describes the production and decay of heavy quarkonia. It has been a desire for 13 years to know the NRQCD NLO predictions for both J/ψ hadroproduction and photoproduction, in order to be able to check the universality of the color octet long distance matrix elements (MEs) by comparing Tevatron and HERA data. In this work we calculate for the first time the NRQCD NLO prediction for direct photoproduction at HERA and compare our result with recent H1 data. Our results show clear evidence that the color octet mechanism of NRQCD is indeed realized in J/ψ photoproduction at HERA. We solved a number of open conceptual problems, probably the most important one being the issue of Coulomb singularities. We found a way to evaluate the virtual corrections without having to deal with them.

Zusammenfassung

Die nichtrelativistische QCD (NRQCD) bildet einen rigorosen Faktorisierungsformalismus zur Beschreibung der Produktions- und Zerfallsraten schwerer Quarkonia. Es besteht seit 13 Jahren der Wunsch, die NRQCD Vorhersagen zur J/ψ Hadroproduktion und Photoproduktion in nächstführender Ordnung (NLO) in α_s zu kennen, um durch den Vergleich von Tevatron- und HERA-Daten die Universalität der Farboktett langreichweitigen Matrixelemente zu testen. In dieser Arbeit berechnen wir zum ersten Mal die NRQCD NLO Vorhersagen zur direkten Photoproduktion bei HERA und vergleichen die Ergebnisse mit aktuellen H1 Daten. Unsere Resultate deuten darauf hin, dass der NRQCD Farkoktettmechanismus in der Tat zur J/ψ Photoproduktion bei HERA beiträgt. In unserer Arbeit haben wir eine Reihe offener konzeptioneller Probleme gelöst. Das wichtigste betrifft wohl die Coulomb-Singularitäten. Wir haben einen Weg gefunden, die virtuellen Korrekturen zu berechnen, ohne dass sie in unserer Rechnung auftauchen.

Contents

1. Introduction **6**

2. Overview and basic definitions **11**
2.1. Our treatment of γ_5 . . . 13

3. Born cross section and virtual corrections **15**
3.1. Implementation of the analytical calculation . . . 22
3.2. Why do we not have Coulomb singularities? . . . 25

4. Loop corrections to the long distance matrix elements **26**

5. Real corrections **31**
5.1. The soft region . . . 33
5.1.1. Soft amplitudes in general . . . 33
5.1.2. Soft amplitudes in our heavy quarkonium production . . . 35
5.1.3. Kinematics of the soft region . . . 37
5.1.4. Soft terms #1 . . . 38
5.1.5. Soft terms #2 . . . 40
5.1.6. Soft terms #3 . . . 41
5.2. The hard collinear region . . . 43
5.2.1. Splitting of the initial QCD parton . . . 43
5.2.2. Splitting of the initial photon . . . 47
5.2.3. Splitting of the final state QCD parton . . . 49
5.2.4. Summary of all hard collinear terms . . . 51
5.3. The hard non-collinear region . . . 52

6. Numerical evaluation and results **56**
6.1. The hadronic cross sections . . . 56
6.2. Parameters used in our analysis . . . 60
6.2.1. The values of the color octet long distance matrix elements . . . 62
6.3. Final results and conclusions . . . 63

7. Summary and outlook **68**

A. Our tensor reduction **70**
A.1. Definition of the tensor integrals and tensor decomposition 70
A.2. Tensor reduction of the generalized A functions 72
A.3. Tensor reduction of the generalized B functions 72
A.4. Tensor reduction of the generalized C functions 74
A.5. Tensor reduction of the generalized D functions 76

B. Use of integration-by-parts **80**

C. The 14 super master integrals **85**

D. The Born squared matrix elements **89**

E. Explicit results for the soft #2 terms **96**

1. Introduction

This doctoral thesis is a contribution to the field of heavy quarkonium physics. Heavy quarkonia are bound states of a heavy quark and its antiquark. The top quark decays too fast to form a bound state, but there are charmonia and bottomonia. Bound by the QCD potential, the heavy quarkonium system can be in different Fock states. Each excitation is considered a particle of its own kind and given its own name. The lower end of the charmonium spectrum is given in table 1. The first time a heavy quarkonium was discovered was in 1974 with the discovery of the J/ψ, the $c\overline{c}$ system in a $1\ ^3S_1$ state. This was the first time a heavy quark was discovered at all and this discovery was very important for establishing QCD, in particular its asymptotic freedom. Ever since then heavy quarkonium physics has been an active field for the study of QCD. The calculation of the mass spectrum is a key application for lattice QCD, and the calculation of the production and decay rates has been one of the first applications of perturbative QCD. The calculation of J/ψ production rates is of special phenomenological interest because of its clear experimental signature with its large branching ratio $\Gamma(J/\psi \to l^+l^-)/\Gamma$ of its leptonic decay modes.

Over the years different methods have been devised to calculate heavy quarkonium production and decay rates. The classic approach is the so called color singlet model. In that approach the cross section is simply assumed to be the cross section for the production/decay of a quarkonium in its physical color singlet, meaning color neutral, state. In case of the J/ψ, this is a $^3S_1^{[1]}$ state, where the upper index 1 stands for color singlet. This cross section then has to be multiplied by the quarkonium wave function at the origin or its derivative, in case of P wave quarkonia. These quantities are treated as numbers extracted from experiment. However, already in the case of P wave quarkonia,

$n\ ^{2S+1}L_J$	Name	Mass
$1\ ^1S_0$	η_c	2980 MeV
$1\ ^3S_1$	J/ψ	3097 MeV
$1\ ^3P_0$	χ_{c0}	3415 MeV
$1\ ^3P_1$	χ_{c1}	3511 MeV
$1\ ^1P_1$	h_c	3526 MeV
$1\ ^3P_2$	χ_{c2}	3556 MeV
$2\ ^1S_0$	η_c'	3637 MeV
$2\ ^3S_1$	ψ'	3686 MeV

Table 1.1.: The lower end of the charmonium spectrum, extracted from [1].

scaling	v^3	v^7	v^{11}
n	${}^3S_1^{[1]}$	${}^1S_0^{[8]}$, ${}^3S_1^{[8]}$, ${}^3P_{0/1/2}^{[8]}$	...

Table 1.2.: Scaling behavior of the leading long distant matrix elements $\langle \mathcal{O}^{J/\psi}[n] \rangle$ as predicted by NRQCD.

there are leftover infrared divergences [2]. This hints at theoretical inconsistencies in this approach.

A newer method is the so called nonrelativistic quantum chromodynamics (NRQCD) [3, 4]. This self consistent effective field theory is based on the energy scale hierarchy

$$Mv^2, Mv \ll \Lambda_{\mathrm{QCD}} \ll M, \tag{1.1}$$

which is observed in the quarkonium system. Here, M is the quarkonium mass and v the relative velocity between the quark and the antiquark. M sets the scale of the pointlike production/decay of the individual quarks, which is accessible in perturbative QCD. The physics of the quarkonium as a whole is however governed by the low energy scales Mv^2, the quarkonium energy, or Mv, the quarkonium momentum scale.

The calculation of the cross section for the production of a heavy quarkonium H within NRQCD is based on the factorization theorem

$$d\sigma(a + b \to H + X) \propto \sum_n d\sigma(a + b \to c\overline{c}[n] + X)\langle \mathcal{O}^H[n] \rangle, \tag{1.2}$$

which states that the production cross section factorizes into a short distance part $\sigma(a + b \to c\overline{c}[n] + X)$, which describes the production of a $c\overline{c}$ pair in a specific Fock state n and is calculated in perturbative QCD, and so called long distance matrix elements (MEs), which are numbers expressing the probability for this $c\overline{c}$ pair to subsequently decay into a physical H via soft gluon radiation. The new feature of NRQCD is that the intermediate state n does not have to be color neutral, it can be a color octet state. The MEs should in principle be calculable in lattice simulations. But as there are currently no reliable calculations available, they are taken to be phenomenological constants extracted by fitting to experimental data. The sum over n is in principal an infinite sum. Fortunately, NRQCD predicts each of the MEs $\langle \mathcal{O}^H[n] \rangle$ to scale with a certain power of v, the relative velocity of the c and $\overline{c}$ in the physical H. This relative velocity is a small number which serves as an expansion parameter. In case of charmonium, $v^2 \approx 0.2$. These velocity scaling rules are for the case of J/ψ production summarized in table 1.2: NRQCD predicts the leading contribution to come from $n = {}^3S_1^{[1]}$. This contribution equals the color singlet model prediction, so the color singlet model is actually incorporated into NRQCD. The higher order contributions from $n = {}^1S_0^{[8]}$, ${}^3S_1^{[8]}$ and ${}^3P_{0/1/2}^{[8]}$ are the so called relativistic corrections, also referred to as *the* color octet contributions. All other MEs scale with even higher powers of v, and are usually neglected in NRQCD analyses.

In this framework, the leftover infrared divergences of the P wave quarkonia are canceled by NRQCD radiative corrections to the MEs of S states, as will be described in chapter 4.

Hadroproduction	${}^3S_1^{[1]}$	${}^1S_0^{[8]}$, ${}^3S_1^{[8]}$, ${}^3P_{0/1/2}^{[8]}$
Born	Baier, Rückl (1981) [7]	Cho, Leibovic (1996) [5]
NLO	Campbell et al. (2007) [8]	———

Photoproduction	${}^3S_1^{[1]}$	${}^1S_0^{[8]}$, ${}^3S_1^{[8]}$, ${}^3P_{0/1/2}^{[8]}$
Born	Berger, Jones (1981) [9]	Ko, Lee, Song (1996) [10]
NLO	Krämer (1995) [11]	THIS WORK

Table 1.3.: Overview of complete Born level and NLO calculations of inclusive J/ψ hadro- and photoproduction so far. We have distinguished between color singlet model calculations and calculations including the color octet states. Only the first complete work of each calculation is cited.

The great breakthrough for NRQCD had been that it was able to explain the cross section for J/ψ hadroproduction at the Tevatron [5], which is orders of magnitude larger than the color singlet model prediction, see figure 1.1. The extracted MEs are in line with the NRQCD velocity scaling rules. However, in order to establish NRQCD as the correct theory for heavy quarkonium production, we must show the significance of the color octet contributions in other high energy experiments as well and proof the universality of the MEs. This has not been achieved so far. One way of proofing the ME universality is to use values for the MEs which were extracted from fits to the Tevatron data and apply them in a calculation of the photoproduction rates at HERA, another source of high precision J/ψ production data. A summary of performed hadroproduction and photoproduction calculations is given in table 1.3. The state of knowledge in HERA photoproduction before our work is summarized in figure 1.2. Krämer's color singlet model prediction at NLO seems to describe the data very well [11]. On the other hand Born level calculations including intermediate color octet states predict a rise in the cross section at high z which is not observed [13, 10]. This situation does not support the universality of the MEs. In order to clarify the situation it is urgently necessary to perform the NRQCD calculation including the intermediate color octet states also at NLO. And exactly that calculation is the subject of this doctoral thesis.

As can be seen from table 1.3, the seeming discrepancy between Tevatron and HERA data was known since 1996, and is one of the open questions of particle phenomenology which has raised much attention during the past 13 years. Nevertheless so far no one has succeeded in evaluating that NLO correction, which certainly hints at serious difficulties. These difficulties lie in the evaluation of the P waves, as the expressions become huge and the virtual correction loop integrals evolve non-standard form, as well as a non-standard divergency structure. These difficulties are first overcome in the present work. Actually, two NLO calculations of quarkonium production with intermediate P states have already been performed: The total J/ψ hadroproduction cross section [14] and the inclusive J/ψ production in two-photon collisions [15]. However, the former calculation

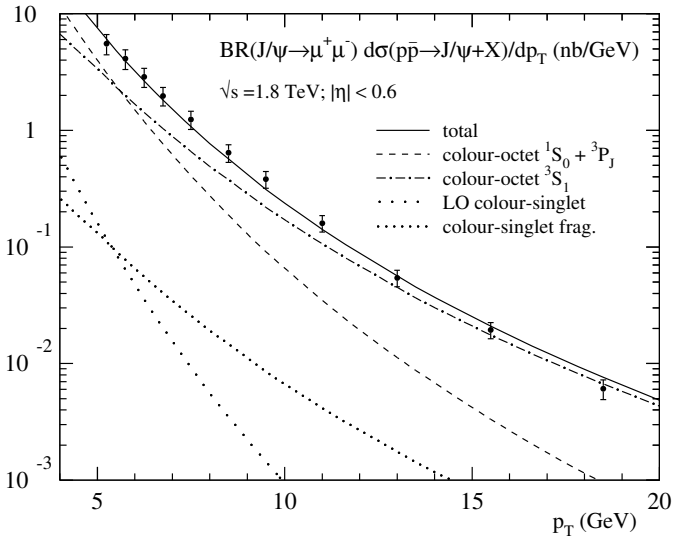

Figure 1.1.: Different leading order contributions to the p_T distribution of inclusive J/ψ hadroproduction at the Tevatron. This figure is taken from [6].

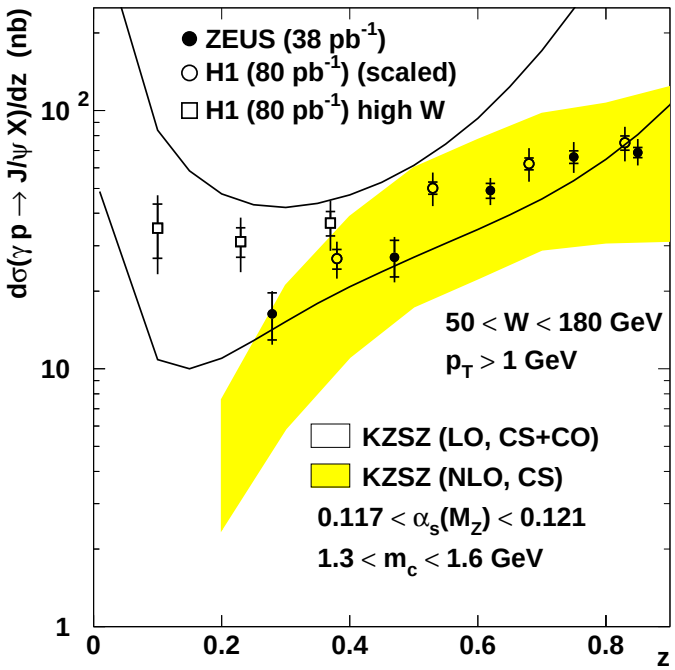

Figure 1.2.: The z distribution of inclusive J/ψ photoproduction at HERA. This figure is taken from [12] and shows the state of knowledge before our work. The open bands represents the leading order color singlet plus color octet contributions in direct and resolved photoproduction. The shaded band shows Krämer's result [11] for the NLO color singlet contribution for direct photoproduction.

evaluates only a $2 \to 1$ process and in the latter one no virtual corrections to P wave states had to be calculated.

This thesis is organized as follows: In chapter 2 we introduce the basic concepts of our calculation. The analytic part of our calculation is described in chapters 3, 4 and 5. Each of these chapters describes one of the three different components which build up the whole NLO cross section: Chapter 3 explains the calculation of the Born cross sections and the virtual corrections and also describes the implementation in our various computer programs. In chapter 4 we calculate the loop corrections to the S wave long distance matrix elements in NRQCD. Chapter 5 then deals with the real corrections. Here, the partly non-standard infrared divergency structure with its cancellations is described in detail. After that, in chapter 6 we describe our numerical evaluation, present results and draw conclusions, before we end with a summary and an outlook in chapter 7. For the interested reader we also add a large appendix with detailed formulas concerning our tensor reduction, the topologies for our integration-by-parts procedure, our master integrals, as well as explicit expressions for the Born terms as well as for the so called soft #2 terms.

2. Overview and basic definitions

We are evaluating the inclusive cross section for direct photoproduction of J/ψ. An overview of the factorization formulas at work is given in figure 2.1: An on-shell bremsstrahlung photon γ, which is radiated off the incoming electron, interacts with a parton i stemming from the incoming proton. We calculate the hadronic cross section by folding the partonic cross section with the proton parton distribution functions (PDFs) $f_{i/p}(y)$ and the Weizsäcker-Williams distribution $f_{\gamma/e}(x)$ [16] according to

$$d\sigma(e+p \to J/\psi + X) = \sum_{i=g;u,\overline{u},d,\overline{d},s,\overline{s}} \int dx f_{\gamma/e}(x) \int dy f_{i/p}(y) \times d\sigma(\gamma + i \to J/\psi + X). \tag{2.1}$$

The parton i can be a gluon or an up, down or strange quark or antiquark. The calculation of the hadronic cross section will be further elaborated in chapter 6.1.

The partonic cross section is calculated according to the NRQCD factorization theorem

$$d\sigma(\gamma + i \to J/\psi + X) = \sum_n d\sigma(\gamma + i \to c\overline{c}[n] + X) \frac{\langle \mathcal{O}^{J/\psi}[n] \rangle}{N_{\text{col}}(n) N_{\text{pol}}(n)}. \tag{2.2}$$

Here it is necessary to divide by the number of color and polarization degrees of freedom of the intermediate $c\overline{c}[n]$, because we sum over them in the evaluation of the short distance cross section $d\sigma(\gamma + i \to c\overline{c}[n] + X)$. This point is further addressed in [14]. $N_{\text{col}}(n)$ is 1 if n is a color singlet state and $2C_A C_F$ if it is a color octet state. Here, $C_A = N_c$ and $C_F = \frac{N_c^2 - 1}{2N_c}$, where $N_c = 3$ in QCD. In four dimensions, $N_{\text{pol}} = 2J + 1$, where J is the total angular momentum quantum number of n.

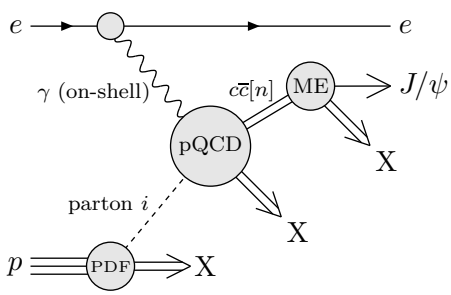

Figure 2.1.: Visualization of the factorization formulas in direct photoproduction of J/ψ

The partonic cross section to produce a $c\overline{c}[n]$ is then calculated via

$$d\sigma(\gamma + i \to c\overline{c}[n] + X) = \frac{1}{2s} d\mathrm{PS} \frac{1}{N_{\mathrm{col,in}} N_{\mathrm{pol,in}}} \sum_{\mathrm{col,pol}} |\mathcal{M}(\gamma + i \to c\overline{c}[n] + X)|^2 \quad (2.3)$$

where the factor $\frac{1}{2s}$ with $s \equiv (k_\gamma + k_i)^2$ is the flux factor, dPS is the differential phase space, and the squared matrix element $|\mathcal{M}(\gamma + i \to c\overline{c}[n] + X)|^2$ is summed over the polarizations and colors of the final state particles and averaged over the polarizations and colors of the initial state particles.

We calculate $\mathcal{M}(\gamma + i \to c\overline{c}[n] + X)$, the amplitude to create a $c\overline{c}$ pair in a Fock state n, by applying certain projectors onto the QCD amplitudes $\mathcal{A}$ for open $c\overline{c}$ production with amputated charm spinors. We follow closely the notation of [14] and use

$$\mathcal{M}_{c\overline{c}[^1S_0^{[8]}]} = \mathrm{Tr}\left[\mathcal{C}_8^c\, \Pi_0\, \mathcal{A}\right]|_{q=0} \quad (2.4)$$

$$\mathcal{M}_{c\overline{c}[^3S_1^{[1]}]} = \mathcal{E}_\alpha \mathrm{Tr}\left[\mathcal{C}_1\, \Pi_1^\alpha\, \mathcal{A}\right]|_{q=0} \quad (2.5)$$

$$\mathcal{M}_{c\overline{c}[^3S_1^{[8]}]} = \mathcal{E}_\alpha \mathrm{Tr}\left[\mathcal{C}_8^c\, \Pi_1^\alpha\, \mathcal{A}\right]|_{q=0} \quad (2.6)$$

$$\mathcal{M}_{c\overline{c}[^3P_J^{[8]}]} = \mathcal{E}_{\alpha\beta}^{(J)} \frac{d}{dq_\beta} \mathrm{Tr}\left[\mathcal{C}_8^c\, \Pi_1^\alpha \mathcal{A}\right]|_{q=0} \qquad (J = 0, 1, 2). \quad (2.7)$$

$\mathcal{E}_\alpha$ and $\mathcal{E}_{\alpha\beta}^{(J)}$ are polarization vectors of the $c\overline{c}$ state. The color and spin projectors $\mathcal{C}$ and Π are to be inserted into the open charm quark chain. The trace is understood to be taken over the charm chain both in Dirac space and in color space. In case of intermediate S states, we have to set the relative momentum $2q$ between the two external charm quarks to zero, and in the case of intermediate P states, we have to evaluate the derivative with respect to q at the point $q = 0$. The c is an open color index which is to be summed over in the squared matrix element. The color projectors are given by

$$\mathcal{C}_1 = \frac{1}{\sqrt{2} C_A} \quad (2.8)$$

$$\mathcal{C}_8^c = \sqrt{2} T^c, \quad (2.9)$$

where T^c is a color matrix. We remark that our expression for $\mathcal{C}_1$ is different from the one given in [14], but that is due to the fact that their normalization of the color singlet MEs is different from the standard one. They have shifted a factor $\frac{1}{2C_A}$ from the projectors into the color singlet MEs. But in order to be consistent with the majority of publications we stick to the normalization in [4]. The projectors onto spin singlet states, Π_0, and onto spin triplet states, Π_1^α, are given by

$$\Pi_0 = \frac{1}{\sqrt{8m_c^3}} \left(\frac{\not{P}}{2} - \not{q} - m_c\right) \gamma_5 \left(\frac{\not{P}}{2} + \not{q} + m_c\right) \quad (2.10)$$

$$\Pi_1^\alpha = \frac{1}{\sqrt{8m_c^3}} \left(\frac{\not{P}}{2} - \not{q} - m_c\right) \gamma^\alpha \left(\frac{\not{P}}{2} + \not{q} + m_c\right). \quad (2.11)$$

The momentum of the outgoing c quark is given by $P/2 + q$ and the momentum of the outgoing $\overline{c}$ by $P/2 - q$. m_c is the charm quark mass.

In our whole calculation we are regularizing all divergences in dimensional regularization with $D = 4 - 2\epsilon$ space-time dimensions. We will make frequent use of the symbol

$$C_\epsilon \equiv \left(\frac{4\pi\mu^2}{m_c^2} e^{-\gamma_E} \right)^\epsilon , \tag{2.12}$$

where μ is the renormalization scale and γ_E Euler's gamma.

When squaring the amplitude and summing over the polarizations of the external particles, we also have to sum over the $c\overline{c}$ polarization vectors. In D dimensions we have

$$\sum_{\text{pol}} \mathcal{E}_\alpha \mathcal{E}^*_{\alpha'} = \Pi_{\alpha\alpha'} \tag{2.13}$$

$$\sum_{\text{pol}} \mathcal{E}^{(0)}_{\alpha\beta} \mathcal{E}^{(0)*}_{\alpha'\beta'} = \frac{1}{D-1} \Pi_{\alpha\beta} \Pi_{\alpha'\beta'} \tag{2.14}$$

$$\sum_{\text{pol}} \mathcal{E}^{(1)}_{\alpha\beta} \mathcal{E}^{(1)*}_{\alpha'\beta'} = \frac{1}{2} \left(\Pi_{\alpha\alpha'} \Pi_{\beta\beta'} - \Pi_{\alpha\beta'} \Pi_{\alpha'\beta} \right) \tag{2.15}$$

$$\sum_{\text{pol}} \mathcal{E}^{(2)}_{\alpha\beta} \mathcal{E}^{(2)*}_{\alpha'\beta'} = \frac{1}{2} \left(\Pi_{\alpha\alpha'} \Pi_{\beta\beta'} + \Pi_{\alpha\beta'} \Pi_{\alpha'\beta} \right) - \frac{1}{D-1} \Pi_{\alpha\beta} \Pi_{\alpha'\beta'} \tag{2.16}$$

where we have abbreviated

$$\Pi_{\alpha\beta} = -g_{\alpha\beta} + \frac{P_\alpha P_\beta}{4m_c^2}. \tag{2.17}$$

2.1. Our treatment of γ_5

Although the basic diagrams we evaluate are pure QCD diagrams, we still have to deal with the problem of γ_5 in dimensional regularization. That is because there is a γ_5 in the spin projector (2.10) onto the spin singlet state. When applying this projector to our amplitudes we have to evaluate a spin trace

$$\mathcal{M}_{c\overline{c}[^1S_0^{[8]}]} \propto \mathrm{Tr}[\gamma_5 \gamma_{\mu_1} \ldots \gamma_{\mu_n}] \tag{2.18}$$

over one γ_5 and up to eight other gamma matrices. As explained for example in [19], the relations

$$\{\gamma_\mu, \gamma_5\} = 0 \tag{2.19}$$

and

$$\mathrm{Tr}[\gamma_5 \gamma_\alpha \gamma_\beta \gamma_\gamma \gamma_\delta] = 4i\epsilon_{\alpha\beta\gamma\delta} \tag{2.20}$$

are incompatible in D dimensions, because the mixed application of both rules leads to ambiguous results. This would be the so called *naive* scheme. Therefore we implement the 't Hooft-Veltman or also called the Breitenlohner-Maison scheme, which was first

proposed in [17] and elaborated in [18]. The aspects important for this calculation are comprehensively summarized in [19]. In this scheme, the anticommutation relation (2.19) is no longer valid, and we evaluate (2.18) by replacing γ_5 by

$$\gamma_5 = \frac{i}{4!}\epsilon_{\alpha_1\alpha_2\alpha_3\alpha_4}\gamma^{\alpha_1}\gamma^{\alpha_2}\gamma^{\alpha_3}\gamma^{\alpha_4}. \tag{2.21}$$

Here, the gamma matrices on the right hand side are D dimensional, but the Levi-Civita tensor ϵ is a 4 dimensional object. The D dimensional Dirac trace in (2.4) can now be performed. The squared amplitude for producing a $c\overline{c}[^1S_0^{[8]}]$ state will then contain exactly two ϵ tensors, which are further evaluated according to

$$\mathcal{M}^*_{c\overline{c}[^1S_0^{[8]}]}\mathcal{M}_{c\overline{c}[^1S_0^{[8]}]} \propto \epsilon_{\alpha_1\alpha_2\alpha_3\alpha_4}\epsilon_{\beta_1\beta_2\beta_3\beta_4} = -\begin{vmatrix} \tilde{g}_{\alpha_1\beta_1} & \tilde{g}_{\alpha_1\beta_2} & \tilde{g}_{\alpha_1\beta_3} & \tilde{g}_{\alpha_1\beta_4} \\ \tilde{g}_{\alpha_2\beta_1} & \tilde{g}_{\alpha_2\beta_2} & \tilde{g}_{\alpha_2\beta_3} & \tilde{g}_{\alpha_2\beta_4} \\ \tilde{g}_{\alpha_3\beta_1} & \tilde{g}_{\alpha_3\beta_2} & \tilde{g}_{\alpha_3\beta_3} & \tilde{g}_{\alpha_3\beta_4} \\ \tilde{g}_{\alpha_4\beta_1} & \tilde{g}_{\alpha_4\beta_2} & \tilde{g}_{\alpha_4\beta_3} & \tilde{g}_{\alpha_4\beta_4} \end{vmatrix}, \tag{2.22}$$

where the $\tilde{g}^{\alpha_i\beta_j}$ are 4 dimensional metric tensors, which are contracted with other objects according to

$$\tilde{g}_{\mu\nu}g^{\nu\rho} = \tilde{g}_\mu{}^\rho \tag{2.23}$$

$$\tilde{g}_{\mu\nu}p^\nu = \tilde{p}_\mu \tag{2.24}$$

$$\tilde{p}_\mu q^\mu = \tilde{p}\cdot\tilde{q} \tag{2.25}$$

$$\tilde{g}_\mu{}^\mu = 4, \tag{2.26}$$

where $g^{\nu\rho}$ and p^ν are D dimensional and $\tilde{p}_\mu$ is 4 dimensional. In order to avoid any misunderstandings, we emphasize that our application of the 't Hooft Veltman scheme does not include any γ_5 related counterterms.

3. Born cross section and virtual corrections

This chapter deals with the calculations of the Born cross sections and the virtual corrections. These are the parts of the calculation with two incoming and two outgoing particles. We are dealing with the partonic level processes

$$\gamma(k_1) + q(k_2) \quad \rightarrow \quad c\overline{c}[n](P) + q(k_3) \qquad (q = u, \overline{u}, d, \overline{d}, s, \overline{s}) \tag{3.1}$$

$$\gamma(k_1) + g(k_2) \quad \rightarrow \quad c\overline{c}[n](P) + g(k_3), \tag{3.2}$$

where the respective particle momenta are given in brackets. We consider the up, down and strange quarks and antiquarks massless. We introduce the Mandelstam invariants

$$s \equiv (k_1 + k_2)^2 = 2k_1 \cdot k_2 \tag{3.3}$$

$$t \equiv (P - k_1)^2 = -2k_2 \cdot k_3 \tag{3.4}$$

$$u \equiv (P - k_2)^2 = -2k_1 \cdot k_3 \tag{3.5}$$

and additionally define

$$s_1 \equiv s - 4m_c^2 = 2P \cdot k_3 \tag{3.6}$$

$$t_1 \equiv t - 4m_c^2 = -2P \cdot k_1 \tag{3.7}$$

$$u_1 \equiv u - 4m_c^2 = -2P \cdot k_2. \tag{3.8}$$

To evaluate the differential phase space, we use the parameterization

$$k_1 = \left(\frac{\sqrt{s}}{2},\, 0,\, 0,\, \frac{\sqrt{s}}{2}\right) \tag{3.9}$$

$$k_2 = \left(\frac{\sqrt{s}}{2},\, 0,\, 0,\, -\frac{\sqrt{s}}{2}\right) \tag{3.10}$$

$$P = \left(E_{J/\psi},\, 0,\, p_{J/\psi}\sin\theta,\, p_{J/\psi}\cos\theta\right), \tag{3.11}$$

where

$$E_{J/\psi} = \frac{t + u - 8m_c^2}{-2\sqrt{s}}, \qquad p_{J/\psi} = \sqrt{E_{J/\psi}^2 - 4m_c^2}, \qquad \cos\theta = \frac{t - u}{2\sqrt{s}\, p_{J/\psi}}, \tag{3.12}$$

so that the phase space in four dimensions is given by

$$\begin{aligned} d\mathrm{PS} &= \frac{d^3P}{(2\pi)^3 2E_{J/\psi}} \frac{1}{(2\pi)^3} d^4k_3 \theta(k_{3,0}) \delta(k_3^2)(2\pi)^4 \delta^{(4)}(k_1 + k_2 - P - k_3) \\ &= \frac{1}{(2\pi)^2} \frac{1}{2E_{J/\psi}} p_{J/\psi}^2 dp_{J/\psi} d(\cos\theta) 2d\varphi\, \delta(s + t + u - 4m_c^2) \\ &= \frac{1}{8\pi^2 s} dt\, du\, d\varphi\, \delta(s + t + u - 4m_c^2) \\ &= \frac{1}{8\pi s} dt. \end{aligned} \tag{3.13}$$

For the change of variables from $(p_{J/\psi}, \cos\theta)$ to (t, u), we used the relations (3.12). We could integrate (from 0 till π) over φ, the azimuthal angle of the J/ψ, because the squared matrix element cannot depend on it. The partonic cross section (2.3) then reads

$$\begin{aligned}
&\frac{d\sigma(\gamma + q/g \to c\overline{c}[n] + q/g)}{dt} \\
&= \frac{1}{16\pi s^2} \frac{1}{N_{\text{col,in}} N_{\text{pol,in}}} \sum_{\text{col,pol}} |\mathcal{M}(\gamma + q/g \to c\overline{c}[n] + q/g)|^2. \qquad (3.14)
\end{aligned}$$

The kinematically allowed region of the phase space is given by

$$\begin{aligned}
4m_c^2 &< \quad s \qquad (3.15) \\
-s_1 &< \quad t \quad < 0. \qquad (3.16)
\end{aligned}$$

The next step is to do a perturbative expansion of the matrix elements in α_s and write $\mathcal{M} = \mathcal{M}_{\text{Tree}} + \mathcal{M}_{\text{virtual}}$, where $\mathcal{M}_{\text{virtual}}$ denotes the virtual corrections of $\mathcal{O}(\alpha_s)$. All corrections of higher order in α_s are neglected. Then

$$\begin{aligned}
\sum_{\text{col,pol}} |\mathcal{M}(\gamma + q \to c\overline{c}[n] + q)|^2 &= \sum_{\text{col,pol}} |\mathcal{M}_{\text{Tree}}(\gamma + q \to c\overline{c}[n] + q)|^2 \\
&+2\,\text{Re} \sum_{\text{col,pol}} \mathcal{M}^*_{\text{Tree}}(\gamma + q \to c\overline{c}[n] + q)\mathcal{M}_{\text{virtual}}(\gamma + q \to c\overline{c}[n] + q) \qquad (3.17)
\end{aligned}$$

and

$$\begin{aligned}
&\sum_{\text{col,pol}} |\mathcal{M}(\gamma + g \to c\overline{c}[n] + g)|^2 \\
&= \sum_{\text{col,pol}^*} \Big[|\mathcal{M}_{\text{Tree}}(\gamma + g \to c\overline{c}[n] + g)|^2 - 2|\mathcal{M}_{\text{Tree}}(\gamma + u_g \to c\overline{c}[n] + u_g)|^2 \Big] \\
&\quad +2\,\text{Re} \sum_{\text{col,pol}^*} \Big[\mathcal{M}^*_{\text{Tree}}(\gamma + g \to c\overline{c}[n] + g)\mathcal{M}_{\text{virtual}}(\gamma + g \to c\overline{c}[n] + g) \\
&\qquad -2\mathcal{M}^*_{\text{Tree}}(\gamma + u_g \to c\overline{c}[n] + u_g)\mathcal{M}_{\text{virtual}}(\gamma + u_g \to c\overline{c}[n] + u_g) \Big]. \qquad (3.18)
\end{aligned}$$

In the evaluation of the squared matrix element for the process $\gamma + g \to c\overline{c}[n] + g$ we have implemented the approach of [20], which speeds up the calculation tremendously. In that approach the gluon polarization sum is taken not only over the physical transverse polarizations, but the complete polarization sum

$$\sum_{\text{pol}^*} \epsilon_\mu \epsilon^*_\nu = -g_{\mu\nu}. \qquad (3.19)$$

is used. In turn, the corresponding gluon ghost process contributions $\gamma + u_g \to c\overline{c}[n] + u_g$ and $\gamma + \overline{u}_g \to c\overline{c}[n] + \overline{u}_g$ have to be subtracted. The contributions from both ghost processes are equal due to charge symmetry, so that we arrive at (3.18).

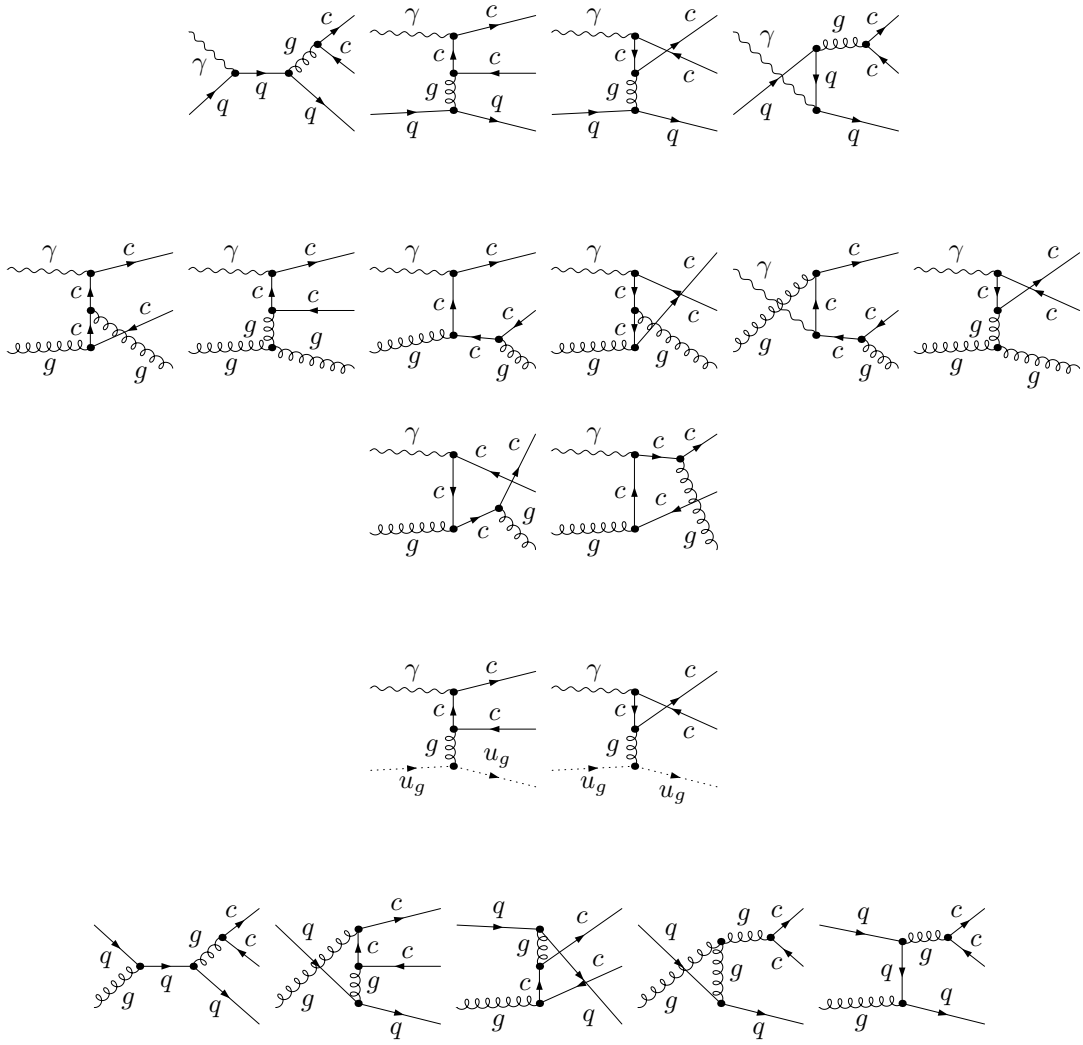

Figure 3.1.: The $2 \to 2$ tree level diagrams needed in our calculation. u_g stands for gluon ghost. The process $q + g \to c\overline{c} + q$ (along with its crossed version $q + \overline{q} \to c\overline{c} + g$) will be needed in the calculation of the hard collinear terms stemming from initial photon splitting.

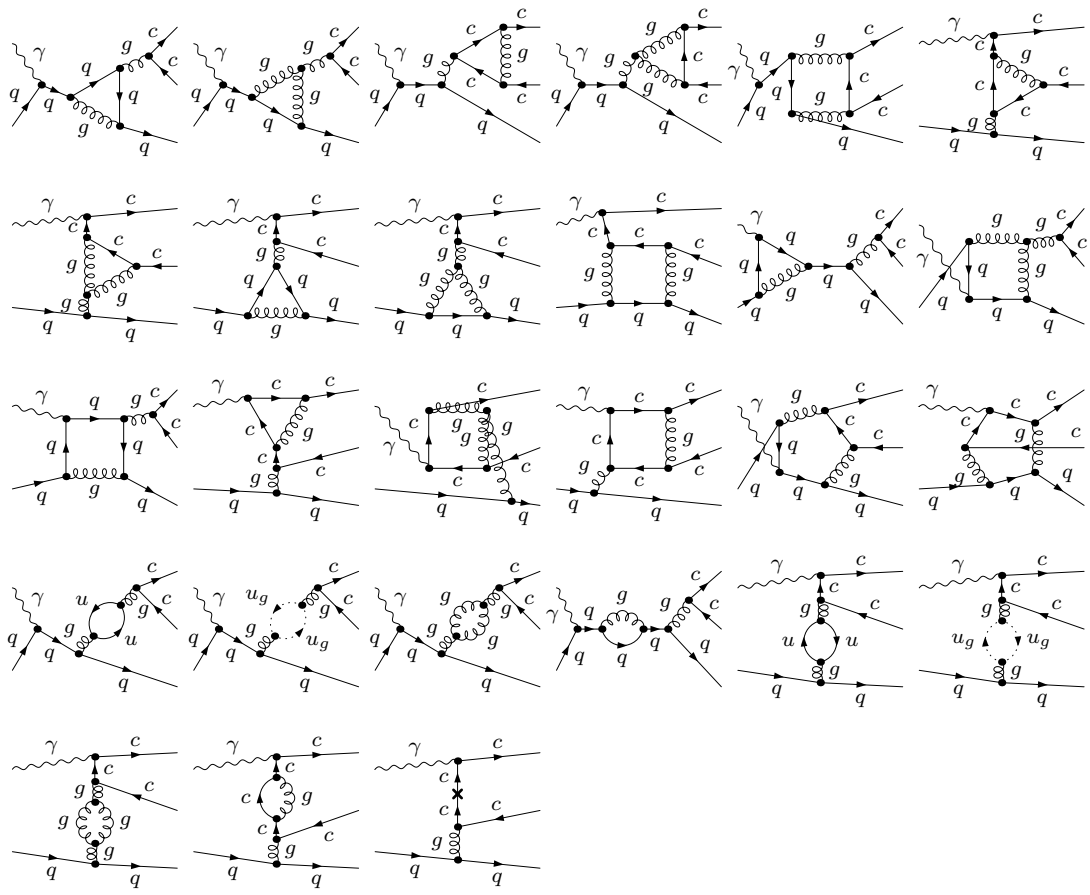

Figure 3.2.: Virtual correction diagrams contributing to the process $\gamma + q \to c\overline{c} + q$. The cross is an insertion of the charm mass counterterm. u_g means gluon ghost and u up quark. 37 diagrams have not been drawn. They differ from the drawn ones only by an exchange of the external c and $\overline{c}$ lines or the external q and $\overline{q}$ lines, or by replacing the up quark loops with down or strange loop.

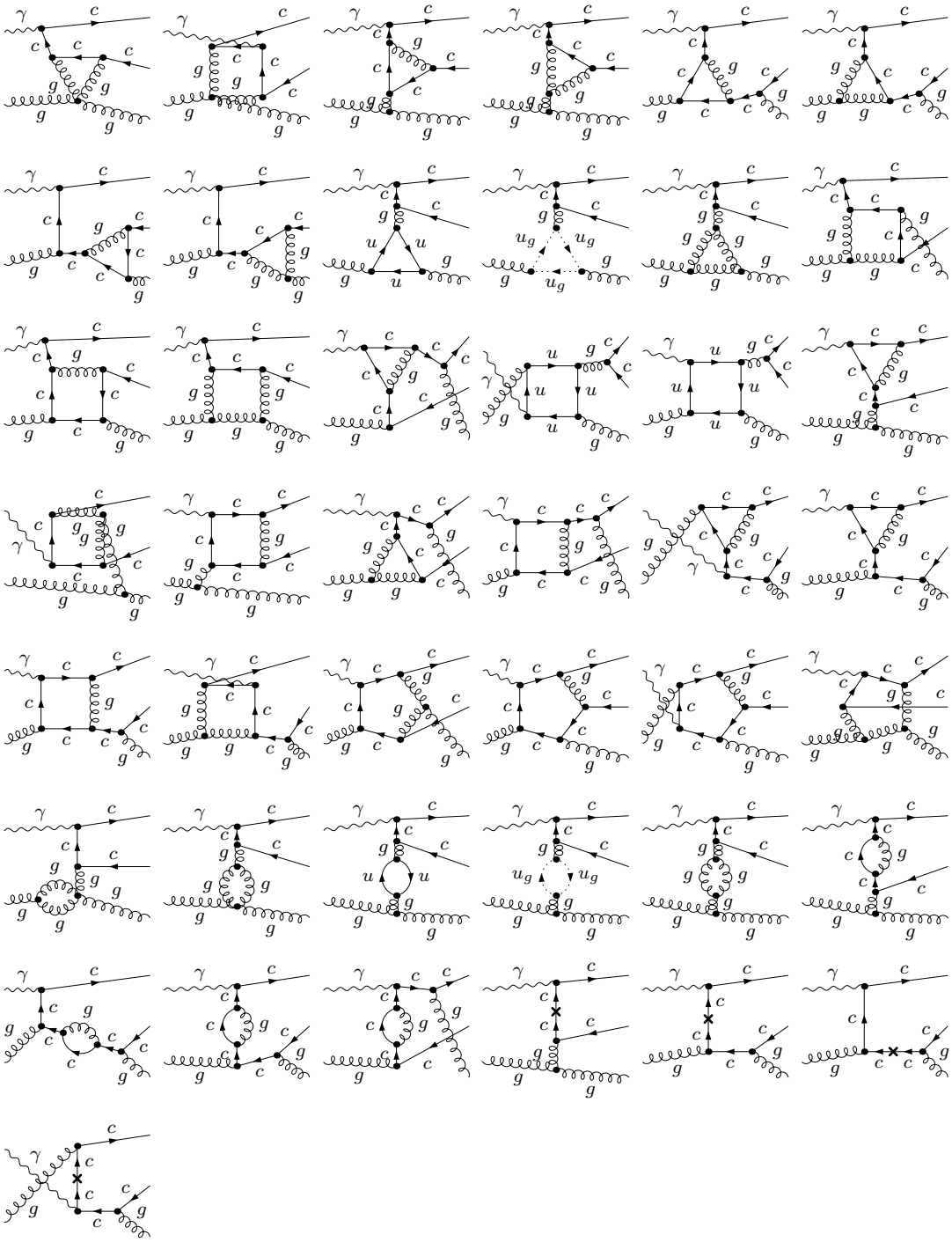

Figure 3.3.: Virtual correction diagrams contributing to the process $\gamma + g \to c\overline{c} + g$. The cross is an insertion of the charm mass counterterm. u_g means gluon ghost and u up quark. 114 diagrams have not been drawn. They differ from the drawn ones only by an exchange of the external c and $\overline{c}$ line or the external gluon lines, or by replacing the up quark loops with down or strange loops.

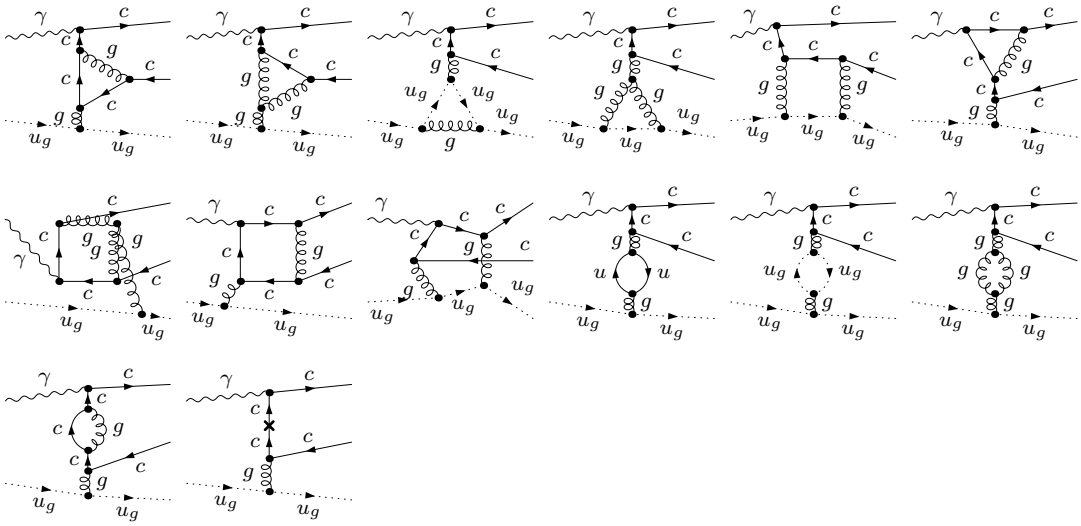

Figure 3.4.: Virtual correction diagrams contributing to the process $\gamma + u_g \to c\overline{c} + u_g$. The cross is an insertion of the charm mass counterterm. u_g means gluon ghost and u up quark. 19 diagrams have not been drawn. They differ from the drawn ones only by an exchange of the external c and $\overline{c}$ line or the external gluon ghost lines, or by replacing the up quark loop with a down or strange loop.

The first terms on the right hand side of (3.17) and (3.18) are the leading order, meaning the Born contributions, which are relatively easy to be calculated. The corresponding Feynman diagrams are drawn in figure 3.1. The results of the squared matrix elements are given in appendix D.

The one-loop diagrams needed for the virtual corrections are drawn in figures 3.2, 3.3 and 3.4. The loop integrals lead to ultraviolet (UV) divergences in the region of large loop momenta and infrared (IR) divergences in the region of small loop momenta. These divergences appear as $\frac{1}{\epsilon}$ poles and, in the case of the infrared divergences, also as $\frac{1}{\epsilon^2}$ poles. The ultraviolet divergences are cancelled by the renormalization of the charm mass m_c, the strong coupling constant $g_s = \sqrt{4\pi\alpha_s}$ and by contributions from external leg insertions, which enter the calculation via wave function renormalization constants. The infrared divergences will be cancelled by complement infrared divergences of the real corrections and by contributions from the wave function renormalization constants as well. We renormalize the bare charm quark mass $m_{c,0}$ by writing it as the sum of the renormalized mass m_c and the mass counterterm δm_c,

$$m_{c,0} = m_c + \delta m_c. \tag{3.20}$$

Fixing this splitting by the usual on-shell condition results in

$$\delta m_c = -\frac{3g_s^2 m_c}{16\pi^2} C_F C_\epsilon \left[\frac{1}{\epsilon_{\mathrm{UV}}} + \frac{4}{3}\right] \tag{3.21}$$

for the expression of order α_s. The symbol C_ϵ was defined in (2.12). We take care of this counterterm by including charm mass counterterm diagrams, as can be seen in figures 3.2, 3.3 and 3.4. We renormalize the bare strong coupling constant $g_{s,0}$ by introducing the counterterm δZ_g via

$$g_{s,0} = (1 + \delta Z_g) g_s \tag{3.22}$$

and fixing it using the $\overline{\mathrm{MS}}$ prescription, which results in

$$\delta Z_g = \frac{g_s^2}{16\pi^2}\left(-\frac{11}{6}C_A + \frac{1}{3}n_{\mathrm{lf}}\right) C_\epsilon \left[\frac{1}{\epsilon_{\mathrm{UV}}} - \ln\frac{\mu^2}{m_c^2}\right], \tag{3.23}$$

for the order α_s expression, where n_{lf} is the number of light flavors, three in our calculation, and μ the renormalization scale. As for the wave function renormalization constants of the charm quark δZ_ψ, the light quarks δZ_{lq}, the gluon δZ_A and the gluon ghosts δZ_u, we fix them using the on-shell condition resulting in

$$\delta Z_\psi = -\frac{g_s^2}{16\pi^2} C_F C_\epsilon \left[\frac{1}{\epsilon_{\mathrm{UV}}} + \frac{2}{\epsilon_{\mathrm{IR}}} + 4\right] \tag{3.24}$$

$$\delta Z_{\mathrm{lq}} = -\frac{g_s^2}{16\pi^2} C_F C_\epsilon \left[\frac{1}{\epsilon_{\mathrm{UV}}} - \frac{1}{\epsilon_{\mathrm{IR}}}\right] \tag{3.25}$$

$$\delta Z_u = \frac{g_s^2}{32\pi^2} C_A C_\epsilon \left[\frac{1}{\epsilon_{\mathrm{UV}}} - \frac{1}{\epsilon_{\mathrm{IR}}}\right] \tag{3.26}$$

$$\delta Z_A = \frac{g_s^2}{48\pi^2}\,(5C_A - 2n_{\rm lf})\,C_\epsilon \left[\frac{1}{\epsilon_{\rm UV}} - \frac{1}{\epsilon_{\rm IR}}\right] \tag{3.27}$$

for the expressions of order α_s. We take care of the strong coupling constant renormalization by doing the replacement (3.22) in the Born expressions of the squared matrix elements. The corrections due to both the strong coupling constant renormalization and the corrections due to external leg insertions are consistently accounted for by defining the symbols $\mathcal{M}_{\rm virtual}(\gamma + q/g/u_g \to c\overline{c}[n] + q/g/u_g)$ in (3.17) and (3.18) to be

$$\begin{aligned}
&\mathcal{M}_{\rm virtual}(\gamma + q \to c\overline{c}[n] + q) \\
&\quad = \mathcal{M}_{\rm loop}(\gamma + q \to c\overline{c}[n] + q) + 2\delta Z_g + \delta Z_\psi + \delta Z_{\rm lq} && (3.28)\\
&\mathcal{M}_{\rm virtual}(\gamma + g \to c\overline{c}[n] + g) \\
&\quad = \mathcal{M}_{\rm loop}(\gamma + g \to c\overline{c}[n] + g) + 2\delta Z_g + \delta Z_\psi + \delta Z_A && (3.29)\\
&\mathcal{M}_{\rm virtual}(\gamma + u_g \to c\overline{c}[n] + u_g) \\
&\quad = \mathcal{M}_{\rm loop}(\gamma + u_g \to c\overline{c}[n] + u_g) + 2\delta Z_g + \delta Z_\psi + \delta Z_u, && (3.30)
\end{aligned}$$

where $\mathcal{M}_{\rm loop}$ means the amplitudes corresponding to the loop diagrams of figures 3.2, 3.3 and 3.4.

3.1. Implementation of the analytical calculation

An overview of the implementation of the analytical calculation of the squared matrix elements is given in figure 3.5.

A. Generation of the diagrams: Our first step is to use FeynArts [21] to generate the diagrams needed for all of our partonic subprocesses, at tree level, and for the virtual corrections also the one loop diagrams and the charm mass counterterm diagrams. At this point we already take out diagrams with massless tadpoles and with light quark triangles with less than three gluon lines attached to it, because these diagrams will vanish anyway. For the four and five point loops we shift the loop momenta for each diagram already at this point, so as to simplify the propagator structure.

B. Treating the amplitudes: After that we run a Mathematica script, which reads the FeynArts output. It separates the color structure from the rest of the amplitudes, applies the color projectors, for color singlet and color octet states separately, and evaluates the color factors for all combinations of diagram times complex conjugated diagram using FeynCalc [22]. The non-color parts of the amplitudes are then further treated by a FORM [23] script. This script applies the spin projectors onto the various $c\overline{c}[n]$ states, squares the amplitudes, performs the polarization sums and fermion traces and recombines the results with the previously calculated color factors.

C.1 Reduction procedure, first method: In the case of the virtual corrections, we still have to perform the loop integrations. We have implemented two different methods

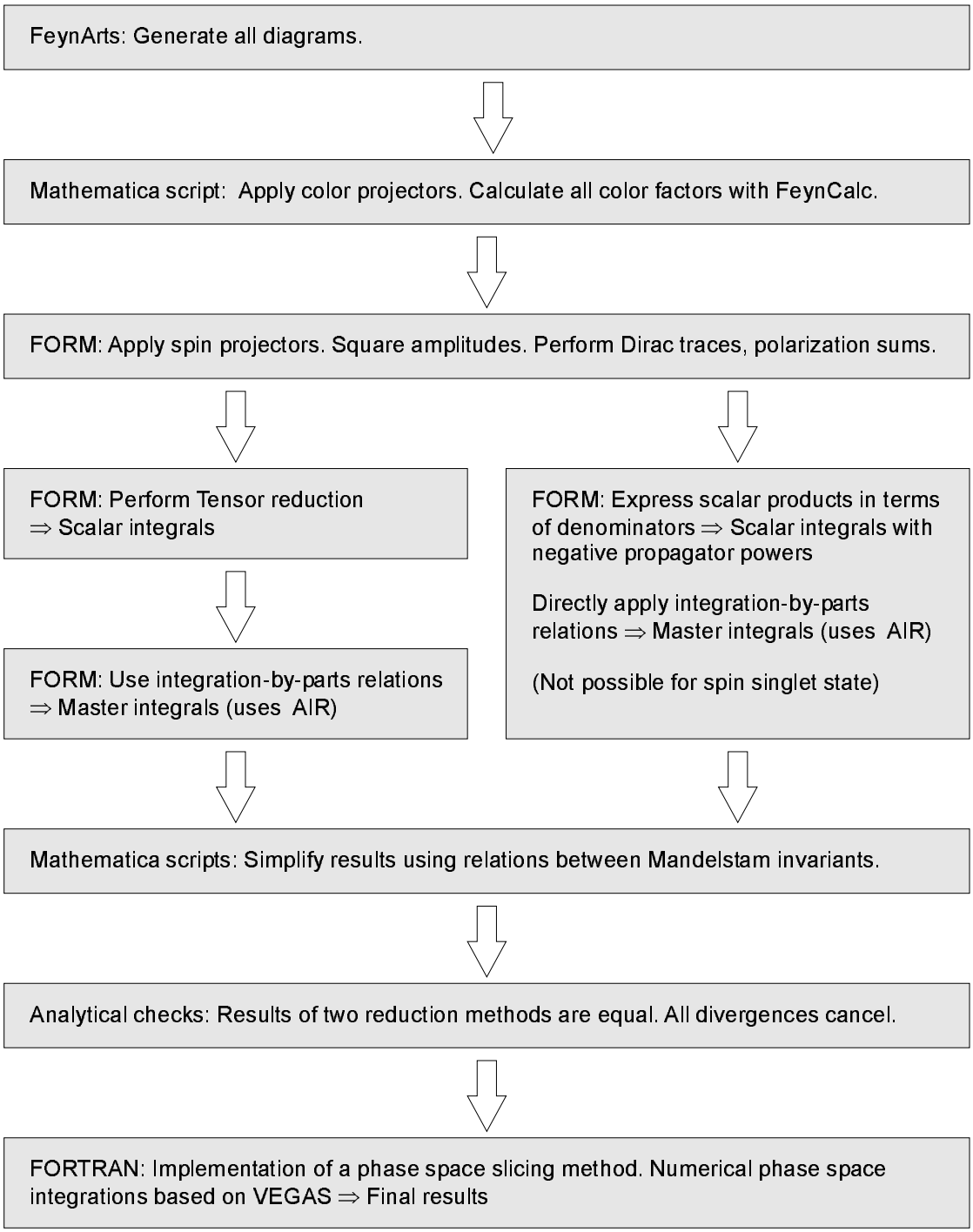

Figure 3.5.: Overview of the implementation of our calculation

for the reduction of the appearing tensor integrals to so called master integrals. Both methods are implemented in a combination of different FORM scripts. In the first method we first apply the tensor reduction procedure which is described in detail in appendix A. It is a generalization of the Passarino-Veltman reduction [24] to the case of linearly dependent propagator momenta, double propagator powers and an arbitrary number of tensor coefficients. The resulting scalar integrals are then reduced further to a set of 14 master integrals by using reduction formulas derived from integration-by-parts relations as described in appendix B.

C.2 Reduction procedure, second method: In the second implementation we do not perform a tensor reduction, but instead express all scalar products in the numerators as a sum of propagators. After a cancellation we then end up with scalar integrals having negative propagator powers. These scalar integrals are now directly reduced to the master integrals by using the integration-by-parts reduction formulas. However, this second method cannot be used for the production of the spin singlet state $c\overline{c}[^1S_0^{[8]}]$. The reason is that the projector (2.10) contains a γ_5. As explained in section 2.1, the scheme we use for dealing with γ_5 in D dimensions leads to 4 dimensional scalar products in the numerators besides the usual D dimensional ones. In case of external momenta, there is no difference between them, but a 4 dimensional loop momentum squared $\tilde{Q}^2$ does not necessarily equal its D dimensional counterpart Q^2. Therefore we cannot cancel a $\tilde{Q}^2$ in the numerator against a Q^2 propagator, so we cannot express tensor integrals with $\tilde{Q}^2$ numerators only in terms of scalar integrals. If we nevertheless cancel a $\tilde{Q}^2$ against a Q^2, we get indeed wrong results.

D. Simplification of the results: The results coming out of these FORM programs are huge, especially for the P states, which are of the order of hundreds of megabytes in size for each subprocess. In order to be able to process the expressions further we use Mathematica scripts which simplify the results basically just by using the identities (3.3) till (3.8) relating the different Mandelstam invariants. This simplification process is the most time consuming part of the implementation of the analytic calculation, but we gain a reduction of the expressions in size by up to a factor 2000. After that the expressions are of manageable size. Mathematica is not able to simplify expressions of the order of hundreds of megabyte at once, so the main job of our scripts is to chunk the expressions automatically into suitable subexpressions, which Mathematica can simplify, then combine the simplified expressions again into chunks of suitable size and so on. We implemented this procedure with many Mathematica instances running parallel. Unfortunately, our simplification procedure only worked for the 2 to 2 kinematics case. In case of the real corrections with 2 to 3 kinematics, the size of the expressions remain of the order of a few megabytes.

E. Analytic checks: We could analytically show that, first, the results of the two reduction methods described above are equal and, second, that all divergences, the ultraviolet and the infrared ones separately, vanish in the sum of all contributions. Finally, we use

Mathematica scripts to convert our results for the squared matrix elements into code for FORTRAN routines which will be used for the numerical phase space integrations, as described in chapter 6.

3.2. Why do we not have Coulomb singularities?

An important feature of previous calculations in the field of heavy quarkonium production, e.g. [11, 14, 15, 25, 26], was the appearance of Coulomb singularities stemming from diagrams with a gluon exchange between the two external heavy quarks lines. A significant amount of effort had to be invested into their regularization and cancellation. However, in our calculation, no Coulomb singularities appear. The reason is that in those mentioned works the loop integration was performed before the projectors (2.4) till (2.7) were applied. Let $I(q)$ be a scalar diagram with a gluon exchanged between the two external heavy quarks. Application of the spin projectors eventually means setting the relative momentum $2q$ between the heavy quarks to 0. But after evaluation of the loop integral, this limit can not be taken, so q has to be kept and is treated as a regularization parameter:

$$\lim_{q\to 0} I(q) = \frac{A}{q^2} + \frac{B}{\epsilon} + C, \tag{3.31}$$

where $\frac{B}{\epsilon}$ is the infrared divergency and $\frac{A}{q^2}$ the Coulomb divergent term. This Coulomb singularity is then either absorbed into the quarkonium wave functions of the color singlet model [11, 25, 26], or canceled by radiative corrections due to longitudinal gluon exchange in the loop corrections to the MEs [14, 15] (see also our remark at the end of chapter 4).

Our approach is different. We first apply the projectors and then perform the loop integration. That means we directly evaluate the integrals at $q = 0$. The result is then free of Coulomb divergences:

$$I(0) = \frac{B}{\epsilon} + C, \tag{3.32}$$

with the same B and C as in (3.31), but without the Coulomb divergent term. It is a well known feature that Coulomb singularities are not apparent in dimensional regularization [27]. Our final results will still be the same as their results. Besides not having to deal with Coulomb singularities, our approach has the advantage that after setting q to zero, we have one mass scale less in the loop integration. However, now our Feynman integrals consist of propagators with linear dependent momenta.

4. Loop corrections to the long distance matrix elements

The long distance matrix element $\langle \mathcal{O}^{J/\psi}[n] \rangle$ describes the probability for the transition of the intermediate $c\bar{c}[n]$ state into a J/ψ plus other particles X, e.g. soft gluons. It can be expressed as the vacuum expectation value of a so called four-fermion operators by rewriting

$$\begin{aligned} \langle \mathcal{O}^{J/\psi}[n] \rangle &= \sum_X \big\langle c\bar{c}[n] \big| J/\psi + X \big\rangle \big\langle J/\psi + X \big| c\bar{c}[n] \big\rangle \\ &= \big\langle 0 \big| \underbrace{\chi^\dagger \mathcal{K}^n_{i,j,a} \psi \, \mathcal{P}^{J/\psi} \, \psi^\dagger \mathcal{K}^n_{i,j,a} \chi}_{\text{4-fermion operator } \mathcal{O}^{J/\psi}[n]} \big| 0 \big\rangle, \end{aligned} \tag{4.1}$$

where

$$\mathcal{P}^{J/\psi} \equiv \sum_X \big| J/\psi + X \big\rangle \big\langle J/\psi + X \big|. \tag{4.2}$$

Here, ψ is the Pauli field operator annihilating a charm quark and χ the Pauli field creating an anticharm quark. The factors $\mathcal{K}^n_{i,j,a}$ consist of Pauli matrices σ_i, color matrices T_a and in case of P states also of field derivation operators. Their definitions

$$\mathcal{K}_a^{{}^1S_0^{[8]}} = T_a \tag{4.3}$$

$$\mathcal{K}_{i,a}^{{}^3S_1^{[8]}} = \sigma_i \, T_a \tag{4.4}$$

$$\mathcal{K}_a^{{}^3P_0^{[8]}} = -\frac{i}{2} \overleftrightarrow{\mathbf{D}} \cdot \boldsymbol{\sigma} \, T_a \tag{4.5}$$

$$\mathcal{K}_{i,a}^{{}^3P_1^{[8]}} = -\frac{i}{2} \big(\overleftrightarrow{\mathbf{D}} \times \boldsymbol{\sigma} \big)_i \, T_a \tag{4.6}$$

$$\mathcal{K}_{i,j,a}^{{}^3P_2^{[8]}} = -\frac{i}{2} \left(\frac{1}{2} \overleftrightarrow{D}_i \, \sigma_j + \frac{1}{2} \overleftrightarrow{D}_j \, \sigma_i - \frac{1}{3} \overleftrightarrow{\mathbf{D}} \cdot \boldsymbol{\sigma} \delta_{ij} \right) T_a \tag{4.7}$$

are given in [4]. $\overleftrightarrow{D}_i$ is the ith component ($i = 1, 2, 3$) of the covariant derivative acting on the spinor to the right minus the ith component of the covariant derivative acting on the spinor to the left. The expressions for the corresponding color singlet states are the same as (4.3) till (4.7), but without the color matrices T_a.

In this interpretation, the long distance matrix elements are viewed as $c\bar{c}$ scattering matrix elements which have to be evaluated nonrelativistically in the $c\bar{c}$ rest frame. At

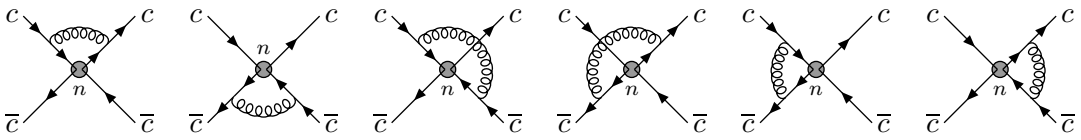

$\mathcal{M}_1[n]$ $\mathcal{M}_2[n]$ $\mathcal{M}_3[n]$ $\mathcal{M}_4[n]$ $\mathcal{M}_5[n]$ $\mathcal{M}_6[n]$

Figure 4.1.: Loop correction diagrams for $\langle \mathcal{O}^{J/\psi}[n] \rangle$

Born level,

$$\langle \mathcal{O}^{J/\psi}[{}^3S_1^{[8]}] \rangle_{\text{Born}} =$$

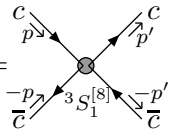

$$= \; C\, \xi^\dagger(\mathbf{p}')\sigma_i T_a \eta(-\mathbf{p}')\; \eta^\dagger(-\mathbf{p})\sigma_i T_a \xi(\mathbf{p}) \tag{4.8}$$

$$\sum_{J=0}^{2} \langle \mathcal{O}^{J/\psi}[{}^3P_J^{[8]}] \rangle_{\text{Born}} =$$

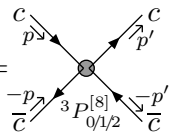

$$= \; C\, \mathbf{p}\cdot\mathbf{p}'\; \xi^\dagger(\mathbf{p}')\sigma_i T_a \eta(-\mathbf{p}')\; \eta^\dagger(-\mathbf{p})\sigma_i T_a \xi(\mathbf{p}), \tag{4.9}$$

where ξ is the Pauli spinor of the incoming c quark and η the Pauli spinor of the outgoing $\overline{c}$ quark. C is a common overall factor. The expressions for the corresponding color singlet long distance matrix elements are the same as (4.8) and (4.9), but without the color matrices T_a.

In a consistent NLO calculation, we also have to compute the $\mathcal{O}(\alpha_s)$ corrections to the MEs. The corresponding loop diagrams are shown in figure 4.1. Because of the non-relativistic structure of the theory, we use the Coulomb gauge for the gluon propagator. As for the charm and anticharm quark propagators and the charm-gluon couplings, we derive the Feynman rules from the heavy quark part of the NRQCD lagrangian [4]

$$\begin{aligned}
\mathcal{L}_{\text{heavy}} &= \psi^\dagger \left(iD_0 + \frac{\mathbf{D}^2}{2m_c} \right) \psi + \chi^\dagger \left(iD_0 - \frac{\mathbf{D}^2}{2m_c} \right) \chi \\
&= \psi^\dagger \left(i\partial_0 + \frac{\boldsymbol{\partial}^2}{2m_c} \right) \psi + g_s \psi^\dagger \left(T_a\, A_{0,a} - \frac{i}{m_c} T_a\, \mathbf{A}_a \cdot \boldsymbol{\partial} \right) \psi \\
&\quad - \frac{g_s^2}{2m_c} T_a T_b\, \mathbf{A}_a \cdot \mathbf{A}_b \psi^\dagger \psi + \chi^\dagger \left(i\partial_0 + \frac{\boldsymbol{\partial}^2}{2m_c} \right) \chi \\
&\quad + g_s \chi^\dagger \left(T_a\, A_{0,a} - \frac{i}{m_c} T_a\, \mathbf{A}_a \cdot \boldsymbol{\partial} \right) \chi + \frac{g_s^2}{2m_c} T_a T_b\, \mathbf{A}_a \cdot \mathbf{A}_b \chi^\dagger \chi,
\end{aligned} \tag{4.10}$$

where ψ and χ are the Pauli fields defined as above, A_0 is the Coulomb component and $\mathbf{A}$ the transverse component of the gluon field. The indices a and b are color indices.

Let us now explicitly calculate the loop corrections to $\langle \mathcal{O}^{J/\psi}[{}^3S_1^{[8]}]\rangle$. The contribution of diagram 1 in figure 4.1 with transverse gluon exchange is then

$\mathcal{M}_{1,\text{transv.}}[{}^3S_1^{[8]}] \;=$ 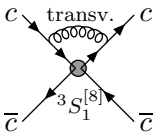

$$= C\,\xi^\dagger(\mathbf{p}')\sigma_i T_b T_a \eta(-\mathbf{p}')\;\eta^\dagger(-\mathbf{p})\sigma_i T_a T_b \xi(\mathbf{p})\; I, \tag{4.11}$$

where

$$\begin{aligned} I \;\equiv\; & -\frac{g_s^2}{m_c^2}\mu^{4-D}\int \frac{d^Dk}{(2\pi)^4} p_i(p'_j-k_j)\frac{i\big(\delta_{ij}-\frac{k_ik_j}{|\mathbf{k}|^2}\big)}{k^2+i\epsilon}\,\frac{i}{\frac{\mathbf{p}^2}{2m_c}-k_0-\frac{(\mathbf{p}-\mathbf{k})^2}{2m_c}+i\epsilon} \\ & \times\frac{i}{\frac{\mathbf{p}'^2}{2m_c}-k_0-\frac{(\mathbf{p}'-\mathbf{k})^2}{2m_c}+i\epsilon}. \end{aligned} \tag{4.12}$$

We have made use of the on-shell conditions $p_0=\frac{\mathbf{p}^2}{2m_c}$ and $p'_0=\frac{\mathbf{p}'^2}{2m_c}$. A crucial feature of NRQCD calculations is that the heavy quark propagator has to be expanded in $1/m_c$ before integration [28, 29]. Otherwise we would get a wrong result, because NRQCD is only valid in the region $\mathbf{k}^2,\mathbf{p}^2,\mathbf{p}'^2 \ll m_c^2$. Keeping only the leading term in $1/m_c$ and performing a contour integration over k_0 yields

$$\begin{aligned} I \;&=\; \frac{g_s^2}{m_c^2}\mu^{4-D}\int\frac{d^{D-1}k}{(2\pi)^3}\left(\mathbf{p}\cdot\mathbf{p}'-\frac{\mathbf{p}\cdot\mathbf{k}\;\mathbf{p}'\cdot\mathbf{k}}{|\mathbf{k}|^2}\right)\frac{1}{2|\mathbf{k}|^3} \\ &=\; \frac{\alpha_s}{3\pi m_c^2}\mu^{4-D}\mathbf{p}\cdot\mathbf{p}'\left(\frac{1}{\epsilon_{\text{UV}}}-\frac{1}{\epsilon_{\text{IR}}}\right). \end{aligned} \tag{4.13}$$

Similarly, diagrams 2, 3 and 4 of figure 4.1 are evaluated to be

$$\mathcal{M}_{2,\text{transv.}}[{}^3S_1^{[8]}] \;=\; C\,\xi^\dagger(\mathbf{p}')\sigma_i T_a T_b \eta(-\mathbf{p}')\;\eta^\dagger(-\mathbf{p})\sigma_i T_b T_a \xi(\mathbf{p})\; I \tag{4.14}$$

$$\mathcal{M}_{3,\text{transv.}}[{}^3S_1^{[8]}] \;=\; C\,\xi^\dagger(\mathbf{p}')\sigma_i T_a T_b \eta(-\mathbf{p}')\;\eta^\dagger(-\mathbf{p})\sigma_i T_a T_b \xi(\mathbf{p})\; I \tag{4.15}$$

$$\mathcal{M}_{4,\text{transv.}}[{}^3S_1^{[8]}] \;=\; C\,\xi^\dagger(\mathbf{p}')\sigma_i T_b T_a \eta(-\mathbf{p}')\;\eta^\dagger(-\mathbf{p})\sigma_i T_b T_a \xi(\mathbf{p})\; I. \tag{4.16}$$

All other diagrams with transverse gluon exchange and all diagrams with Coulomb gluon exchange vanish exactly. Consider for example diagram 5 with Coulomb gluon exchange, which is after expansion in $1/m_c$

$$\begin{aligned} \mathcal{M}_{5,\text{Coulomb}}[{}^3S_1^{[8]}] \;&=\; C\,\xi^\dagger(\mathbf{p}')\sigma_i T_a \eta(-\mathbf{p}')\;\eta^\dagger(-\mathbf{p})\sigma_i T_b T_a T_b \xi(\mathbf{p}) \\ &\quad\times ig_s^2\mu^{4-D}\int\frac{d^Dk}{(2\pi)^4}\frac{1}{|\mathbf{k}|^2}\,\frac{1}{(k_0+i\epsilon)(k_0-i\epsilon)}, \end{aligned} \tag{4.17}$$

which is zero in dimensional regularization. In the same way, also the heavy quark self energy diagram is exactly zero, so that there are also no contribution due to external leg insertions.

Using the identity

$$T_aT_b \otimes T_bT_a + T_aT_b \otimes T_aT_b = \frac{C_F}{C_A}(1 \otimes 1) + \left(\frac{C_A}{2} - \frac{2}{C_A}\right)(T_a \otimes T_a) \tag{4.18}$$

for tensorproducts of color matrices, the sum of (4.11), (4.14), (4.15) and (4.16) becomes

$$\begin{aligned}\langle \mathcal{O}^{J/\psi}[^3S_1^{[8]}]\rangle_{\rm loop} &= C\ \xi^\dagger(\mathbf{p}')\sigma_i\eta(-\mathbf{p}')\ \eta^\dagger(-\mathbf{p})\sigma_i\xi(\mathbf{p}) \cdot \frac{2C_F}{C_A} I \\ &+ \xi^\dagger(\mathbf{p}')\sigma_i T_a\eta(-\mathbf{p}')\ \eta^\dagger(-\mathbf{p})\sigma_i T_a\xi(\mathbf{p}) \cdot \left(C_A - \frac{4}{C_A}\right) I. \end{aligned} \tag{4.19}$$

A comparison with (4.9) shows that

$$\begin{aligned}\langle \mathcal{O}^{J/\psi}[^3S_1^{[8]}]\rangle &= \langle \mathcal{O}^{J/\psi}[^3S_1^{[8]}]\rangle_{\rm Born} + \frac{2\alpha_s}{3\pi m_c^2}\mu^{4-D}\left(\frac{1}{\epsilon_{\rm UV}} - \frac{1}{\epsilon_{\rm IR}}\right) \\ &\times \sum_J \left[\frac{C_F}{C_A}\langle \mathcal{O}^{J/\psi}[^3P_J^{[1]}]\rangle_{\rm Born} + \left(\frac{C_A}{2} - \frac{2}{C_A}\right)\langle \mathcal{O}^{J/\psi}[^3P_J^{[8]}]\rangle_{\rm Born}\right]. \end{aligned} \tag{4.20}$$

This bare long distance matrix operator is both ultraviolet and infrared divergent. We remove the ultraviolet singularity by renomalizating $\langle \mathcal{O}^{J/\psi}[^3S_1^{[8]}]\rangle$. We have freedom in choosing an appropriate renormalization condition, but in order to be consistent with previous calculations [14, 15], we define

$$\begin{aligned}\langle \mathcal{O}^{J/\psi}[^3S_1^{[8]}]\rangle_{\rm ren} &\equiv \langle \mathcal{O}^{J/\psi}[^3S_1^{[8]}]\rangle - \frac{2\alpha_s}{3\pi m_c^2}\left(\frac{1}{\epsilon_{\rm UV}} + \ln 4\pi - \gamma_E + \ln\frac{\mu^2}{\mu_\Lambda^2}\right) \\ &\times \sum_J \left[\frac{C_F}{C_A}\langle \mathcal{O}^{J/\psi}[^3P_J^{[1]}]\rangle_{\rm Born} + \left(\frac{C_A}{2} - \frac{2}{C_A}\right)\langle \mathcal{O}^{J/\psi}[^3P_J^{[8]}]\rangle_{\rm Born}\right], \end{aligned} \tag{4.21}$$

where the additional scale μ_Λ is introduced, which is called the NRQCD scale. Our final result for $\langle \mathcal{O}^{J/\psi}[^3S_1^{[8]}]\rangle$, which multiplies our short distance cross section, is then

$$\begin{aligned}\langle \mathcal{O}^{J/\psi}[^3S_1^{[8]}]\rangle_{\rm Born} &= \langle \mathcal{O}^{J/\psi}[^3S_1^{[8]}]\rangle_{\rm ren} + \frac{2\alpha_s}{3\pi m_c^2}\left(\frac{4\pi\mu^2}{\mu_\Lambda^2}e^{-\gamma_E}\right)^\epsilon \frac{1}{\epsilon_{\rm IR}} \\ &\times \sum_J \left[\frac{C_F}{C_A}\langle \mathcal{O}^{J/\psi}[^3P_J^{[1]}]\rangle_{\rm Born} + \left(\frac{C_A}{2} - \frac{2}{C_A}\right)\langle \mathcal{O}^{J/\psi}[^3P_J^{[8]}]\rangle_{\rm Born}\right]. \end{aligned} \tag{4.22}$$

Similarly, the $\mathcal{O}(\alpha_s)$ expression for $\langle \mathcal{O}^{J/\psi}[^3S_1^{[1]}]\rangle$ is evaluated to be

$$\begin{aligned}\langle \mathcal{O}^{J/\psi}[^3S_1^{[1]}]\rangle_{\rm Born} &= \langle \mathcal{O}^{J/\psi}[^3S_1^{[1]}]\rangle_{\rm ren} \\ &+ \frac{4\alpha_s}{3\pi m_c^2}\left(\frac{4\pi\mu^2}{\mu_\Lambda^2}e^{-\gamma_E}\right)^\epsilon \frac{1}{\epsilon_{\rm IR}}\sum_J \langle \mathcal{O}^{J/\psi}[^3P_J^{[8]}]\rangle_{\rm Born}. \end{aligned} \tag{4.23}$$

The loop corrections to $\langle \mathcal{O}^{J/\psi}[^1S_0^{[8]}]\rangle$ and $\langle \mathcal{O}^{J/\psi}[^3P_J^{[8]}]\rangle$ are proportional to long distance matrix elements which scale with powers of v that are already beyond the order considered in our calculation.

The renormalized MEs $\langle \mathcal{O}^{J/\psi}[^3S_1^{[8]}]\rangle_{\text{ren}}$ and $\langle \mathcal{O}^{J/\psi}[^3S_1^{[1]}]\rangle_{\text{ren}}$ are are actually objects which depend on the scale μ_Λ. A renormalization group equation, which describes this dependence, can be derived out of (4.22) and (4.23). However, in our calculation we consider μ_Λ to be constant and assume it to be the same in all processes and experiments, so we do not examine this scale dependence.

We remark that in the case of the diagram 5 and 6 of figure 4.1 with Coulomb gluon exchange the authors of [14, 15] perform the loop integration before expanding in $1/m_c$. Then these diagrams give rise to Coulomb divergent terms, which they need in order to cancel the Coulomb divergence they encounter in their calculation of the short distance cross sections. However their calculation is inconsistent, because in the case of transverse gluon exchange, they do nevertheless, like us, first expand in $1/m_c$ and then do the loop integration, in order to produce the correct infrared singular term.

5. Real corrections

This chapter deals with the calculation of the real correction processes, which are processes with two incoming and three outgoing particles. At the partonic level these are

$$\gamma(k_1) + q(k_2) \rightarrow c\overline{c}[n](P) + q(k_3) + g(k_4) \qquad (q = u, \overline{u}, d, \overline{d}, s, \overline{s}) \tag{5.1}$$
$$\gamma(k_1) + g(k_2) \rightarrow c\overline{c}[n](P) + g(k_3) + g(k_4) \tag{5.2}$$
$$\gamma(k_1) + g(k_2) \rightarrow c\overline{c}[n](P) + q(k_3) + \overline{q}(k_4) \qquad (q = u, d, s), \tag{5.3}$$

where the momenta of the respective particles are given in brackets. We define the $2 \rightarrow 3$ kinematics Mandelstam invariants

$$s \equiv (k_1 + k_2)^2 = 2k_1 \cdot k_2 \tag{5.4}$$
$$s_3 \equiv (k_3 + k_4)^2 = 2k_3 \cdot k_4 \tag{5.5}$$
$$s_4 \equiv (P + k_4)^2 - 4m_c^2 = 2P \cdot k_4 \tag{5.6}$$
$$s_5 \equiv (P + k_3)^2 - 4m_c^2 = 2P \cdot k_3 \tag{5.7}$$
$$t_1 \equiv (P - k_1)^2 - 4m_c^2 = -2P \cdot k_1 \tag{5.8}$$
$$t_6 \equiv (k_2 - k_3)^2 = -2k_2 \cdot k_3 \tag{5.9}$$
$$u_6 \equiv (k_1 - k_3)^2 = -2k_1 \cdot k_3 \tag{5.10}$$
$$u_1 \equiv (P - k_2)^2 - 4m_c^2 = -2P \cdot k_2 \tag{5.11}$$
$$t' \equiv (k_1 - k_4)^2 = -2k_1 \cdot k_4 \tag{5.12}$$
$$u' \equiv (k_2 - k_4)^2 = -2k_2 \cdot k_4, \tag{5.13}$$

taking over the notation of [11]. Note that the invariants s, t_1 and u_1 coincide with the respective definitions (3.3), (3.7) and (3.8), where there is one outgoing parton less. Like in the $2 \rightarrow 2$ kinematics case we therefore further define

$$s_1 \equiv s - 4m_c^2 \tag{5.14}$$
$$t \equiv t_1 + 4m_c^2 \tag{5.15}$$
$$u \equiv u_1 + 4m_c^2. \tag{5.16}$$

Note that s, s_1, s_3, s_4 and s_5 are positive, t, t_1, t_6, u, u_6, u_1, t' and u' negative. Of all these Mandelstam variables (5.4) till (5.16), only a set of five can be linearly independent.

In contrast to the case of the virtual corrections, the evaluation of the real correction's squared matrix elements is straight forward and does not pose any conceptual difficulties. But in the case of real corrections the difficulties arise in the phase space integration of the squared matrix elements. A completely numerical integration over the three particle phase space is not possible, because the integrals are divergent in the regions, where

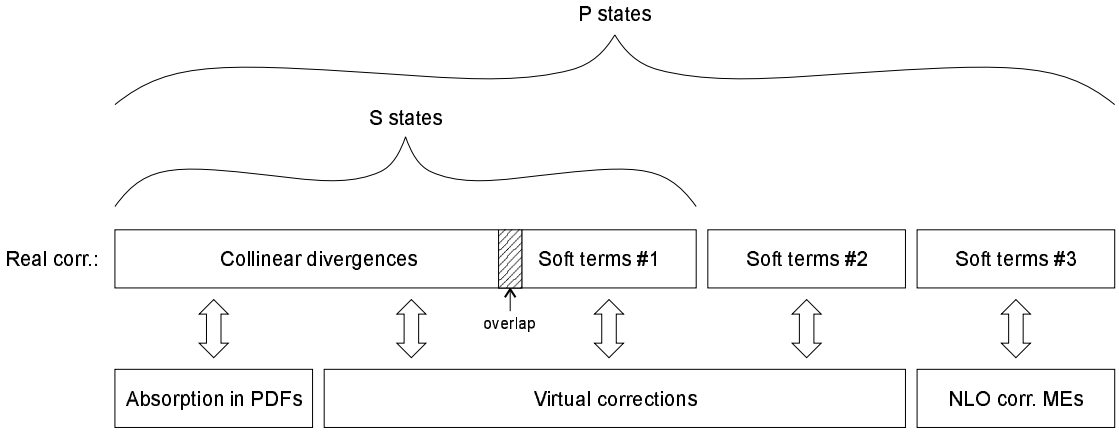

Figure 5.1.: Overview of the infrared singularity structure and its cancellations

an outgoing gluon is soft or two external light particles are collinear to each other, so that the integrations have to be performed in $D = 4 - 2\epsilon$ dimensions. However, a D dimensional analytic integration over the complete phase space is far beyond reach of our current computational abilities. Therefore, in this work we implement a phase space slicing method, where follow the lines of [30], which we had to adapt to our heavy quarkonium production case. In that method we divide the phase space into three parts:

1. The *soft* region, in which one of the outgoing gluons is soft.
2. The *hard collinear* region, in which all outgoing gluons are hard, but two external light particles are collinear to each other.
3. The *hard non-collinear* region, in which the outgoing gluons are hard, and no two external light particles are collinear to each other.

The hard non-collinear region is free of divergences, therefore we perform its phase space integration completely numerically in four dimensions, as will be described in section 5.3. On the other hand, in the soft and hard collinear regions, certain factorization rules apply to both phase space and squared matrix elements, which facilitate analytic phase space integrations in D dimensions, as will be described in detail in sections 5.1 and 5.2. In these analytic integrations, the soft and collinear divergences will become apparent as $\frac{1}{\epsilon^2}$ and $\frac{1}{\epsilon}$ poles, which cancel against infrared divergences stemming from different other sources. An overview of these cancellations is depicted in figure 5.1: The so called soft #1 divergences and the collinear divergences are cancelled by the infrared singularities from the virtual corrections. Furthermore universal parts from the incoming collinear divergences are absorbed into the parton distribution functions of the incoming parton and the photon. We remark that the overlap between the soft #1 terms and the collinear terms is the origin of the $\frac{1}{\epsilon^2}$ poles. (We view this region as part of our soft region.) In case of intermediate P states, there are additionally soft #2 terms, which are also cancelled

by infrared divergent terms of the virtual corrections, and soft #3 terms, which are cancelled by loop corrections to the long distance matrix elements $\langle \mathcal{O}^{J/\psi}[^3S_1^{[8]}]\rangle$ and $\langle \mathcal{O}^{J/\psi}[^3S_1^{[1]}]\rangle$.

We have not yet stated precisely, what parts of the phase space we consider soft, and what collinear. For that purpose we introduce the two *slicing parameters* δ_s and δ_c, and we define that a phase space point is soft if

$$\frac{2E_3}{\sqrt{s}} = \frac{s - s_4 - 4m_c^2}{s} < \delta_s \quad \text{or} \quad \frac{2E_4}{\sqrt{s}} = \frac{s - s_5 - 4m_c^2}{s} < \delta_s, \tag{5.17}$$

and that it is collinear if

$$\frac{s_3}{s} < \delta_c \quad \text{or} \quad \frac{-t_6}{s} < \delta_c \quad \text{or} \quad \frac{-u_6}{s} < \delta_c \quad \text{or} \quad \frac{-t'}{s} < \delta_c \quad \text{or} \quad \frac{-u'}{s} < \delta_c. \tag{5.18}$$

E_3 means the energy of the parton with momentum k_3 and E_4 the energy of the parton with momentum k_4. Now the integration results of all three integration regions will depend on the unphysical parameters δ_s and δ_c. But if δ_s and δ_c are sufficiently small, so that the soft and collinear approximations used are sufficiently correct, then the sum of the integration results of the three regions must be independent of the specific choice of δ_s and δ_c. This phase space slicing parameter independence is an important check on our calculation.

5.1. The soft region

5.1.1. Soft amplitudes in general

Soft divergences arise from diagrams, where an external gluon is attached to another external gluon or quark line. In the limit where that gluon is soft, the amplitude of that diagram factorizes into the Born amplitude without the soft gluon and a so called eikonal factor. More precisely, in the case where a soft gluon is attached to an incoming quark, we have

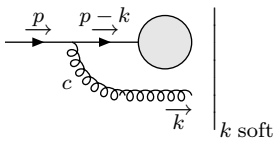

$$= g_s \frac{p \cdot \epsilon^*(k)}{p \cdot k} A(p)(-T_c)u(p), \tag{5.19}$$

where

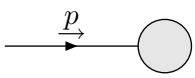

$$\equiv A(p)u(p). \tag{5.20}$$

In the case where a soft gluon is attached to an outgoing quark, we have

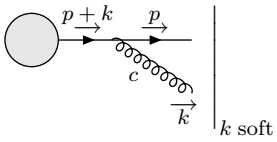

$$= g_s \frac{p \cdot \epsilon^*(k)}{p \cdot k} \overline{u}(p) T_c A(p), \tag{5.21}$$

where

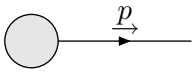

$$\equiv \overline{u}(p)A(p). \tag{5.22}$$

In the case where a soft gluon is attached to an outgoing antiquark, we have

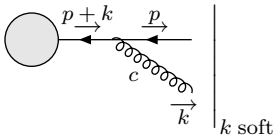

$$= g_s \frac{p \cdot \epsilon^*(k)}{p \cdot k} A(p)(-T_c)v(p), \tag{5.23}$$

where

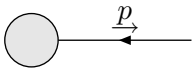

$$\equiv A(p)v(p). \tag{5.24}$$

In the case where a soft gluon is attached to an incoming antiquark, we have

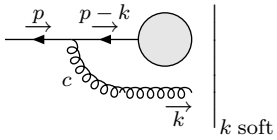

$$= g_s \frac{p \cdot \epsilon^*(k)}{p \cdot k} \overline{v}(p)T_c A(p), \tag{5.25}$$

where

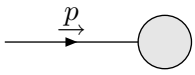

$$\equiv \overline{v}(p)A(p). \tag{5.26}$$

Finally, in the case where a soft gluon is attached to another gluon line, no matter if incoming or outgoing, we have

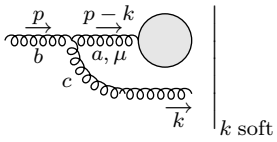

$$= g_s \frac{p \cdot \epsilon^*(k)}{p \cdot k} \epsilon_\mu(p) i f_{bca} A^\mu_a(p), \tag{5.27}$$

where

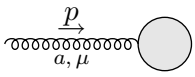

$$\equiv \epsilon_\mu(p) A^\mu_a(p). \tag{5.28}$$

In equations (5.19) till (5.28), T_c are color matrices and f_{bca} the usual antisymmetric SU(3) structure constants.

We summarize all these cases of soft gluon insertions by introducing the abbreviated notation used in [31]: If $|A\rangle$ denotes a Born amplitude

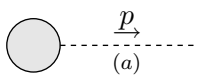

$$\equiv |A\rangle, \tag{5.29}$$

then the diagrams with a soft gluon attached to an external QCD parton line i with momentum p is given by

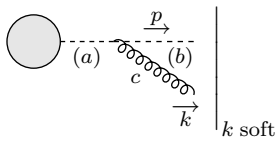

$$= g_s \frac{p \cdot \epsilon^*(k)}{p \cdot k} \mathbf{T}_i |A\rangle. \tag{5.30}$$

We call the object $\mathbf{T}_i$ a color operator, and it is defined by acting on the Born amplitude $|A\rangle$ by the insertion of the color structure

T_c	if	i is an outgoing quark or incoming antiquark
$-T_c$	if	i is an incoming quark or outgoing antiquark
if_{bca}	if	i is a gluon

into the amplitude $|A\rangle$ at the position of parton i. Furthermore we define

$$\langle A|\mathbf{T}_x \mathbf{T}_y|B\rangle \equiv (\mathbf{T}_x|A\rangle)^* \left(\mathbf{T}_y|B\rangle\right). \tag{5.31}$$

In order to prevent possible confusion, we emphasize that the bras and kets do not mean quantum mechanical states, but are short notations for amplitudes.

5.1.2. Soft amplitudes in our heavy quarkonium production

The real correction processes which exhibit soft divergences are the two processes (5.1) and (5.2). Let us denote the corresponding amplitudes in the limit where the gluon with momentum k_4 is soft by

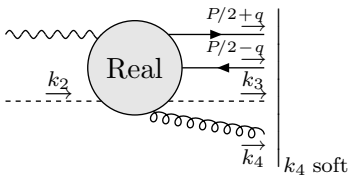

$$\equiv \big|k_4 \text{ soft}\big\rangle, \tag{5.32}$$

where the dashed line is either a gluon or a light quark (or antiquark). We evaluate $\big|k_4 \text{ soft}\big\rangle$ by attaching a soft gluon with momentum k_4 in turn to the external gluon, light quark and charm quark lines of the corresponding Born processes (3.1) or (3.2)

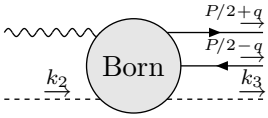

$$\equiv \big|\text{Born}\big\rangle. \tag{5.33}$$

Application of rule (5.30) for each soft gluon insertion then yields

$$\begin{aligned}\big|k_4\text{ soft}\big\rangle &= g_s\Bigg(\frac{\left(\frac{P}{2}+q\right)\cdot\epsilon^*(k_4)}{\left(\frac{P}{2}+q\right)\cdot k_4}\mathbf{T}_c+\frac{\left(\frac{P}{2}-q\right)\cdot\epsilon^*(k_4)}{\left(\frac{P}{2}-q\right)\cdot k_4}\mathbf{T}_{\overline{c}}\\ &\quad+\frac{k_2\cdot\epsilon^*(k_4)}{k_2\cdot k_4}\mathbf{T}_2+\frac{k_3\cdot\epsilon^*(k_4)}{k_3\cdot k_4}\mathbf{T}_3\Bigg)\big|\text{Born}\big\rangle. \end{aligned}\tag{5.34}$$

We evaluate the soft regions of the real corrections using the axial gauge with

$$\sum_{\text{pol}}\epsilon_\mu(k_4)\epsilon^*_\nu(k_4)=-g_{\mu\nu}+\frac{P_\mu k_{4\nu}+k_{4\mu}P_\nu}{P\cdot k_4}-\frac{P^2k_{4\mu}k_{4\nu}}{(P\cdot k_4)^2}\tag{5.35}$$

for the gluons so that

$$P\cdot\epsilon(k_4)=0.\tag{5.36}$$

Then

$$\big|k_4\text{ soft}\big\rangle\Big|_{q=0}=g_s\sum_{i=2}^{3}\frac{k_i\cdot\epsilon^*(k_4)}{k_i\cdot k_4}\mathbf{T}_i\big|\text{Born}\big\rangle\Big|_{q=0}\tag{5.37}$$

and

$$\begin{aligned}\frac{\partial}{\partial q_\beta}\big|k_4\text{ soft}\big\rangle\Big|_{q=0} &= g_s\frac{2\epsilon^{*\beta}(k_4)}{P\cdot k_4}(\mathbf{T}_c-\mathbf{T}_{\overline{c}})\big|\text{Born}\big\rangle\Big|_{q=0}\\ &\quad+g_s\sum_{i=2}^{3}\frac{k_i\cdot\epsilon^*(k_4)}{k_i\cdot k_4}\mathbf{T}_i\frac{\partial}{\partial q_\beta}\big|\text{Born}\big\rangle\Big|_{q=0}, \end{aligned}\tag{5.38}$$

so that the application of the projectors (2.4) till (2.7) then yields for the real corrections to the $c\overline{c}[n]$ production amplitudes in the limit where k_4 is soft

$$\big|{}^1S_0^{[8]},k_4\text{ soft}\big\rangle = \text{Tr}\left[\mathcal{C}_8\Pi_0\big|k_4\text{ soft}\big\rangle\right]\Big|_{q=0}=g_s\sum_{i=2}^{3}\frac{k_i\cdot\epsilon^*(k_4)}{k_i\cdot k_4}\mathbf{T}_i\big|{}^1S_0^{[8]},\text{Born}\big\rangle\tag{5.39}$$

$$\begin{aligned}\big|{}^3S_1^{[1/8]},k_4\text{ soft}\big\rangle &= \epsilon_\alpha\text{Tr}\left[\mathcal{C}_{1/8}\Pi_1^\alpha\big|k_4\text{ soft}\big\rangle\right]\Big|_{q=0}\\ &= g_s\sum_{i=2}^{3}\frac{k_i\cdot\epsilon^*(k_4)}{k_i\cdot k_4}\mathbf{T}_i\big|{}^3S_1^{[1/8]},\text{Born}\big\rangle \end{aligned}\tag{5.40}$$

$$\begin{aligned}\big|{}^3P_J^{[8]},k_4\text{ soft}\big\rangle &= \mathcal{E}^{(J)}_{\alpha\beta}\frac{\partial}{\partial q_\beta}\text{Tr}\left[\mathcal{C}_8\Pi_1^\alpha\big|k_4\text{ soft}\big\rangle\right]\Big|_{q=0}\\ &= \sum_{i=2}^{3}\frac{k_i\cdot\epsilon^*(k_4)}{k_i\cdot k_4}\mathbf{T}_i\big|{}^3P_J^{[8]},\text{Born}\big\rangle\\ &\quad+\mathcal{E}^{(J)}_{\alpha\beta}g_s\frac{2\epsilon^{*\beta}(k_4)}{P\cdot k_4}(\mathbf{T}_c-\mathbf{T}_{\overline{c}})\text{Tr}\left[\mathcal{C}_8\Pi_1^\alpha\big|\text{Born}\big\rangle\right]\Big|_{q=0}. \end{aligned}\tag{5.41}$$

The corresponding squared matrix elements are then evaluated to be

$$\begin{aligned}
\left|\mathcal{M}_{k_4\,\mathrm{soft}}({}^1S_0^{[8]})\right|^2 &= S_1({}^1S_0^{[8]}) && (5.42)\\
\left|\mathcal{M}_{k_4\,\mathrm{soft}}({}^3S_1^{[1/8]})\right|^2 &= S_1({}^3S_1^{[1/8]}) && (5.43)\\
\left|\mathcal{M}_{k_4\,\mathrm{soft}}({}^3P_J^{[8]})\right|^2 &= S_1({}^3P_J^{[8]}) + S_2({}^3P_J^{[8]}) + S_3({}^3P_J^{[8]}), && (5.44)
\end{aligned}$$

where we have abbreviated

$$S_1(n) = g_s \sum_{i,j=2}^{3} \frac{k_i\cdot\epsilon(k_4)\,k_j\cdot\epsilon^*(k_4)}{k_i\cdot k_4\,k_j\cdot k_4}\langle n,\,\mathrm{Born}\big|\mathbf{T}_i\mathbf{T}_j\big|n,\,\mathrm{Born}\rangle \tag{5.45}$$

$$\begin{aligned}
S_2({}^3P_J^{[8]}) &= 4g_s^2\sum_{i=2}^{3}\frac{k_i\cdot\epsilon(k_4)\,\epsilon^{*\beta}(k_4)}{k_i\cdot k_4\,P\cdot k_4}\mathcal{E}^J_{\alpha\beta}\\
&\quad\times\big\langle{}^3P_J^{[8]},\mathrm{Born}\big|\mathbf{T}_i(\mathbf{T}_c-\mathbf{T}_{\overline{c}})\mathrm{Tr}\left[\mathcal{C}_8\Pi_1^\alpha\big|\mathrm{Born}\rangle\right]\Big|_{q=0} && (5.46)
\end{aligned}$$

$$\begin{aligned}
S_3({}^3P_J^{[8]}) &= 4g_s\frac{\epsilon^{\beta'}(k_4)\epsilon^{*\beta}(k_4)\mathcal{E}^{(J)*}_{\alpha'\beta'}\mathcal{E}^{(J)}_{\alpha\beta}}{(P\cdot k_4)^2}\\
&\quad\times\mathrm{Tr}\big[\langle\mathrm{Born}\big|\Pi_1^{*\alpha'}\mathcal{C}_8\big]\Big|_{q=0}(\mathbf{T}_c-\mathbf{T}_{\overline{c}})(\mathbf{T}_c-\mathbf{T}_{\overline{c}})\mathrm{Tr}\left[\mathcal{C}_8\Pi_1^\alpha\big|\mathrm{Born}\rangle\right]\Big|_{q=0}. && (5.47)
\end{aligned}$$

We call $S_1(n)$ the soft #1 terms, which appear in both intermediate S and intermediate P states, and $S_2({}^3P_J^{[8]})$ and $S_3({}^3P_J^{[8]})$ the soft #2 and soft #3 terms, which appear only in squared amplitudes for intermediate P states.

5.1.3. Kinematics of the soft region

For the phase space integration in the soft region $k_4 \to 0$, we parameterize the momenta in the center of mass frame of the incoming particles, which is here at the same time the center of mass frame of the J/ψ and the outgoing parton with momentum k_3:

$$\begin{aligned}
k_1 &= E_2(1,\,0,\,-\sin\theta,\,-\cos\theta) && (5.48)\\
k_2 &= E_2(1,\,0,\,\sin\theta,\,\cos\theta) && (5.49)\\
P &= (E_{J/\psi},\,0,\,0,\,-E_3) && (5.50)\\
k_3 &= E_3(1,\,0,\,0,\,1) && (5.51)\\
k_4 &= E_4(1,\,\sin\theta_1\sin\theta_2,\,\sin\theta_1\cos\theta_2,\,\cos\theta_1), && (5.52)
\end{aligned}$$

where

$$E_2 = \frac{\sqrt{s}}{2},\qquad E_3 = \frac{s_1}{2\sqrt{s}},\qquad E_{J/\psi} = \frac{s+4m_c^2}{2\sqrt{s}},\qquad \cos\theta = \frac{t-u}{s_1}. \tag{5.53}$$

The corresponding contribution to the real correction cross section is given by

$$d\sigma_{\text{soft}}(n) = \frac{1}{2s} d\text{PS}_{2\to 2} \int_{\text{soft}} d\text{PS}_{k_4} \frac{1}{N_{\text{col,in}} N_{\text{pol,in}}} \sum_{\text{col,pol}} |\mathcal{M}_{k_4\ \text{soft}}(n)|^2, \tag{5.54}$$

where $d\text{PS}_{2\to 2}$ is the two particle phase space (3.13) and

$$\begin{aligned}\int_{\text{soft}} d\text{PS}_{k_4} &\equiv \int_{\text{soft}} \frac{\mu^{4-D} d^{D-1} k_4}{2(2\pi)^{D-1} E_4} \\ &= \frac{(\pi\mu^2)^\epsilon}{(2\pi)^3} \frac{\Gamma(1-\epsilon)}{\Gamma(1-2\epsilon)} \int_0^{\frac{\delta_s\sqrt{s}}{2}} E_4^{1-2\epsilon} dE_4 \int_0^\pi \sin^{1-2\epsilon}\theta_1 d\theta_1 \int_0^\pi \sin^{-2\epsilon}\theta_2 d\theta_2. \end{aligned} \tag{5.55}$$

We have to perform the integrations over $d\text{PS}_{k_4}$ analytically in D dimensions in order to make the infrared poles explicit. In the following subsections we will need the results of the integrals

$$\int_{\text{soft}} \frac{d\text{PS}_{k_4}}{(P\cdot k_4)^2} = \frac{1}{32\pi^2 m_c^2} C_\epsilon \left[-\frac{1}{\epsilon} - \frac{s+4m_c^2}{s_1} \ln\left(\frac{s}{4m_c^2}\right) + \ln\left(\frac{\delta_s^2 s}{m_c^2}\right)\right] \tag{5.56}$$

$$\begin{aligned}&\int_{\text{soft}} \frac{d\text{PS}_{k_4}}{k_3\cdot k_4\, P\cdot k_4} \\ &= \frac{1}{8\pi^2 s_1} C_\epsilon \left[\frac{1}{\epsilon^2} - \frac{1}{\epsilon}\ln\left(\frac{s^2\delta_s^2}{4m_c^4}\right) + \frac{1}{2}\ln^2\left(\frac{s^2\delta_s^2}{4m_c^4}\right) + 2\,\text{Li}_2\left(\frac{-s_1}{4m_c^2}\right) - \frac{\pi^2}{4}\right]\end{aligned} \tag{5.57}$$

$$\begin{aligned}&\int_{\text{soft}} \frac{d\text{PS}_{k_4}}{k_2\cdot k_4\, k_3\cdot k_4} \\ &= -\frac{1}{4\pi^2 t} C_\epsilon \left[\frac{1}{\epsilon^2} - \frac{1}{\epsilon}\ln\left(\frac{-st\delta_s^2}{s_1 m_c^2}\right) + \frac{1}{2}\ln^2\left(\frac{-st\delta_s^2}{s_1 m_c^2}\right) + \text{Li}_2\left(\frac{-u}{s_1}\right) - \frac{\pi^2}{4}\right]\end{aligned} \tag{5.58}$$

$$\begin{aligned}&\int_{\text{soft}} \frac{d\text{PS}_{k_4}}{k_2\cdot k_4\, P\cdot k_4} \\ &= -\frac{1}{8\pi^2 u_1} C_\epsilon \left[\frac{1}{\epsilon^2} - \frac{1}{\epsilon}\ln\left(\frac{u_1^2\delta_s^2}{4m_c^4}\right) + \ln^2\left(\frac{-u_1}{4m_c^2}\right) - \frac{1}{2}\ln^2\left(\frac{s}{4m_c^2}\right) + \frac{1}{2}\ln^2\left(\frac{s\delta_s^2}{m^2}\right)\right. \\ &\quad \left. + \ln\left(\frac{u_1^2}{4m_c^2 s}\right)\ln\left(\frac{s\delta_s^2}{m_c^2}\right) + 2\,\text{Li}_2\left(\frac{u}{4m_c^2}\right) - 2\,\text{Li}_2\left(\frac{-t}{u_1}\right) - \frac{\pi^2}{4}\right],\end{aligned} \tag{5.59}$$

which are expressed in terms of the Mandelstam variables (3.3) till (3.8).

5.1.4. Soft terms #1

Using (5.45) in combination with (5.35) and the property

$$\langle n, \text{Born}|\mathbf{T}_2\mathbf{T}_2|n, \text{Born}\rangle = \langle n, \text{Born}|\mathbf{T}_3\mathbf{T}_3|n, \text{Born}\rangle, \tag{5.60}$$

the integral of the polarization and color summed soft #1 terms over the soft region of phase space yields

$$\begin{aligned}
\int_{\text{soft}} d\text{PS}_{k_4} \sum_{\text{col,pol}} S_1(n) &= g_s^2 \sum_{\text{col,pol}} \langle n, \text{Born} \big| \mathbf{T}_2 \mathbf{T}_3 \big| n, \text{Born} \rangle \\
&\quad \times \int_{\text{soft}} d\text{PS}_{k_4} \left(-\frac{2k_2 \cdot k_3}{k_2 \cdot k_4\, k_3 \cdot k_4} + \frac{2P \cdot k_2}{k_2 \cdot k_4\, P \cdot k_4} + \frac{2P \cdot k_3}{k_3 \cdot k_4\, P \cdot k_4} - \frac{2P^2}{(P \cdot k_4)^2} \right) \\
&+ g_s^2 \sum_{\text{col,pol}} \langle n, \text{Born} \big| \mathbf{T}_2 \mathbf{T}_2 \big| n, \text{Born} \rangle \\
&\quad \times \int_{\text{soft}} d\text{PS}_{k_4} \left(\frac{2P \cdot k_2}{k_2 \cdot k_4\, P \cdot k_4} + \frac{2P \cdot k_3}{k_3 \cdot k_4\, P \cdot k_4} - \frac{2P^2}{(P \cdot k_4)^2} \right). \qquad (5.61)
\end{aligned}$$

A direct calculation using our automated programs shows that

$$\sum_{\text{col,pol}} \langle n, \text{Born} \big| \mathbf{T}_2 \mathbf{T}_3 \big| n, \text{Born} \rangle = C_1 \sum_{\text{col,pol}} |\mathcal{M}_{\text{Born}}(n)|^2 \qquad (5.62)$$

$$\sum_{\text{col,pol}} \langle n, \text{Born} \big| \mathbf{T}_2 \mathbf{T}_2 \big| n, \text{Born} \rangle = C_2 \sum_{\text{col,pol}} |\mathcal{M}_{\text{Born}}(n)|^2 \qquad (5.63)$$

with

$$C_1 \equiv \begin{cases} \frac{1}{2C_A} & \text{for processes } \gamma q \to c\bar{c}[\text{color octet}] + qg \\ -C_A & \text{for processes } \gamma g \to c\bar{c}[\text{color singlet}] + gg \\ -\frac{C_A}{2} & \text{for processes } \gamma g \to c\bar{c}[\text{color octet}] + gg \end{cases} \qquad (5.64)$$

$$C_2 \equiv \begin{cases} C_F & \text{for processes } \gamma q \to c\bar{c}[n] + qg \\ C_A & \text{for processes } \gamma g \to c\bar{c}[n] + gg \end{cases}. \qquad (5.65)$$

Plugging (5.56) till (5.59) into (5.61), then in turn plugging that result into (5.54) and comparing with (3.14), the contributions of the soft #1 terms to the differential cross section are finally evaluated to be

$$\begin{aligned}
&d\sigma_{\text{soft}\#1}(\gamma + g/q \to c\bar{c}[n] + g/q + g) \\
&= \frac{g_s^2}{8\pi^2} C_1 C_\epsilon d\sigma_{\text{Born}}(\gamma + g/q \to c\bar{c}[n] + g/q) \\
&\quad \times \left[\frac{1}{\epsilon} \left(2 - 2\ln\left(\frac{s_1 u_1}{4m_c^2 t} \right) \right) - \ln^2\left(\frac{-\delta_s^2 st}{s_1 m_c^2} \right) + \ln^2\left(\frac{-u_1}{4m_c^2} \right) - \frac{1}{2}\ln^2\left(\frac{s}{4m_c^2} \right) \right. \\
&\quad + \frac{1}{2}\ln^2\left(\frac{\delta_s^2 s}{m_c^2} \right) + \ln\left(\frac{u_1^2}{4m_c^2 s} \right) \ln\left(\frac{\delta_s^2 s}{m_c^2} \right) + \frac{1}{2}\ln^2\left(\frac{\delta_s^2 s^2}{4m_c^4} \right) + 2\frac{s + 4m_c^2}{s_1} \ln\left(\frac{s}{4m_c^2} \right) \\
&\quad \left. -2\ln\left(\frac{\delta_s^2 s}{m_c^2} \right) - 2\text{Li}_2\left(\frac{-u}{s_1} \right) + 2\text{Li}_2\left(\frac{u}{4m_c^2} \right) - 2\text{Li}_2\left(\frac{-t}{u_1} \right) + 2\text{Li}_2\left(\frac{-s_1}{4m_c^2} \right) \right] \\
&+ \frac{g_s^2}{8\pi^2} C_2 C_\epsilon d\sigma_{\text{Born}}(\gamma + g/q \to c\bar{c}[n] + g/q) \\
&\quad \times \left[\frac{2}{\epsilon^2} + \frac{1}{\epsilon} \left(2 - 2\ln\left(\frac{-u_1 s \delta_s^2}{4m_c^4} \right) \right) + \ln^2\left(\frac{-u_1}{4m_c^2} \right) - \frac{1}{2}\ln^2\left(\frac{s}{4m_c^2} \right) \right.
\end{aligned}$$

$$+\frac{1}{2}\ln^2\left(\frac{\delta_s^2 s}{m_c^2}\right)+\ln\left(\frac{u_1^2}{4m_c^2 s}\right)\ln\left(\frac{\delta_s^2 s}{m_c^2}\right)+\frac{1}{2}\ln^2\left(\frac{\delta_s^2 s^2}{4m_c^4}\right)+2\frac{s+4m_c^2}{s_1}\ln\left(\frac{s}{4m_c^2}\right)$$
$$-2\ln\left(\frac{\delta_s^2 s}{m_c^2}\right)+2\mathrm{Li}_2\left(\frac{u}{4m_c^2}\right)-2\mathrm{Li}_2\left(\frac{-t}{u_1}\right)+2\mathrm{Li}_2\left(\frac{-s_1}{4m_c^2}\right)-\frac{\pi^2}{2}\Bigg]. \tag{5.66}$$

We remark that in the case of the process $\gamma + g \to c\bar{c}[n] + g + g$ there is in fact also a contribution in the case when the gluon momentum k_3 is soft. For symmetry reasons this contribution is the same as the one when k_4 is soft, so actually there is an additional factor 2. However, there is also an additional factor $\frac{1}{2}$ because there are now two identical particles in the final state, so that the net effect is that no additional factor has to be considered. This argument will apply in the same way also to the soft #2 and the soft #3 terms.

5.1.5. Soft terms #2

As for the soft #2 terms, let us first evaluate the integrals of the fraction in (5.46) over the soft region, which becomes after using the polarization sum (5.35)

$$\begin{aligned}
&\int_{\text{soft}} d\mathrm{PS}_{k_4}\sum_{\text{col,pol}}\frac{k_i\cdot\epsilon(k_4)\,\epsilon^{*\beta}(k_4)}{k_i\cdot k_4\,P\cdot k_4}\\
&= \int_{\text{soft}} d\mathrm{PS}_{k_4}\left(-\frac{k_i^\beta}{k_i\cdot k_4\,P\cdot k_4}+\frac{P^\beta}{(P\cdot k_4)^2}+\frac{(P\cdot k_i)k_4^\beta}{(k_i\cdot k_4)(P\cdot k_4)^2}-\frac{P^2 k_4^\beta}{(P\cdot k_4)^3}\right)\\
&= \left(P^\beta-\frac{P^2}{P\cdot k_i}k_i^\beta\right)\int_{\text{soft}}\frac{d\mathrm{PS}_{k_4}}{(P\cdot k_4)^2},
\end{aligned} \tag{5.67}$$

where in the last transformation we have performed a simple tensor reduction. Using (5.56), the contribution of the soft #2 terms are then

$$\begin{aligned}
\frac{d\sigma_{\text{soft}\#2}(\gamma+g/q\to c\bar{c}[^3P_J^{[8]}]+g/q+g)}{dt} &= \frac{1}{2s}\,\frac{1}{8\pi s}\,\frac{1}{N_{\text{col,in}}N_{\text{pol,in}}}\\
&\times\frac{g_s^2}{8\pi^2 m_c^2}C_\epsilon\left[-\frac{1}{\epsilon}-\frac{s+4m_c^2}{s_1}\ln\left(\frac{s}{4m_c^2}\right)+\ln\left(\frac{\delta_s^2 s}{m_c^2}\right)\right]\mathcal{S}(^3P_J^{[8]}),
\end{aligned} \tag{5.68}$$

where the terms

$$\begin{aligned}
\mathcal{S}(^3P_J^{[8]}) &\equiv \sum_{i=2}^{3}\left(P^\beta-\frac{P^2}{P\cdot k_i}k_i^\beta\right)\\
&\times\sum_{\text{pol,col}}\mathcal{E}^{(J)}_{\alpha\beta}\langle{}^3P_J^{[8]},\mathrm{Born}|\mathbf{T}_i(\mathbf{T}_c-\mathbf{T}_{\bar{c}})\mathrm{Tr}\left[\mathcal{C}_8\Pi_1^\alpha|\mathrm{Born}\rangle\right]\Big|_{q=0}
\end{aligned} \tag{5.69}$$

cannot be simplified further in a general form. In particular, they do not factorize with a Born cross section. We evaluate the expressions (5.69) directly using our automated programs. The results are listed in appendix E.

5.1.6. Soft terms #3

As for the soft #3 terms, let us first evaluate the integrals of the fraction in (5.47) over the soft phase space, which becomes using the polarization sum (5.35)

$$\begin{aligned}
&\int_{\text{soft}} d\text{PS}_{k_4} \sum_{\text{col,pol}} \frac{\epsilon^{\beta'}(k_4)\epsilon^{*\beta}(k_4)\mathcal{E}^{(J)*}_{\alpha'\beta'}\mathcal{E}^{(J)}_{\alpha\beta}}{(P\cdot k_4)^2} \\
&= \int_{\text{soft}} d\text{PS}_{k_4} \left(-\frac{g^{\beta\beta'}}{(P\cdot k_4)^2} + \frac{P^\beta k_4^{\beta'} + P^{\beta'} k_4^\beta}{(P\cdot k_4)^3} - \frac{P^2 k_4^\beta k_4^{\beta'}}{(P\cdot k_4)^4}\right) \sum_{\text{col,pol}} \mathcal{E}^{(J)*}_{\alpha'\beta'}\mathcal{E}^{(J)}_{\alpha\beta} \\
&= \frac{D-2}{D-1}\left(-g^{\beta\beta'} + \frac{P^\beta P^{\beta'}}{P^2}\right) \int_{\text{soft}} \frac{d\text{PS}_{k_4}}{(P\cdot k_4)^2} \sum_{\text{col,pol}} \mathcal{E}^{(J)*}_{\alpha'\beta'}\mathcal{E}^{(J)}_{\alpha\beta} \\
&= \frac{D-2}{(D-1)^2} N_{\text{pol}}({}^3P_J^{[8]}) \left(-g_{\alpha\alpha'} + \frac{P_\alpha P_{\alpha'}}{P^2}\right) \int_{\text{soft}} \frac{d\text{PS}_{k_4}}{(P\cdot k_4)^2}. \qquad (5.70)
\end{aligned}$$

Here, in the second transformation we have performed a simple tensor reduction, and in the third step we have evaluated the polarization sum over the $\mathcal{E}$ tensors according to formulas (2.14) till (2.16), where the symbol $N_{\text{pol}}({}^3P_J^{[8]})$ is the number of polarization degrees of freedom in D dimensions, which is given by

$$N_{\text{pol}}({}^3P_J^{[8]}) = \sum_{\text{pol}} \mathcal{E}^{(J)*}_{\mu\nu}\mathcal{E}^{(J)\mu\nu} = \begin{cases} 1 & \text{if } J=0 \\ \frac{1}{2}(D-1)(D-2) & \text{if } J=1 \\ \frac{1}{2}(D+1)(D-2) & \text{if } J=2 \end{cases}. \qquad (5.71)$$

Using (5.70) and recalling (2.13) together with the definition of the projector onto the ${}^3S_1^{[8]}$ state (2.6), the phase space integral of the complete polarization and color summed soft #3 terms (5.47) over the soft region then is

$$\begin{aligned}
&\int_{\text{soft}} d\text{PS}_{k_4} \sum_{\text{col,pol}} S_3(n) = 4g_s^2 \frac{D-2}{(D-1)^2} N_{\text{pol}}({}^3P_J^{[8]}) \int_{\text{soft}} \frac{d\text{PS}_{k_4}}{(P\cdot k_4)^2} \\
&\quad \times \sum_{\text{col,pol}} \left\langle {}^3S_1^{[8]}, \text{Born} \middle| (\mathbf{T}_c - \mathbf{T}_{\overline{c}})(\mathbf{T}_c - \mathbf{T}_{\overline{c}}) \middle| {}^3S_1^{[8]}, \text{Born} \right\rangle \qquad (5.72)
\end{aligned}$$

Using our programs we could explicitly show that at least for the processes $\gamma + g/q \to c\overline{c} + g/q$ the relation

$$\begin{aligned}
&\sum_{\text{col,pol}} \left\langle {}^3S_1^{[8]}, \text{Born} \middle| (\mathbf{T}_c - \mathbf{T}_{\overline{c}})(\mathbf{T}_c - \mathbf{T}_{\overline{c}}) \middle| {}^3S_1^{[8]}, \text{Born} \right\rangle \\
&= \sum_{\text{col,pol}} \left(\frac{C_A^2 - 4}{C_A} \left|\mathcal{M}_{\text{Born}}({}^3S_1^{[8]})\right|^2 + 8C_A C_F \left|\mathcal{M}_{\text{Born}}({}^3S_1^{[1]})\right|^2 \right) \qquad (5.73)
\end{aligned}$$

is true. Therefore, using (5.56),

$$\begin{aligned}
&\int_{\text{soft}} d\text{PS}_{k_4} \sum_{\text{col,pol}} S_3(n) \\
&= \frac{g_s^2}{36\pi^2 m_c^2} N_{\text{pol}}({}^3P_J^{[8]}) C_\epsilon \left[-\frac{1}{\epsilon} - \frac{s+4m_c^2}{s_1} \ln\left(\frac{s}{4m_c^2}\right) + \ln\left(\frac{\delta_s^2 s}{m_c^2}\right) - \frac{1}{3} \right] \\
&\quad \times \sum_{\text{col,pol}} \left(\frac{C_A^2-4}{C_A} \left|\mathcal{M}_{\text{Born}}({}^3S_1^{[8]})\right|^2 + 8C_A C_F \left|\mathcal{M}_{\text{Born}}({}^3S_1^{[1]})\right|^2 \right),
\end{aligned} \tag{5.74}$$

so that finally

$$\begin{aligned}
&d\sigma_{\text{soft}\#3}(\gamma + g/q \to c\overline{c}[{}^3P_J^{[8]}] + g/q + g) \\
&= \frac{g_s^2}{36\pi^2 m_c^2} N_{\text{pol}}({}^3P_J^{[8]}) C_\epsilon \left[-\frac{1}{\epsilon} - \frac{s+4m_c^2}{s_1} \ln\left(\frac{s}{4m_c^2}\right) + \ln\left(\frac{\delta_s^2 s}{m_c^2}\right) - \frac{1}{3} \right] \\
&\quad \times \Bigg(\frac{C_A^2-4}{C_A} d\sigma_{\text{Born}}(\gamma + g/q \to c\overline{c}[{}^3S_1^{[8]}] + g/q) \\
&\quad + 8C_A C_F \, d\sigma_{\text{Born}}(\gamma + g/q \to c\overline{c}[{}^3S_1^{[1]}] + g/q) \Bigg).
\end{aligned} \tag{5.75}$$

This infrared divergence will be cancelled by the contributions due to the loop corrections of the operator matrix elements $\langle \mathcal{O}^{J/\psi}[{}^3S_1^{[8]}]\rangle$ and $\langle \mathcal{O}^{J/\psi}[{}^3S_1^{[1]}]\rangle$, given by (4.22) and (4.23). In the following we proof this cancellation and calculate the finite remainder. We do not consider the $\langle \mathcal{O}^{J/\psi}[{}^3P_J^{[1]}]\rangle$ term, because this operator matrix element scales with a power of v which is beyond the order we consider in our calculation, as can be seen in table 1.2. Plugging (4.22) into (2.2) yields

$$\begin{aligned}
&d\sigma_{\langle \mathcal{O}^{J/\psi}[{}^3S_1^{[8]}]\rangle\,\text{corr.}}(\gamma + g/q \to J/\psi + g/q) \\
&= \frac{g_s^2}{12\pi^2 m_c^2} \frac{C_A^2-4}{C_A} \left(\frac{4\pi\mu^2}{\mu_\Lambda^2} e^{-\gamma_E} \right)^\epsilon \frac{1}{\epsilon} \sum_{J=0}^{2} \frac{\langle \mathcal{O}^{J/\psi}[{}^3P_J^{[8]}]\rangle}{N_{\text{col}}({}^3S_1^{[8]}) N_{\text{pol}}({}^3S_1^{[8]})} \\
&\quad \times d\sigma_{\text{Born}}(\gamma + g/q \to c\overline{c}[{}^3S_1^{[8]}] + g/q) \\
&= \frac{g_s^2}{36\pi^2 m_c^2} \frac{C_A^2-4}{C_A} \frac{1}{2C_A C_F} C_\epsilon \left[\frac{1}{\epsilon} + \ln\left(\frac{m_c^2}{\mu_\Lambda^2}\right) + \frac{2}{3} \right] \sum_{J=0}^{2} \langle \mathcal{O}^{J/\psi}[{}^3P_J^{[8]}]\rangle \\
&\quad \times d\sigma_{\text{Born}}(\gamma + g/q \to c\overline{c}[{}^3S_1^{[8]}] + g/q),
\end{aligned} \tag{5.76}$$

where we have used that $N_{\text{pol}}({}^3S_1^{[8]}) = D-1$ in D dimensions. Similarly,

$$\begin{aligned}
&d\sigma_{\langle \mathcal{O}^{J/\psi}[{}^3S_1^{[1]}]\rangle\,\text{corr.}}(\gamma + g/q \to J/\psi + g/q) \\
&= \frac{4g_s^2}{36\pi^2 m_c^2} C_\epsilon \left[\frac{1}{\epsilon} + \ln\left(\frac{m_c^2}{\mu_\Lambda^2}\right) + \frac{2}{3} \right] \sum_{J=0}^{2} \langle \mathcal{O}^{J/\psi}[{}^3P_J^{[8]}]\rangle \\
&\quad \times d\sigma_{\text{Born}}(\gamma + g/q \to c\overline{c}[{}^3S_1^{[1]}] + g/q).
\end{aligned} \tag{5.77}$$

The sum of all contributions from soft #3 terms to the partonic J/ψ production cross section is given by

$$\begin{aligned} & d\sigma_{\text{all soft}\#3}(\gamma + g/q \to J/\psi + g/q + g) \\ &= \sum_{J=0}^{2} d\sigma_{\text{soft}\#3}(\gamma + g/q \to c\overline{c}[^3P_J^{[8]}] + g/q + g) \frac{\langle \mathcal{O}^{J/\psi}[^3P_J^{[8]}]\rangle}{N_{\text{col}}(^3P_J^{[8]})N_{\text{pol}}(^3P_J^{[8]})}. \end{aligned} \tag{5.78}$$

Using (5.75), the sum of (5.76), (5.77) and (5.78) is finally given by

$$\begin{aligned} & d\sigma_{\text{all soft}\#3}(\gamma + g/q \to J/\psi + g/q + g) + d\sigma_{\text{all ME corr.}}(\gamma + g/q \to J/\psi + g/q) \\ &= \frac{g_s^2}{36\pi^2 m_c^2}\left(-\frac{s+4m_c^2}{s_1}\ln\left(\frac{s}{4m_c^2}\right) + \ln\left(\frac{\delta_s^2 s}{\mu_\Lambda^2}\right) + \frac{1}{3}\right)\sum_{J=0}^{2}\langle \mathcal{O}^{J/\psi}[^3P_J^{[8]}]\rangle \\ &\quad \times\Bigg(\frac{C_A^2-4}{C_A}\frac{1}{2C_AC_F}d\sigma_{\text{Born}}(\gamma + g/q \to c\overline{c}[^3S_1^{[8]}] + g/q) \\ &\qquad +4\,d\sigma_{\text{Born}}(\gamma + g/q \to c\overline{c}[^3S_1^{[1]}] + g/q)\Bigg), \end{aligned} \tag{5.79}$$

which is indeed finite.

5.2. The hard collinear region

Diagrams, in which a massless line splits into two massless external lines give rise to collinear divergences in the phase space region in which the respective two external particles are collinear. In the following we will consider separately the three different cases of collinear divergences in our calculation: The divergences due to the splitting of the initial parton line, the ones due to the splitting of the initial photon line and the ones due to the splitting of the outgoing parton line. The considerations of this section follow the lines of [30].

5.2.1. Splitting of the initial QCD parton

Let us first consider the phase space region in which the incoming QCD parton (which we just call *parton 2*) is collinear to the outgoing QCD parton with momentum k_4 (which we just call *parton 4*). In this limit the divergent contributions stem from the diagrams with $2 \to 2' + 4$ splitting

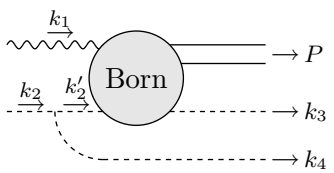

. (5.80)

We will have to distinguish clearly between the photon - parton 2 invariant mass

$$s_{12} \equiv (k_1 + k_2)^2 \tag{5.81}$$

and the photon - parton 2' invariant mass

$$s_{12'} \equiv (k_1 + k_2')^2 = x_b s_{12}, \tag{5.82}$$

where x_b is the splitting parameter, that is the fraction of the parton 2 momentum which is taken away by parton 2'. In the collinear limit $k_2 \parallel k_4$, we use the parameterization

$$\begin{aligned}
k_1 &= \left(\frac{\sqrt{s_{12}}}{2},\ 0,\ 0,\ -\frac{\sqrt{s_{12}}}{2}\right) && (5.83)\\
k_2 &= \left(\frac{\sqrt{s_{12}}}{2},\ 0,\ 0,\ \frac{\sqrt{s_{12}}}{2}\right) && (5.84)\\
k_2' &= \left(x_b\frac{\sqrt{s_{12}}}{2} + \frac{p_\perp^2}{x_b\sqrt{s_{12}}},\ 0,\ p_\perp,\ x_b\frac{\sqrt{s_{12}}}{2}\right) && (5.85)\\
k_4 &= \left((1-x_b)\frac{\sqrt{s_{12}}}{2} + \frac{p_\perp^2}{(1-x_b)\sqrt{s_{12}}},\ 0,\ -p_\perp,\ (1-x_b)\frac{\sqrt{s_{12}}}{2}\right) && (5.86)
\end{aligned}$$

for the external momenta. $p_\perp$ is a small transverse momentum which we allow the partons 2' and 4 to have despite their collinearity. At leading order in $p_\perp$,

$$\begin{aligned}
k_2' &= x_b k_2 && (5.87)\\
k_4 &= (1-x_b)k_2 && (5.88)\\
u' &= -2k_2\cdot k_4 = -\frac{p_\perp^2}{1-x_b}. && (5.89)
\end{aligned}$$

The phase space of parton 4 can in the collinear limit be written as

$$\begin{aligned}
d\mathrm{PS}_{k_4} &= \frac{\mu^{2\epsilon} d^{D-1}k_4}{2(2\pi)^{D-1}E_4}\\
&= \frac{(4\pi\mu^2)^\epsilon}{8\pi^2\Gamma(1-\epsilon)}\,\frac{2}{(1-x_b)\sqrt{s_{12}}}\,p_\perp^{1-2\epsilon}\,dp_\perp\,dk_{4,z}\\
&= \frac{(4\pi\mu^2)^\epsilon}{16\pi^2\Gamma(1-\epsilon)}\left(-(1-x_b)u'\right)^{-\epsilon}dx_b\,du'. && (5.90)
\end{aligned}$$

For the change of variables in the second transformation we have used (5.86) and (5.89), and we have kept only terms of the leading order in $p_\perp$.

At the same time, the matrix element of the process $\gamma + 2 \to c\bar{c}[n] + 3 + 4$ factorizes according to

$$\begin{aligned}
&\frac{1}{N_{\mathrm{col,in}}(k_1,k_2)N_{\mathrm{pol,in}}(k_1,k_2)}\sum_{\mathrm{col,pol}}\left|\mathcal{M}_{2\to 2'4}(\gamma+2\to c\bar{c}[n]+3+4)\right|^2\\
&= -\frac{2g_s^2}{x_b u'}\left(P_{2'2}(x_b)+\epsilon P_{2'2}'(x_b)\right)\frac{1}{N_{\mathrm{col,in}}(k_1,k_2')N_{\mathrm{pol,in}}(k_1,k_2')}\\
&\quad\times\sum_{\mathrm{col,pol}}\left|\mathcal{M}_{\mathrm{Born}}(\gamma+2'(x_b)\to c\bar{c}[n]+3)\right|^2, && (5.91)
\end{aligned}$$

where the squared matrix element of the Born process $\gamma + 2' \to c\overline{c}[n] + 3$ depends on x_b. The functions $P_{2'2}(x_b)$ and $P'_{2'2}(x_b)$ are the D dimensional versions of the Altarelli-Parisi splitting functions [32]

$$
\begin{aligned}
P_{qq}(z) &= C_F \frac{1+z^2}{1-z} && (5.92)\\
P'_{qq}(z) &= -C_F(1-z) && (5.93)\\
P_{gq}(z) &= C_F \frac{1+(1-z)^2}{z} && (5.94)\\
P'_{gq}(z) &= -C_F z && (5.95)\\
P_{gg}(z) &= 2C_A \left(\frac{z}{1-z} + \frac{1-z}{z} + z(1-z) \right) && (5.96)\\
P'_{gg}(z) &= 0 && (5.97)\\
P_{qg}(z) &= \frac{1}{2}\left(z^2 + (1-z)^2\right) && (5.98)\\
P'_{qg}(z) &= -z(1-z), && (5.99)
\end{aligned}
$$

where g stands for a gluon and q for a quark.

Now let us express the partonic hard collinear cross section

$$
\begin{aligned}
d\sigma_{2\to 2'4,\mathrm{hard}}(\gamma + 2 \to c\overline{c}[n] + 3 + 4) &= \frac{1}{2s_{12}} d\mathrm{PS}_{2\to 2} \int_{\text{hard coll.}} d\mathrm{PS}_{k_4} \\
&\times \frac{1}{N_{\mathrm{col,in}}(k_1,k_2) N_{\mathrm{pol,in}}(k_1,k_2)} \sum_{\mathrm{col,pol}} \left| \mathcal{M}_{2\to 2'4}(\gamma + 2 \to c\overline{c}[n] + 3 + 4) \right|^2 \quad (5.100)
\end{aligned}
$$

in terms of

$$
\begin{aligned}
d\sigma_{\mathrm{Born}}(\gamma + 2'(x_b) \to c\overline{c}[n] + 3) &= \frac{1}{2s_{12'}} d\mathrm{PS}_{2\to 2} \frac{1}{N_{\mathrm{col,in}}(k_1,k'_2) N_{\mathrm{pol,in}}(k_1,k'_2)} \\
&\times \sum_{\mathrm{col,pol}} \left| \mathcal{M}_{\mathrm{Born}}(\gamma + 2'(x_b) \to c\overline{c}[n] + 3) \right|^2. \quad (5.101)
\end{aligned}
$$

Plugging (5.90) and (5.91) into (5.100) and comparing with (5.101) results in

$$
\begin{aligned}
& d\sigma_{2\to 2'4,\mathrm{hard}}(\gamma + 2 \to c\overline{c}[n] + 3 + 4) \\
&= \left(1 - \frac{\delta_{3,4}}{2}\right) \frac{g_s^2}{8\pi^2} \frac{(4\pi\mu^2)^\epsilon}{\Gamma(1-\epsilon)} \int_{-\delta_c s_{12}}^{0} (-u')^{-1-\epsilon} du' \int_{x_{b,\min}}^{1-\delta_s \delta_{4,\mathrm{Gluon}}} dx_b \, (1-x_b)^{-\epsilon} \\
&\quad \times \left(P_{2'2}(x_b) + \epsilon P'_{2'2}(x_b) \right) d\sigma_{\mathrm{Born}}(\gamma + 2'(x_b) \to c\overline{c}[n] + 3) \\
&= \left(1 - \frac{\delta_{3,4}}{2}\right) \frac{g_s^2}{8\pi^2} \left(\frac{4\pi\mu^2}{\delta_c s_{12}}\right)^\epsilon \frac{1}{\Gamma(1-\epsilon)} \left(-\frac{1}{\epsilon}\right) \int_{x_{b,\min}}^{1-\delta_s \delta_{4,\mathrm{Gluon}}} dx_b \, (1-x_b)^{-\epsilon} \\
&\quad \times \left(P_{2'2}(x_b) + \epsilon P'_{2'2}(x_b) \right) d\sigma_{\mathrm{Born}}(\gamma + 2'(x_b) \to c\overline{c}[n] + 3). \quad (5.102)
\end{aligned}
$$

The factor $(1 - \frac{\delta_{3,4}}{2})$ takes care about the additional factor $\frac{1}{2}$ in the case of two external gluons in the final state. The upper limit of the x_b integration is 1 if parton 4 is a quark

and $1-\delta_s$ if it is a gluon. The reason is that we have to exclude the soft region in the hard collinear integration. Thereby the prescription $x_b < 1-\delta_s$ follows directly from (5.17) when we make use of the relation $s_5 = s_{12'} - 4m_c^2$, which is true in the collinear limit $k_2 \parallel k_4$. The lower limits $x_{b,\min}$ will be determined later in chapter 6.1 in the context of the hadronic cross section.

The collinear divergence in (5.102) is universal, which means process independent, and is absorbed into the bare proton parton distribution function $f_{2'/p}(x)$ used in the Born process $\gamma + 2' \to c\overline{c}[n] + 3$: We define the scale dependent parton distribution function

$$\begin{aligned} f_{2'/p}(x,\mu_f) &\equiv f_{2'/p}(x) - \sum_{\text{parton } 2} \frac{g_s^2}{8\pi^2}\left(-\frac{1}{\epsilon}\right)\left(\frac{4\pi\mu^2}{\mu_f^2}\right)^{\epsilon}\frac{1}{\Gamma(1-\epsilon)} \\ &\quad \times \int_{x_{b,\min}}^{1} \frac{dx_b}{x_b} P_{2'2}(x_b) f_{2/p}\left(\frac{x}{x_b}\right) \end{aligned} \tag{5.103}$$

following the $\overline{\text{MS}}$ convention, where μ_f is the factorization scale and x the fraction of the proton momentum which the parton $2'$ takes away, so that $\frac{x}{x_b}$ is the fraction of the proton momentum which parton 2 takes away. The additional second term is called the mass factorization counterterm. Summing its contribution and (5.102) eventually yields

$$\begin{aligned} & d\sigma_{2\to 2'4,\text{hard}}(\gamma + 2 \to c\overline{c}[n] + 3 + 4) + d\sigma_{\text{mass fact. CT}}(\gamma + 2' \to c\overline{c}[n] + 3) \\ &= \left(1 - \frac{\delta_{3,4}}{2}\right)\frac{g_s^2}{8\pi^2}\int_{x_{b,\min}}^{1-\delta_s\delta_{4,\text{Gluon}}} dx_b \left(P_{2'2}(x_b)\ln\left(\frac{\delta_c s_{12'}(1-x_b)}{x_b\mu_f^2}\right) - P'_{2'2}(x_b)\right) \\ &\quad \times d\sigma_{\text{Born}}(\gamma + 2'(x_b) \to c\overline{c}[n] + 3) \\ &\quad + \left(1 - \frac{\delta_{3,4}}{2}\right)\frac{g_s^2}{8\pi^2} C_\epsilon \left[\frac{1}{\epsilon} - \ln\left(\frac{\mu_f^2}{m_c^2}\right)\right] \int_{1-\delta_s\delta_{4,\text{Gluon}}}^{1} dx_b P_{2'2}(x_b) \\ &\quad \times d\sigma_{\text{Born}}(\gamma + 2'(x_b) \to c\overline{c}[n] + 3). \end{aligned} \tag{5.104}$$

The integral of the first term is evaluated numerically. The infrared divergent second term appears due to the fact that in (5.103) the complete collinear divergence is subtracted, including the terms arising from the soft collinear region, which are not part of our hard collinear terms. If parton 4 is a quark, then these terms are zero. If it is a gluon, then we can directly calculate them after replacing the Altarelli-Parisi splitting functions $P_{2'2}$ by their plus-regularized versions [32]

$$P_{qq}^{+}(z) = C_F\left(\frac{1+z^2}{(1-z)_+} + \frac{3}{2}\delta(1-z)\right) \tag{5.105}$$

$$P_{gg}^{+}(z) = 2C_A\left(\frac{z}{(1-z)_+} + \frac{1-z}{z} + z(1-z)\right) + \left(\frac{11}{6}C_A - \frac{1}{3}n_{\text{lf}}\right)\delta(1-z), \tag{5.106}$$

so that the integrals converge and yield

$$\begin{aligned}
&\int_{1-\delta_s}^{1} P_{qq}^{+}(x_b) d\sigma_{\text{Born}}(\gamma + 2'(x_b) \to c\bar{c}[n] + 3) \\
&= C_F \left(2\ln(\delta_s) + \frac{3}{2} - 2\delta_s + \mathcal{O}(\delta_s^2) \right) d\sigma_{\text{Born}}(\gamma + 2'(x_b = 1) \to c\bar{c}[n] + 3) \quad (5.107)
\end{aligned}$$

and

$$\begin{aligned}
&\int_{1-\delta_s}^{1} P_{gg}^{+}(x_b) d\sigma_{\text{Born}}(\gamma + 2'(x_b) \to c\bar{c}[n] + 3) \\
&= \left(2C_A \ln(\delta_s) + \frac{11}{6} C_A - \frac{1}{3} n_{\text{lf}} - 2C_A \delta_s + \mathcal{O}(\delta_s^2) \right) \\
&\quad \times d\sigma_{\text{Born}}(\gamma + 2'(x_b = 1) \to c\bar{c}[n] + 3). \quad (5.108)
\end{aligned}$$

5.2.2. Splitting of the initial photon

The collinear divergences of the phase space region in which k_1 is collinear to k_4 stem from the diagrams

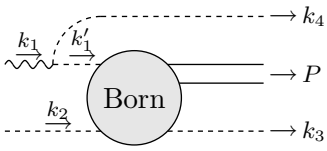

, (5.109)

in which the incoming photon splits into a quark 1' and the outgoing quark 4. The kinematical situation is very similar to the case of the initial parton's splitting. Therefore here we will be less detailed in the derivation of the respective expressions. We define x_a to be the fraction of the photon momentum which is taken away by quark 1', so that

$$k_1' = x_a k_1 \quad (5.110)$$

$$k_4 = (1 - x_a) k_1 \quad (5.111)$$

and

$$s_{12} \equiv (k_1 + k_2)^2 \quad (5.112)$$

$$s_{1'2} \equiv (k_1' + k_2)^2 = x_a s_{12}. \quad (5.113)$$

The phase space of quark 4 is given by

$$d\text{PS}_{k_4} = \frac{(4\pi\mu^2)^\epsilon}{16\pi^2 \Gamma(1-\epsilon)} \left(-(1 - x_a) t' \right)^{-\epsilon} dx_a \, dt' \quad (5.114)$$

and the squared matrix element factorizes in the limit $k_1 \parallel k_4$ according to

$$\begin{aligned}
&\frac{1}{N_{\text{col,in}}(k_1,k_2)N_{\text{pol,in}}(k_1,k_2)} \sum_{\text{col,pol}} \left|\mathcal{M}_{1\to 1'4}(\gamma+2\to c\bar{c}[n]+3+4)\right|^2 \\
&= -\frac{2e^2Q_q^2}{x_a t'}\left(P_{q\gamma}(x_a)+\epsilon P'_{q\gamma}(x_a)\right)\frac{1}{N_{\text{col,in}}(k_1',k_2)N_{\text{pol,in}}(k_1',k_2)} \\
&\quad \times \sum_{\text{col,pol}} \left|\mathcal{M}_{\text{Born}}(1'(x_a)+2\to c\bar{c}[n]+3)\right|^2, \qquad (5.115)
\end{aligned}$$

where Q_q is the electric charge of the quark q in units of the elementary charge e and

$$P_{q\gamma}(x_a) = C_A\left(x_a^2+(1-x_a)^2\right) \qquad (5.116)$$

$$P'_{q\gamma}(x_a) = -2C_A x_a(1-x_a). \qquad (5.117)$$

The hard collinear partonic cross section is then given by

$$\begin{aligned}
d\sigma_{1\to 1'4,\text{hard}}(\gamma+2\to c\bar{c}[n]+3+4) &= \frac{e^2Q_q^2}{8\pi^2}\left(\frac{4\pi\mu^2}{\delta_c s_{12}}\right)^{\epsilon}\frac{1}{\Gamma(1-\epsilon)}\left(-\frac{1}{\epsilon}\right) \\
&\times \int_{x_{a,\min}}^1 dx_a\,(1-x_a)^{-\epsilon}\left(P_{q\gamma}(x_a)+\epsilon P'_{q\gamma}(x_a)\right) d\sigma_{\text{Born}}(1'(x_a)+2\to c\bar{c}[n]+3). \qquad (5.118)
\end{aligned}$$

This collinear divergence is actually only canceled when we include NLO corrections to the resolved photoproduction process

$$d\sigma_{\text{resolved}}(\gamma+2\to c\bar{c}[n]+3) = \sum_{\text{parton } 1'} d\sigma_{\text{Born}}(1'(x_a)+2\to c\bar{c}[n]+3) f_{1'/\gamma}(x_a)dx_a \qquad (5.119)$$

in our calculation, because then this collinear singularity can be absorbed into the parton distribution function $f_{1'/\gamma}(x_a)$ of the photon. We make use of this absorption, although we do actually not yet compute the resolved photoproduction case, and redefine

$$f_{1'/\gamma}(x_a,\mu_f) \equiv f_{1'/\gamma}(x_a) - \frac{e^2Q_q^2}{8\pi^2}\left(\frac{4\pi\mu^2}{\mu_f^2}\right)^{\epsilon}\frac{1}{\Gamma(1-\epsilon)}\left(-\frac{1}{\epsilon}\right)P_{1'\gamma}(x_a). \qquad (5.120)$$

The second term is again called the mass factorization counterterm. The sum of its contribution and (5.118),

$$\begin{aligned}
&d\sigma_{1\to 1'4,\text{hard}}(\gamma+2\to c\bar{c}[n]+3+4) + d\sigma_{\text{resolved,mass fact. CT}}(\gamma+2\to c\bar{c}[n]+3) \\
&= \frac{e^2Q_q^2}{8\pi^2}\int_{x_{a,\min}}^1 dx_a\left(P_{q\gamma}(x_a)\ln\left(\frac{\delta_c s_{1'2}(1-x_a)}{x_a\mu_f^2}\right) - P'_{q\gamma}(x_a)\right) \\
&\quad \times d\sigma_{\text{Born}}(1'(x_a)+2\to c\bar{c}[n]+3), \qquad (5.121)
\end{aligned}$$

is finite. The lower limit $x_{a,\min}$ will be determined in chapter 6.1 in the context of the hadronic cross section. The integral will be performed numerically. We do not have to take special care about the soft collinear limit, because parton 4 is a quark.

5.2.3. Splitting of the final state QCD parton

The collinear divergences of the phase space region in which k_3 is collinear to k_4 stem from the diagrams

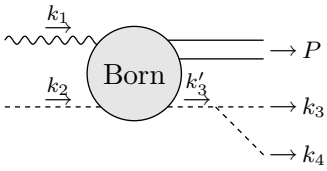

, (5.122)

in which the parton 3' splits into the two outgoing partons 3 and 4, whose momenta we parameterize as

$$k_3 = \left(zP + \frac{p_\perp^2}{2zP},\, 0,\, p_\perp,\, zP\right) \tag{5.123}$$

$$k_4 = \left((1-z)P + \frac{p_\perp^2}{2(1-z)P},\, 0,\, -p_\perp,\, (1-z)P\right) \tag{5.124}$$

so that

$$s_3 = 2k_3 \cdot k_4 = \frac{p_\perp^2}{z(1-z)} \tag{5.125}$$

at leading order in $p_\perp$. The phase space factorizes according to

$$\begin{aligned} d\mathrm{PS}_{2\to 3} &= \frac{\mu^{2\epsilon} d^{D-1}P}{2(2\pi)^{D-1}E_{J/\psi}} \frac{\mu^{2\epsilon} d^{D-1}k_3}{2(2\pi)^{D-1}E_3} \frac{\mu^{2\epsilon} d^{D-1}k_4}{2(2\pi)^{D-1}E_4} \\ &\quad \times (2\pi)^D \delta^{(D)}(k_1 + k_2 - P - k_3 - k_4) \\ &= d\mathrm{PS}^*_{2\to 2} \times d\mathrm{PS}^*_{k_4} \end{aligned} \tag{5.126}$$

with

$$d\mathrm{PS}^*_{2\to 2} \equiv \frac{\mu^{2\epsilon} d^{D-1}P}{2(2\pi)^{D-1}E_{J/\psi}} \frac{\mu^{2\epsilon} d^{D-1}k_{3'}}{2(2\pi)^{D-1}k_{3',0}} (2\pi)^D \delta^{(D)}(k_1 + k_2 - P - k_{3'}) \tag{5.127}$$

$$d\mathrm{PS}^*_{k_4} \equiv \frac{\mu^{2\epsilon} d^{D-1}k_4}{2(2\pi)^{D-1}E_4} \frac{k_{3',0}}{E_3}. \tag{5.128}$$

Here, we have just done a change of variables from k_3 to $k_{3'} = k_3 + k_4$ and regrouped the terms. In the collinear limit $k_3 \parallel k_4$, we further evaluate $d\mathrm{PS}^*_{k_4}$ to be

$$d\mathrm{PS}^*_{k_4} = \frac{(4\pi\mu^2)^\epsilon}{16\pi^2\Gamma(1-\epsilon)} \left(z(1-z)s_3\right)^{-\epsilon} dz\, ds_3, \tag{5.129}$$

where we have made use of (5.124) and (5.125). The squared matrix element factorizes according to

$$\begin{aligned} \sum_{\mathrm{col,pol}} \left|\mathcal{M}_{3'\to 34}(\gamma + 2 \to c\bar{c}[n] + 3 + 4)\right|^2 &= \frac{2g_s^2}{s_3}\left(P_{33'}(z) + \epsilon P'_{33'}(z)\right) \\ \times \sum_{\mathrm{col,pol}} \left|\mathcal{M}_{\mathrm{Born}}(\gamma + 2 \to c\bar{c}[n] + 3')\right|^2, \end{aligned} \tag{5.130}$$

so that

$$
\begin{aligned}
d\sigma_{3'\to 34,\mathrm{hard}}(\gamma+2\to c\overline{c}[n]+3+4) &= \left(1-\frac{\delta_{3,4}}{2}\right) d\sigma_{\mathrm{Born}}(\gamma+2\to c\overline{c}[n]+3') \\
&\quad\times\frac{g_s^2}{8\pi^2}\frac{(4\pi\mu^2)^\epsilon}{\Gamma(1-\epsilon)}\int_0^{\delta_c s} ds_3 s_3^{-1-\epsilon}\int_{z_{\min}}^{z_{\max}} dz\,(z(1-z))^{-\epsilon}\left(P_{33'}(z)+\epsilon P'_{33'}(z)\right) \\
&= \left(1-\frac{\delta_{3,4}}{2}\right) d\sigma_{\mathrm{Born}}(\gamma+2\to c\overline{c}[n]+3')\frac{g_s^2}{8\pi^2}\left(\frac{4\pi\mu^2}{\delta_c s}\right)^\epsilon\frac{1}{\Gamma(1-\epsilon)}\left(-\frac{1}{\epsilon}\right) \\
&\quad\times\int_{z_{\min}}^{z_{\max}} dz\,(z(1-z))^{-\epsilon}\left(P_{33'}(z)+\epsilon P'_{33'}(z)\right). \qquad (5.131)
\end{aligned}
$$

The factor $(1-\frac{\delta_{3,4}}{2})$ takes care about the additional factor $\frac{1}{2}$ in the case of two external gluons in the final state. The upper and lower limits of the z integration depend on whether the partons 3 and 4 are gluons or quarks, because, again, we have to exclude the soft region in the hard collinear integration. Making use of (5.17) we see that

$$
z_{\min} = \begin{cases} 0 & \text{if 3 is a quark} \\ \frac{\delta_s s}{s_1} & \text{if 3 is a gluon} \end{cases} \qquad (5.132)
$$

$$
z_{\max} = \begin{cases} 1 & \text{if 4 is a quark} \\ 1-\frac{\delta_s s}{s_1} & \text{if 4 is a gluon} \end{cases}. \qquad (5.133)
$$

Integrating (5.131) analytically results in

$$
\begin{aligned}
d\sigma_{3'\to 34,\mathrm{hard}}(\gamma+q\to c\overline{c}[n]+q+g) &= d\sigma_{\mathrm{Born}}(\gamma+q\to c\overline{c}[n]+q) \\
&\quad\times\frac{g_s^2 C_F}{8\pi^2}C_\epsilon\left[\frac{1}{\epsilon}\left(2\ln\left(\frac{\delta_s s}{s_1}\right)+\frac{3}{2}\right)-\left(2\ln\left(\frac{\delta_s s}{s_1}\right)+\frac{3}{2}\right)\ln\left(\frac{\delta_c s}{m_c^2}\right)-\ln^2\left(\frac{\delta_s s}{s_1}\right)\right. \\
&\qquad\left.+\frac{7}{2}-\frac{\pi^2}{3}+\mathcal{O}\left(\frac{\delta_s s}{s_1}\right)\right] \qquad (5.134)
\end{aligned}
$$

for $q\to q+g$ splitting,

$$
\begin{aligned}
d\sigma_{3'\to 34,\mathrm{hard}}(\gamma+g\to c\overline{c}[n]+g+g) &= d\sigma_{\mathrm{Born}}(\gamma+g\to c\overline{c}[n]+g) \\
&\quad\times\frac{g_s^2 C_A}{8\pi^2}C_\epsilon\left[\frac{1}{\epsilon}\left(2\ln\left(\frac{\delta_s s}{s_1}\right)+\frac{11}{6}\right)-\left(2\ln\left(\frac{\delta_s s}{s_1}\right)+\frac{11}{6}\right)\ln\left(\frac{\delta_c s}{m_c^2}\right)\right. \\
&\qquad\left.-\ln^2\left(\frac{\delta_s s}{s_1}\right)+\frac{67}{18}-\frac{\pi^2}{3}+\mathcal{O}\left(\frac{\delta_s s}{s_1}\right)\right] \qquad (5.135)
\end{aligned}
$$

for $g\to g+g$ splitting and

$$
\begin{aligned}
d\sigma_{3'\to 34}(\gamma+g\to c\overline{c}[n]+q+\overline{q}) &= d\sigma_{\mathrm{Born}}(\gamma+g\to c\overline{c}[n]+g) \\
&\quad\times\frac{g_s^2}{24\pi^2}C_\epsilon\left[-\frac{1}{\epsilon}+\ln\left(\frac{\delta_c s}{m_c^2}\right)-\frac{5}{3}+\mathcal{O}\left(\frac{\delta_s s}{s_1}\right)\right] \qquad (5.136)
\end{aligned}
$$

for $g\to q+\overline{q}$ splitting.

5.2.4. Summary of all hard collinear terms

To summarize this section, the hard collinear cross sections of our real correction processes (5.1), (5.2) and (5.3) plus their respective mass factorization counterterms are given by

$$d\sigma_{\text{hard coll.}}(\gamma + q \to c\bar{c}[n] + q + g) \;+\; \text{mass fact. CTs}$$

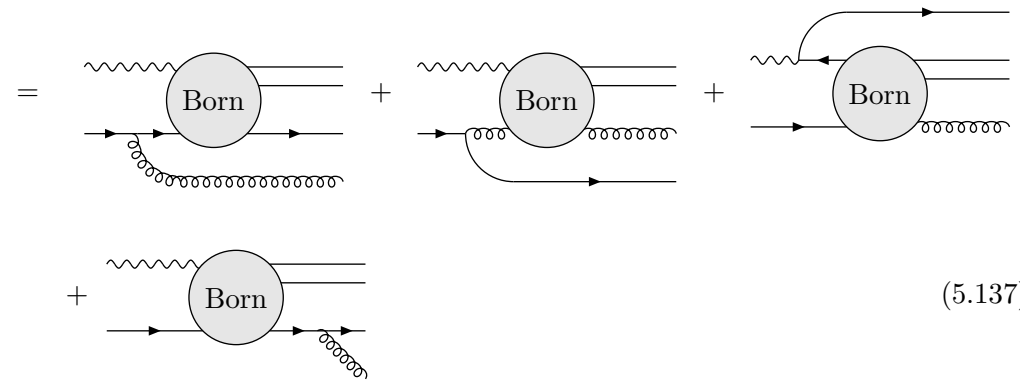

(5.137)

$$d\sigma_{\text{hard coll.}}(\gamma + g \to c\bar{c}[n] + g + g) \;+\; \text{mass fact. CTs}$$

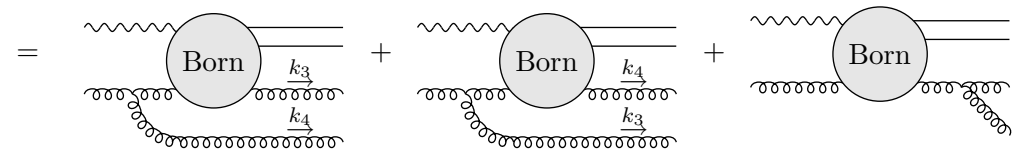

(5.138)

$$d\sigma_{\text{hard coll.}}(\gamma + g \to c\bar{c}[n] + q + \bar{q}) \;+\; \text{mass fact. CTs}$$

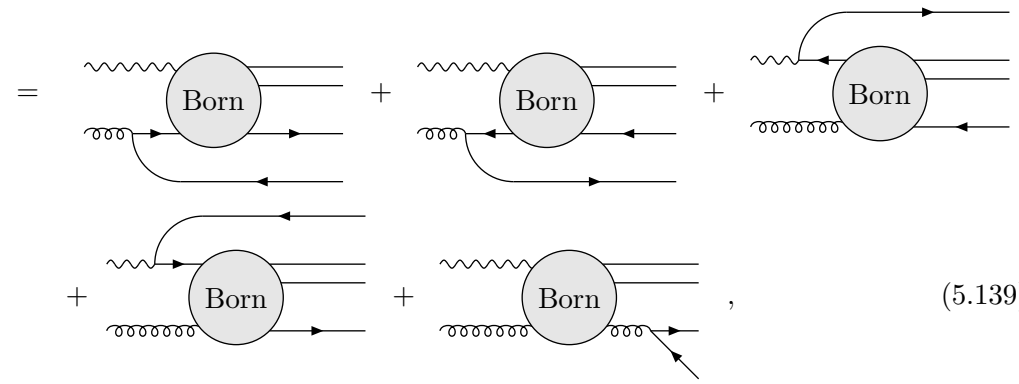

(5.139)

where each diagram stands for one of the respective expressions (5.104), (5.121) or (5.134). The formulas (5.104) and (5.121), which were actually derived for the collinear limits $k_4 \parallel k_1$ and $k_4 \parallel k_2$, also describe the limits $k_3 \parallel k_1$ and $k_3 \parallel k_2$.

5.3. The hard non-collinear region

The integration of the real corrections over the hard non-collinear region does not lead to divergences. Therefore we can perform the phase space integration in four dimensions. As described in [33], we insert the identity

$$1 = ds_3 d^4k_{3'}\delta(k_{3'}^2 - s_3)\delta^{(4)}(k_3' - k_3 - k_4) \tag{5.140}$$

into the three particle phase space

$$d\mathrm{PS}_{2\to 3} = \frac{d^3P}{2(2\pi)^3 E_{J/\psi}}\frac{d^3k_3}{2(2\pi)^3 E_3}\frac{d^3k_4}{2(2\pi)^3 E_4}(2\pi)^4\delta^{(4)}(k_1 + k_2 - P - k_3 - k_4), \tag{5.141}$$

so that it factorizes according to

$$d\mathrm{PS}_{2\to 3} = \frac{1}{(2\pi)^5}ds_3 \times d\mathrm{PS}^{**}_{2\to 2} \times d\mathrm{PS}'_{1\to 2} \tag{5.142}$$

where

$$d\mathrm{PS}^{**}_{2\to 2} \equiv \frac{d^3P}{2E_{J/\psi}}d^4k_{3'}\theta(k_{3',0})\delta(k_{3'}^2 - s_3)\delta^{(4)}(k_1 + k_2 - P - k_{3'}) \tag{5.143}$$

$$d\mathrm{PS}'_{1\to 2} \equiv \frac{d^3k_3}{2E_3}d^4k_4\theta(k_{4,0})\delta(k_4^2)\delta^{(4)}(k_{3'} - k_3 - k_4). \tag{5.144}$$

We calculate $d\mathrm{PS}^{**}_{2\to 2}$ in the center of mass system of the incoming particles, and like in the 2 to 2 kinematics case we use the parameterization

$$k_1 = \left(\frac{\sqrt{s}}{2},\, 0,\, 0,\, \frac{\sqrt{s}}{2}\right) \tag{5.145}$$

$$k_2 = \left(\frac{\sqrt{s}}{2},\, 0,\, 0,\, -\frac{\sqrt{s}}{2}\right) \tag{5.146}$$

$$P = \left(E_{J/\psi},\, 0,\, p_{J/\psi}\sin\theta,\, p_{J/\psi}\cos\theta\right) \tag{5.147}$$

where

$$E_{J/\psi} = \frac{t + u - 8m_c^2}{-2\sqrt{s}}, \qquad p_{J/\psi} = \sqrt{E_{J/\psi}^2 - 4m_c^2}, \qquad \cos\theta = \frac{t - u}{2\sqrt{s}\,p_{J/\psi}}. \tag{5.148}$$

After integration over the first delta function we arrive at

$$\begin{aligned} d\mathrm{PS}^{**}_{2\to 2} &= \frac{1}{2E_{J/\psi}}p_{J/\psi}^2 dp_{J/\psi}d(\cos\theta)2d\varphi\,\delta(s + t + u - 4m_c^2 - s_3) \\ &= \frac{1}{2s}dt\,du\,d\varphi\,\delta(s + t + u - 4m_c^2 - s_3), \end{aligned} \tag{5.149}$$

where we have made a change of variables from $(p_{J/\psi}, \cos\theta)$ to (t, u). As the squared matrix element cannot depend on φ, the azimuthal angel of the J/ψ, we integrate over it (from 0 till π) and integrate over the delta function as well, so that

$$d\mathrm{PS}^{**}_{2\to 2} = \frac{\pi}{2s}dt. \tag{5.150}$$

As for $d\mathrm{PS}'_{1\to 2}$, we calculate it in the rest frame of the particles 3 and 4, in which we use the parameterization

$$
\begin{aligned}
k_1 &= E'_1\left(1,\,0,\,\sin\theta'_1,\,\cos\theta'_1\right) && (5.151)\\
k_2 &= \left(E'_2,\,0,\,-E'_1\sin\theta'_1,\,p'_{J/\psi}-E'_1\cos\theta'_1\right) && (5.152)\\
P &= \left(E'_{J/\psi},\,0,\,0,\,p'_{J/\psi}\right) && (5.153)\\
k_3 &= \frac{\sqrt{s_3}}{2}\left(1,\,\sin\theta'\sin\varphi',\,\sin\theta'\cos\varphi',\,\cos\theta'\right) && (5.154)\\
k_4 &= \frac{\sqrt{s_3}}{2}\left(1,\,-\sin\theta'\sin\varphi',\,-\sin\theta'\cos\varphi',\,-\cos\theta'\right) && (5.155)
\end{aligned}
$$

for the respective momenta, where

$$
\begin{aligned}
&E'_1=\frac{s+t_1}{2\sqrt{s_3}},\qquad E'_2=\frac{s_3-t}{2\sqrt{s_3}},\qquad E'_{J/\psi}=\frac{s-s_3-4m_c^2}{2\sqrt{s_3}},\\
&p'_{J/\psi}=\sqrt{E'^2_{J/\psi}-4m_c^2},\qquad \cos\theta'_1=\frac{1}{p'_{J/\psi}}\left(E'_{J/\psi}+\frac{t_1}{2E'_1}\right),\\
&\cos\theta'=\frac{1}{p'_{J/\psi}}\left(\frac{s_4}{\sqrt{s_3}}-E'_{J/\psi}\right),\qquad \cos\varphi'=\frac{1+\frac{u_6}{\sqrt{s_3}E'_1}-\cos\theta'_1\cos\theta'}{\sin\theta'_1\sin\theta'}. \qquad (5.156)
\end{aligned}
$$

Integrating over the first delta function in (5.144) leads to

$$
\begin{aligned}
d\mathrm{PS}'_{1\to 2} &= \frac{k_{3,0}}{2}dk_{3,0}d(\cos\theta')2d\varphi'\delta(s_3-2\sqrt{s_3}k_{3,0})\\
&= \frac{1}{4}d(\cos\theta')d\varphi'. && (5.157)
\end{aligned}
$$

Plugging (5.150) and (5.157) into (5.142) and using (2.3) we arrive at

$$
\begin{aligned}
\frac{d\sigma(\gamma+i\to c\bar{c}[n]+j+k)}{dt} &= \frac{1}{2s}\,\frac{1}{256\pi^4 s}ds_3d(\cos\theta')d\varphi'\\
&\times\left(1-\frac{\delta_{3,4}}{2}\right)\frac{1}{N_{\mathrm{col,in}}N_{\mathrm{pol,in}}}\sum_{\mathrm{col,pol}}|\mathcal{M}(\gamma+i\to c\bar{c}[n]+j+k)|^2. \qquad (5.158)
\end{aligned}
$$

The factor $(1-\frac{\delta_{3,4}}{2})$ is added for the case of the process $\gamma+g\to c\bar{c}[n]+g+g$, in which there are two identical particles in the final state.

To summarize, in comparison to the 2 to 2 kinematics case, there are three additional integrations: Over s_3, $\cos\theta'$ and over φ'. For given s and t their integration ranges are given by

$$
0<s_3<t+\frac{st}{t_1},\qquad -1<\cos\theta'<1,\qquad 0<\varphi'<\pi. \qquad (5.159)
$$

For our actual calculation, however, we will use another expression for the upper limit of s_3 which we will derive in chapter 6.1 in the context of the hadronic cross section.

For the squared matrix elements, we do not make any approximation, but evaluate the Feynman diagrams drawn in figures 5.2, 5.3 and 5.4 directly using our automated programs. Thereby we will need the expressions of all Mandelstam invariants (5.4) till (5.13) in terms of the integration variables. The corresponding relations are easily derived from the formulas (5.151) till (5.156). In the evaluation of the process $\gamma + g \to c\overline{c}[n] + g + g$ we again apply the full polarization sum

$$\sum_{\text{pol}^*} \epsilon_\mu \epsilon_\nu^* = -g_{\mu\nu}, \tag{5.160}$$

but subtract all gluon ghost contributions according to

$$\begin{aligned} &\sum_{\text{col,pol}} |\mathcal{M}(\gamma + g \to c\overline{c}[n] + g + g)|^2 \\ &= \sum_{\text{col,pol}^*} \Big[|\mathcal{M}(\gamma + g \to c\overline{c}[n] + g + g)|^2 - 2|\mathcal{M}(\gamma + u_g \to c\overline{c}[n] + u_g + g)|^2 \\ &\quad -2|\mathcal{M}(\gamma + u_g \to c\overline{c}[n] + g + u_g)|^2 - 2|\mathcal{M}(\gamma + g \to c\overline{c}[n] + u_g + \overline{u}_g)|^2 \Big]. \end{aligned} \tag{5.161}$$

It is the integration over the hard non-collinear part which is the most time consuming part of the numerical integration.

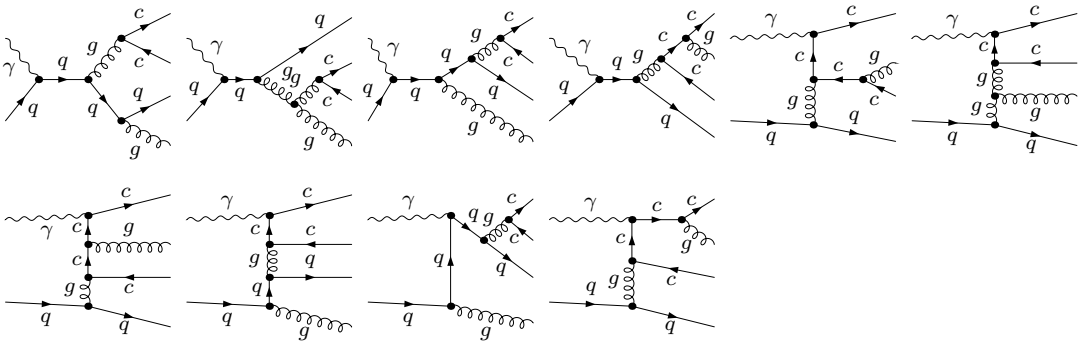

Figure 5.2.: Tree level diagrams of the process $\gamma + q \to c\overline{c} + q + g$. 14 diagrams have not been drawn. They differ from the drawn ones only by an exchange of the external c and $\overline{c}$ lines or the external q and $\overline{q}$ lines. The diagrams of the process $\gamma + g \to c\overline{c} + q + \overline{q}$ can be inferred just by crossing the external particles accordingly.

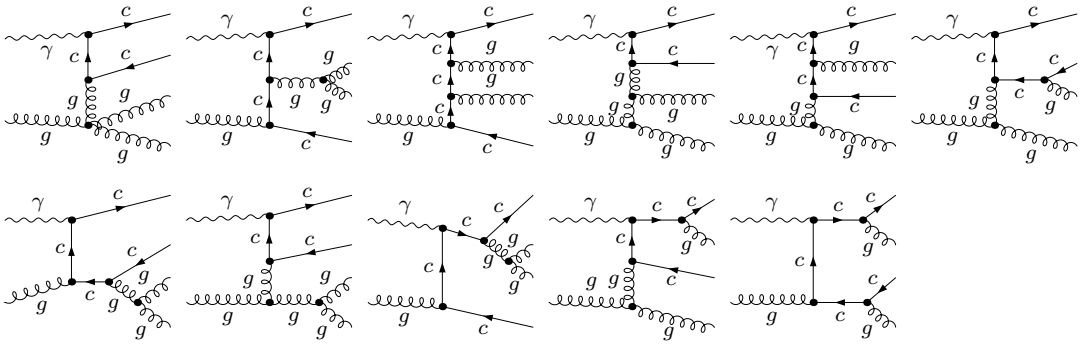

Figure 5.3.: Tree level diagrams of the process $\gamma + g \to c\overline{c} + g + g$. 39 diagrams have not been drawn. They differ from the drawn ones only by an exchange of the external c and $\overline{c}$ lines or the external gluon lines.

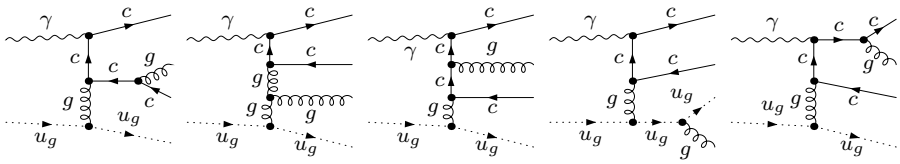

Figure 5.4.: Tree level diagrams of the process $\gamma + u_g \to c\overline{c} + u_g + g$. u_g stands for gluon ghost. 7 diagrams have not been drawn. They differ from the drawn ones only by an exchange of the external c and $\overline{c}$ lines or the external gluon ghost lines. The diagrams of the other processes with gluon ghosts needed for the real corrections can be inferred by crossing of the external particles.

6. Numerical evaluation and results

The numerical phase space integrations are implemented in FORTRAN. The underlying integration routine used is VEGAS [34]. Due to the large size of the hard non-collinear part of the real corrections, especially to the partonic processes $\gamma + g \to c\overline{c}[^3P_J^{[8]}] + g + g$, the calculation was quite extensive. About 200 processes were running for three weeks. In section 6.1 we derive the expressions for the actual quantities we are going to calculate along with the integration limits. In section 6.2, we specify the parameters used in our calculation before presenting our final results in section 6.3.

6.1. The hadronic cross sections

Up to this point we have dealt primarily with the partonic cross sections and learned how to calculate the different contributions to $d\sigma(i + j \to J/\psi + X)/dt$. We already know that the hadronic cross section is calculated according to (2.1), but in this section we want to examine in detail how to relate $d\sigma(i+j \to J/\psi+X)/dt$ to the experimentally accessible quantities.

We investigate the general kinematical situation depicted in figure 6.1. In the center of mass frame of the incoming electron (with momentum k_e) and proton (with momentum k_p), a bremsstrahlung photon with momentum $k_1 = x_\gamma k_e$ is radiated off the electron. This photon then emits a parton 1' with momentum $k_1' = x_a k_1$. On the other hand, the parton 2 with momentum $k_2 = x_B k_p$ stemming from the proton, itself emits another parton 2' with momentum $k_2' = x_b k_2$. The partons 1' and 2' then take part in the actual partonic reaction and produce, among other particles, the J/ψ with momentum P. In

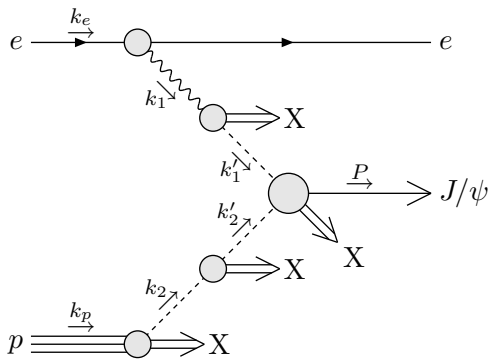

Figure 6.1.: Overview of the kinematics of the hadronic cross section

particular, we use the parameterization

$$k_e = \frac{\sqrt{S_H}}{2}(1,\,0,\,0,\,1) \tag{6.1}$$

$$k_1 = x_\gamma \frac{\sqrt{S_H}}{2}(1,\,0,\,0,\,1) \tag{6.2}$$

$$k_1' = x_\gamma x_a \frac{\sqrt{S_H}}{2}(1,\,0,\,0,\,1) \tag{6.3}$$

$$k_p = \frac{\sqrt{S_H}}{2}(1,\,0,\,0,\,-1) \tag{6.4}$$

$$k_2 = x_B \frac{\sqrt{S_H}}{2}(1,\,0,\,0,\,-1) \tag{6.5}$$

$$k_2' = x_B x_b \frac{\sqrt{S_H}}{2}(1,\,0,\,0,\,-1) \tag{6.6}$$

$$P = (m_T \cosh\eta,\, p_T \cos\phi,\, p_T \sin\phi,\, m_T \sinh\eta) \tag{6.7}$$

for the momenta, where

$$m_T \equiv \sqrt{p_T^2 + 4m_c^2}, \tag{6.8}$$

and we call S_H the hadronic center of mass energy, p_T the transverse momentum of the J/ψ and η its rapidity.

The Mandelstam variables of the partonic process are then given by

$$s = (k_1' + k_2')^2 = x_\gamma x_a x_B x_b S_H \tag{6.9}$$

$$t = (P - k_1')^2 = 4m_c^2 - x_\gamma x_a \sqrt{S_H} m_T e^{-\eta} \tag{6.10}$$

$$u = (P - k_2')^2 = 4m_c^2 - x_B x_b \sqrt{S_H} m_T e^{\eta}, \tag{6.11}$$

so that

$$x_\gamma x_a = \frac{x_B x_b \sqrt{S_H} m_T e^{\eta} - 4m_c^2 + s_3}{x_B x_b S_H - m_T \sqrt{S_H} e^{-\eta}} \tag{6.12}$$

$$x_B x_b = \frac{x_\gamma x_a \sqrt{S_H} m_T e^{-\eta} - 4m_c^2 + s_3}{x_\gamma x_a S_H - m_T \sqrt{S_H} e^{\eta}}. \tag{6.13}$$

This is the general form, which is valid for the real corrections with 2 to 3 kinematics. To get the corresponding expressions in the case with just two external particles, simply set $s_3 = 0$ in (6.12) and (6.13).

The general form of the hadronic cross section is given by

$$\frac{d\sigma(e+p \to J/\psi + X)}{dx_\gamma dx_a dx_B dx_b dt} = \sum_{\text{parton } i} \sum_{\text{parton } j} \sum_{\text{parton } k} f_{\gamma/e}(x_\gamma) f_{i/\gamma}(x_a) f_{j/p}(x_B) f_{k/j}(x_b) \times \frac{d\sigma(i+k \to J/\psi + X)}{dt} \tag{6.14}$$

The symbol $f_{j/p}(x_B)$ is the parton distribution function which gives the probability to find the parton j inside the proton with a momentum fraction x_B. We use the

scale dependent proton PDFs, which additionally depend on the factorization scale μ_f. The function $f_{\gamma/e}(x_a)$ is the distribution of bremsstrahlung photons radiated off the incoming electron in the equivalent photon approximation. We use the Weizsäcker-Williams formula [16]

$$f_{\gamma/e}(x_\gamma) = \frac{e^2}{8\pi^2}\left(\frac{1+(1-x_\gamma)^2}{x_\gamma}\ln\left(\frac{Q^2_{\max}}{Q^2_{\min}}\right) + 2m_e^2 x_\gamma\left(\frac{1}{Q^2_{\max}} - \frac{1}{Q^2_{\min}}\right)\right) \tag{6.15}$$

with

$$Q^2_{\min} \equiv \frac{m_e^2 x_\gamma^2}{1-x_\gamma}. \tag{6.16}$$

$Q_{\max}$ is the maximum virtuality we allow the photon to have in the photoproduction limit and m_e the electron mass. In direct photoproduction, which we consider in this project,

$$f_{i/\gamma}(x_a) = \delta(1-x_a) \qquad \text{and} \qquad f_{k/j}(x_b) = \delta(1-x_b). \tag{6.17}$$

However, as described in section 5.2, in the calculation of the initial state collinear singularities, we have to consider $k_1 \to k_1'$ and $k_2 \to k_2'$ splitting: The expression (5.121) is equal to $d\sigma_{\text{Born}}(1'+2 \to c\overline{c}[n]+3)$ evaluated with

$$f_{i/\gamma}(x_a) = \frac{e^2 Q_i^2}{8\pi^2}\left(P_{i\gamma}(x_a)\ln\left(\frac{\delta_c s(1-x_a)}{x_a\mu_f^2}\right) - P'_{i\gamma}(x_a)\right) \tag{6.18}$$

$$f_{k/j}(x_b) = \delta(1-x_b). \tag{6.19}$$

And the first term in (5.104) is equal to $d\sigma_{\text{Born}}(\gamma+2' \to c\overline{c}[n]+3)$ evaluated with

$$f_{i/\gamma}(x_a) = \delta(1-x_a) \tag{6.20}$$

$$f_{k/j}(x_b) = \frac{g_s^2}{8\pi^2}\left(P_{kj}(x_b)\ln\left(\frac{\delta_c s(1-x_b)}{x_b\mu_f^2}\right) - P'_{kj}(x_b)\right) \times\left(1-\frac{\delta_{3,4}}{2}\right)\theta(1-\delta_s\delta_{4,\text{Gluon}}-x_b). \tag{6.21}$$

In photoproduction cross sections, the two additional quantities

$$W \equiv \sqrt{(k_1+k_p)^2} = \sqrt{x_\gamma S_H} \tag{6.22}$$

$$z \equiv \frac{P\cdot k_p}{k_1\cdot k_p} = \frac{m_T e^\eta}{x_\gamma\sqrt{S_H}} \tag{6.23}$$

are defined. W is the photon-proton invariant mass. In the proton rest frame, z is the fraction of the photon energy which is transferred to the J/ψ. After a change of variables from (x_γ, x_B, t) to (W, z, p_T^2) in (6.14), the hadronic cross section reads

$$\frac{d\sigma(e+p\to J/\psi+X)}{dW\,dz\,dp_T^2\,dx_a\,dx_b} = \sum_{i,j,k} f_{\gamma/e}(x_\gamma)f_{i/\gamma}(x_a)f_{j/p}(x_B)f_{k/j}(x_b) \times\frac{2x_B W(t-4m_c^2)}{zS_H(t+p_T^2)}\,\frac{d\sigma(i+k\to J/\psi+X)}{dt}. \tag{6.24}$$

Our final goal is to calculate the differential cross sections

$$\frac{d\sigma}{dp_T^2} = \int_{z_{\min}}^{z_{\max}} dz \int_{W_{\min}}^{\sqrt{S_H}} dW \int_{x_{a,\min}}^{1} dx_a \int_{x_{b,\min}}^{1} dx_b \, \frac{d\sigma}{dW\,dz\,dp_T^2 dx_a dx_b} \tag{6.25}$$

$$\frac{d\sigma}{dz} = \int_{0}^{p_{t,\max}^2} dp_T^2 \int_{W_{\min}}^{\sqrt{S_H}} dW \int_{x_{a,\min}}^{1} dx_a \int_{x_{b,\min}}^{1} dx_b \, \frac{d\sigma}{dW\,dz\,dp_T^2 dx_a dx_b} \tag{6.26}$$

$$\frac{d\sigma}{dW} = \int_{0}^{p_{t,\max}^{2'}} dp_T^2 \int_{z'_{\min}}^{z'_{\max}} dz \int_{x_{a,\min}}^{1} dx_a \int_{x_{b,\min}}^{1} dx_b \, \frac{d\sigma}{dW\,dz\,dp_T^2 dx_a dx_b} \tag{6.27}$$

$$\frac{d\sigma}{dW\,dz\,dp_T^2} = \int_{x_{a,\min}}^{1} dx_a \int_{x_{b,\min}}^{1} dx_b \, \frac{d\sigma}{dW\,dz\,dp_T^2 dx_a dx_b}, \tag{6.28}$$

where

$$x_{b,\min} = \frac{x_\gamma x_a \sqrt{S_H} m_T e^{-\eta} - 4m_c^2}{x_\gamma x_a S_H - m_T \sqrt{S_H} e^{\eta}} \tag{6.29}$$

$$x_{a,\min} = \frac{\sqrt{S_H} m_T e^{\eta} - 4m_c^2}{x_\gamma \left(S_H - m_T \sqrt{S_H} e^{-\eta}\right)} \tag{6.30}$$

$$W_{\min} = \sqrt{\frac{p_T^2}{z(1-z)} + \frac{4m_c^2}{z}} \tag{6.31}$$

$$z_{\min} = \frac{1}{2S_H}\left(S_H + 4m_c^2 - \sqrt{(S_H - 4m_c^2)^2 - 4S_H p_T^2}\right) \tag{6.32}$$

$$z_{\max} = \frac{1}{2S_H}\left(S_H + 4m_c^2 + \sqrt{(S_H - 4m_c^2)^2 - 4S_H p_T^2}\right) \tag{6.33}$$

$$p_{t,\max}^2 = (1-z)\left(zS_H - 4m_c^2\right) \tag{6.34}$$

$$z'_{\min} = \frac{1}{2W^2}\left(W^2 + 4m_c^2 - \sqrt{(W^2 - 4m_c^2)^2 - 4W^2 p_T^2}\right) \tag{6.35}$$

$$z'_{\max} = \frac{1}{2W^2}\left(W^2 + 4m_c^2 + \sqrt{(W^2 - 4m_c^2)^2 - 4W^2 p_T^2}\right) \tag{6.36}$$

$$p_{t,\max}^{2'} = \frac{\left(W^2 - 4m_c^2\right)^2}{4W^2}. \tag{6.37}$$

All of these integrations are performed numerically. In the calculation of the hard non-collinear region of the real corrections further three integrations over s_3, $\cos\theta'$ and φ' have to be performed, see (5.158). Thereby the integration range of s_3 is

$$0 < s_3 < x_b W^2 \left(x_a - z\right) - \frac{x_a m_T^2}{z} + 4m_c^2. \tag{6.38}$$

Please note that all the integration limits given describe only the kinematically accessible parameter space. In the actual integrations we will apply additional cuts on W, p_T and z, in order to compare our results with the corresponding experimentally measured quantities.

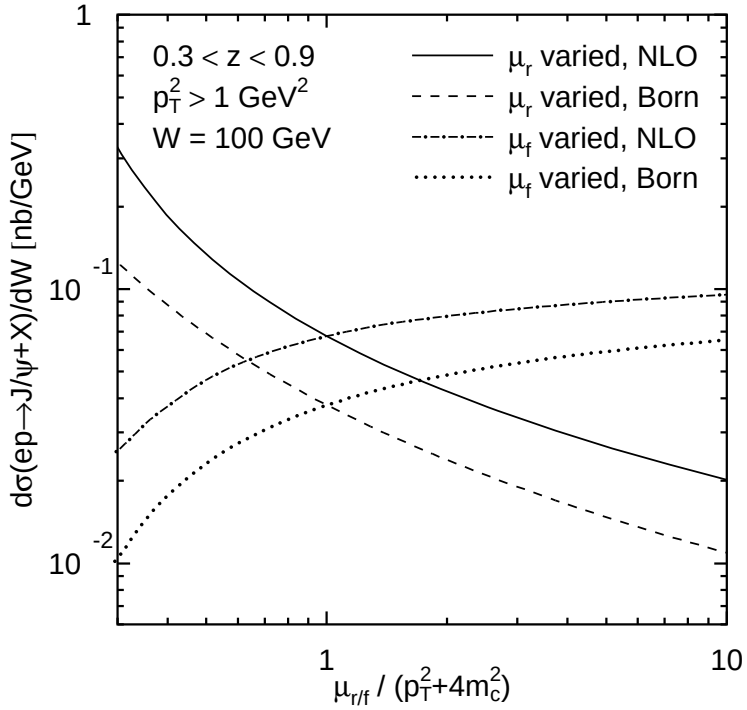

Figure 6.2.: Renormalization scale μ_r and factorization scale μ_f dependence of $d\sigma(ep \to J/\psi + X)/dW$ at $W = 100$ GeV.

6.2. Parameters used in our analysis

At HERA, electrons with an energy of 27.6 GeV are colliding with protons with an energy of 920 GeV. We use the same kinematical ranges like the H1 group used in their analyses [35, 36], with which we will compare our results: We take Q^2_{max} to be 2 GeV^2 and apply the integration cuts

$$60 \text{ GeV} < W < 240 \text{ GeV} \tag{6.39}$$

$$0.3 < z < 0.9 \tag{6.40}$$

$$1 \text{ GeV}^2 < p_T^2 \quad . \tag{6.41}$$

At lower values of z the cross sections should be dominated by resolved photoproduction and in the range $z \approx 1$ diffractive processes are expected to dominate. But in the given region of z it is sensible to compare our direct photoproduction results with the data.

For the running strong coupling constant $\alpha_s(\mu_r^2)$ we employ the one-loop (two-loop) formula for the Born (NLO) cross sections with $n_{\text{lf}} = 3$ active flavors. For the parton distribution functions we use QTEC6L1 (QTEC6M) [37] for the Born (NLO) cross sections, and we use their $\Lambda^{(4)}_{\text{QCD}} = 215$ MeV (326 MeV), so that $\Lambda^{(3)}_{\text{QCD}} = 249$ MeV (388.5 MeV). As renormalization and factorization scales we use $\mu_r^2 = \mu_f^2 = p_T^2 + 4m_c^2$ and for the NRQCD scale $\mu_\Lambda = m_c$. We have investigated the dependence of our cross sections

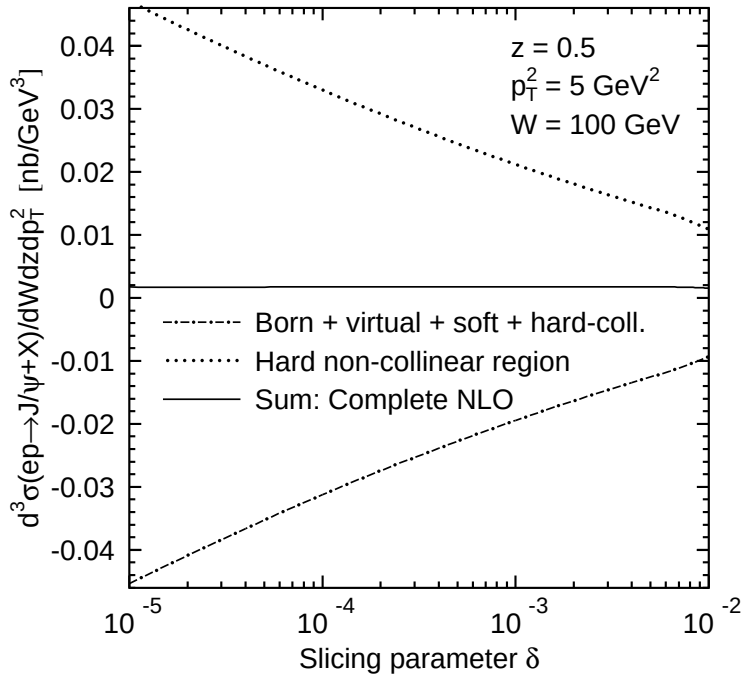

Figure 6.3.: Numerical verification of the phase space slicing mechanism at one typical point in (W, p_T, z) space. We set $\delta_s = \delta$ and $\delta_c = \delta/100$.

on the renormalization and factorization scales by varying them around their default values. The corresponding graphs for $d\sigma(ep \to J/\psi + X)/dW$ are drawn in figure 6.2.

Furthermore we use the values

$$\alpha = \frac{e^2}{4\pi} = \frac{1}{137.036} \tag{6.42}$$

$$m_e = 0.51100 \text{ keV} \tag{6.43}$$

$$m_c \equiv \frac{M_{J/\psi}}{2} = \frac{3.0969 \text{ GeV}}{2} \tag{6.44}$$

from the particle data group [1].

Our cross sections are independent of the unphysical slicing parameters. We have checked this independence numerically by a variation of the slicing parameters over a large range of small values, as is shown in figure 6.3. For our actual analysis we use the values $\delta_s = 10^{-3}$ and $\delta_c = 10^{-5}$.

As for the color singlet long distance matrix element, we calculate it as usual from the J/ψ decay width into an electron positron pair Γ_{ee}:

$$\langle \mathcal{O}^{J/\psi}(^3S_1^{[1]})\rangle = \frac{81 m_c^2}{8\pi\alpha^2} \frac{\Gamma_{ee}}{1 - \frac{16\alpha_s(4m_c^2)}{3\pi}}, \tag{6.45}$$

where we set the NLO correction term $\frac{16\alpha_s(4m_c^2)}{3\pi}$ in (6.45) to zero when calculating Born

cross sections. We use $\Gamma_{ee} = 5.55$ keV [1], so that

$$\langle \mathcal{O}^{J/\psi}(^3S_1^{[1]})\rangle = 0.81 \text{ GeV}^3 \tag{6.46}$$

in the Born case and

$$\langle \mathcal{O}^{J/\psi}(^3S_1^{[1]})\rangle = 1.38 \text{ GeV}^3 \tag{6.47}$$

in the NLO case.

6.2.1. The values of the color octet long distance matrix elements

The great uncertainty of the whole analysis lies in the values of the color octet long distance matrix elements (MEs). They are usually extracted by fitting predictions for J/ψ hadroproduction to Tevatron data. In the process of this fitting, not all color octet matrix elements are considered as independent fit parameters. First, due to the spin symmetry of the $c\overline{c}$ system, we have

$$\langle \mathcal{O}^{J/\psi}(^3P_J^{[8]})\rangle = J\langle \mathcal{O}^{J/\psi}(^3P_0^{[8]})\rangle. \tag{6.48}$$

Second, the contributions of intermediate $^1S_0^{[8]}$ and $^3P_J^{[8]}$ states to the p_T distribution of the hadroproduction are highly correlated, as they have a very similar slope, see figure 1.1. Therefore it has become common to define the linear combination

$$M_r^{J/\psi} \equiv \langle \mathcal{O}^{J/\psi}(^1S_0^{[8]})\rangle + \frac{r}{m_c^2}\langle \mathcal{O}^{J/\psi}(^3P_0^{[8]})\rangle \tag{6.49}$$

and use the three quantities $\langle \mathcal{O}^{J/\psi}(^3S_1^{[8]})\rangle$, $M_r^{J/\psi}$ and r as fit parameters. Of course, considering just (6.49), the values of $\langle \mathcal{O}^{J/\psi}(^1S_0^{[8]})\rangle$ and $\langle \mathcal{O}^{J/\psi}(^3P_0^{[8]})\rangle$ are not unambiguously determined. We will assume the democratic split

$$\langle \mathcal{O}^{J/\psi}(^1S_0^{[8]})\rangle = \frac{M_r^{J/\psi}}{2} \tag{6.50}$$

$$\langle \mathcal{O}^{J/\psi}(^3P_0^{[8]})\rangle = \frac{M_r^{J/\psi} m_c^2}{2r}. \tag{6.51}$$

For a consistent NLO analysis, we would have to use color octet long distance matrix elements obtained by fitting an NLO prediction for hadroproduction to Tevatron data. Unfortunately, currently only leading order fits are on the market, as a complete NLO calculation is so far not available. However, we expect the NLO corrections to be rather large and positive, as can already be inferred from the NLO calculation of the color singlet model prediction [8]. An increase of both color singlet and color octet short distance coefficients would significantly decrease the values of the color octet MEs.

We decide to use the values obtained in [38] form fitting to CDF data [39]. That analysis has two advantages: First, besides doing a thorough leading order fit, they present values for so called "higher order improved" MEs, which are obtained by using

the results of the Monte Carlo simulation analysis [40] for multi gluon radiation in color octet hadroproduction processes. The second advantage is that the values they use for the color singlet long distance matrix elements in their leading and higher order fits are consistent with our values (6.46) and (6.47). Of course, there are fits to more recent Tevatron data available, but we note that the theoretical uncertainties of the short distance cross sections are much larger than the experimental precision gained since the analysis [38], as can be seen in the results of the recent fit published in [41] to Tevatron Run II data [42].

To be concrete, we use the values

$$\langle \mathcal{O}^{J/\psi}(^3S_1^{[8]})\rangle = 3.94 \cdot 10^{-3}\ \mathrm{GeV}^3 \tag{6.52}$$

$$M_{3.7}^{J/\psi} = 6.52 \cdot 10^{-2}\ \mathrm{GeV}^3 \tag{6.53}$$

$$r = 3.47 \tag{6.54}$$

of [38] for our color octet contributions. We indicate the expected decrease of the color octet MEs in a thorough NLO fit by shaded bands, where we use the values of their "higher order improved" long distance matrix elements, namely

$$\langle \mathcal{O}^{J/\psi}(^3S_1^{[8]})\rangle = 2.73 \cdot 10^{-3}\ \mathrm{GeV}^3 \tag{6.55}$$

$$M_{3.54}^{J/\psi} = 5.72 \cdot 10^{-3}\ \mathrm{GeV}^3 \tag{6.56}$$

$$r = 3.54, \tag{6.57}$$

for the lower end of that band.

6.3. Final results and conclusions

The figures 6.4 till 6.6 show our results for the differential cross sections $d\sigma(ep \to J/\psi + X)/dp_T^2$, $d\sigma(ep \to J/\psi + X)/dW$ and $d\sigma(ep \to J/\psi + X)/dz$ for direct photoproduction. The lower graphs show the contributions of the various intermediate states to the respective NLO cross sections. $^3P_{0/1/2}^{[8]}$ means the sum of all P wave contributions. We do not give results for the three P wave states separately, as the ratios of their long distance matrix elements are fixed by $c\bar{c}$ spin symmetry anyway. In the upper graphs we have plotted the Born and the NLO predictions for the intermediate color singlet state alone and for the sum of intermediate color singlet and color octet states. The shaded bands indicate the expected decrease of the color octet MEs in an NLO fit to Tevatron data as explained in section 6.2.1. We compare our predictions to H1 data, namely to the published results of the HERA I run [35] and to the preliminary analysis of a part of the HERA II data [36].

The first conclusion we can draw from our analysis is that the color singlet contribution alone is not sufficient to explain the photoproduction data. The data points are about a factor 4 larger than the prediction, which is an indication for the significance of color octet states. This seems to be in contrast to Krämer's NLO color singlet model analysis [11, 6], which suggests good agreement with data. But this disagreement is due to a

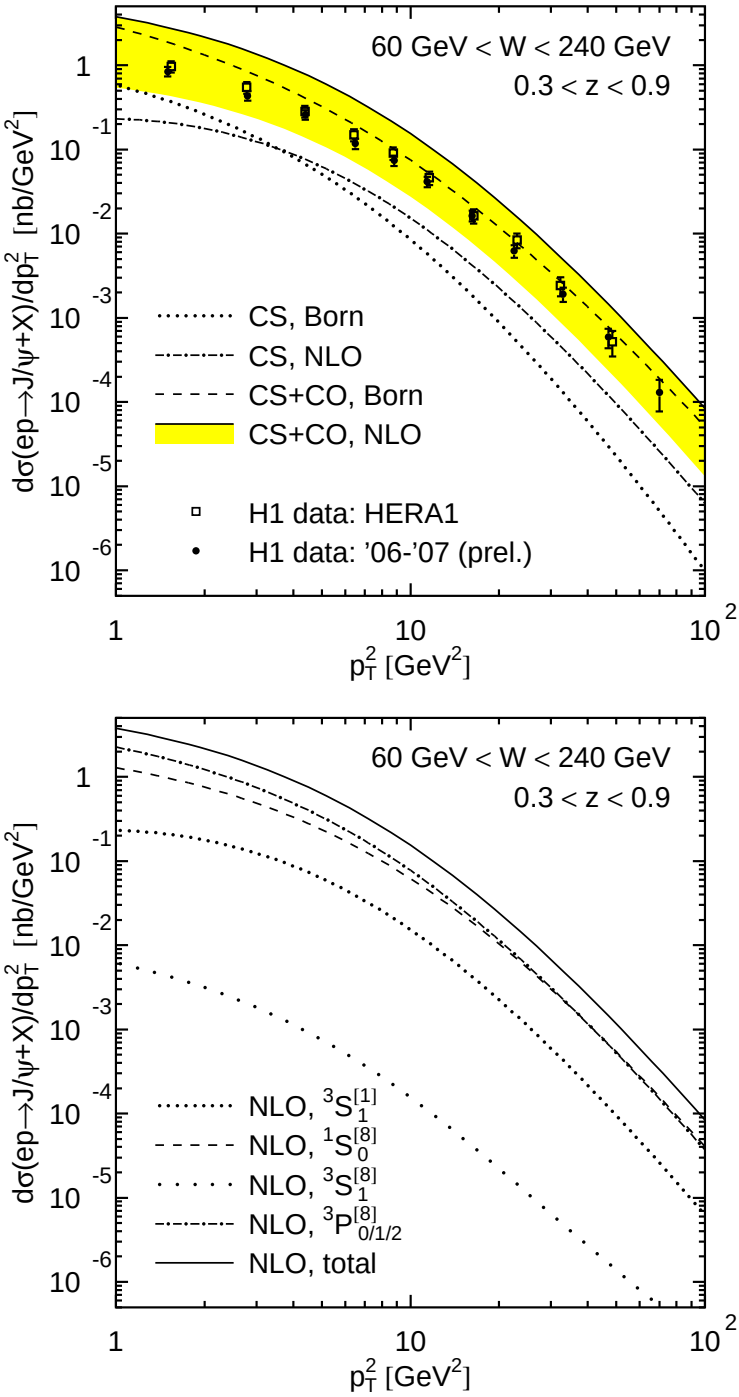

Figure 6.4.: The differential cross section $d\sigma(ep \to J/\psi + X)/dp_T^2$ of direct J/ψ photoproduction at HERA. Upper graph: Born and NLO predictions compared to H1 data, for the color singlet contributions only and for the sum of color singlet and color octet contributions. Lower graph: The contributions of the different intermediate states to the NLO prediction.

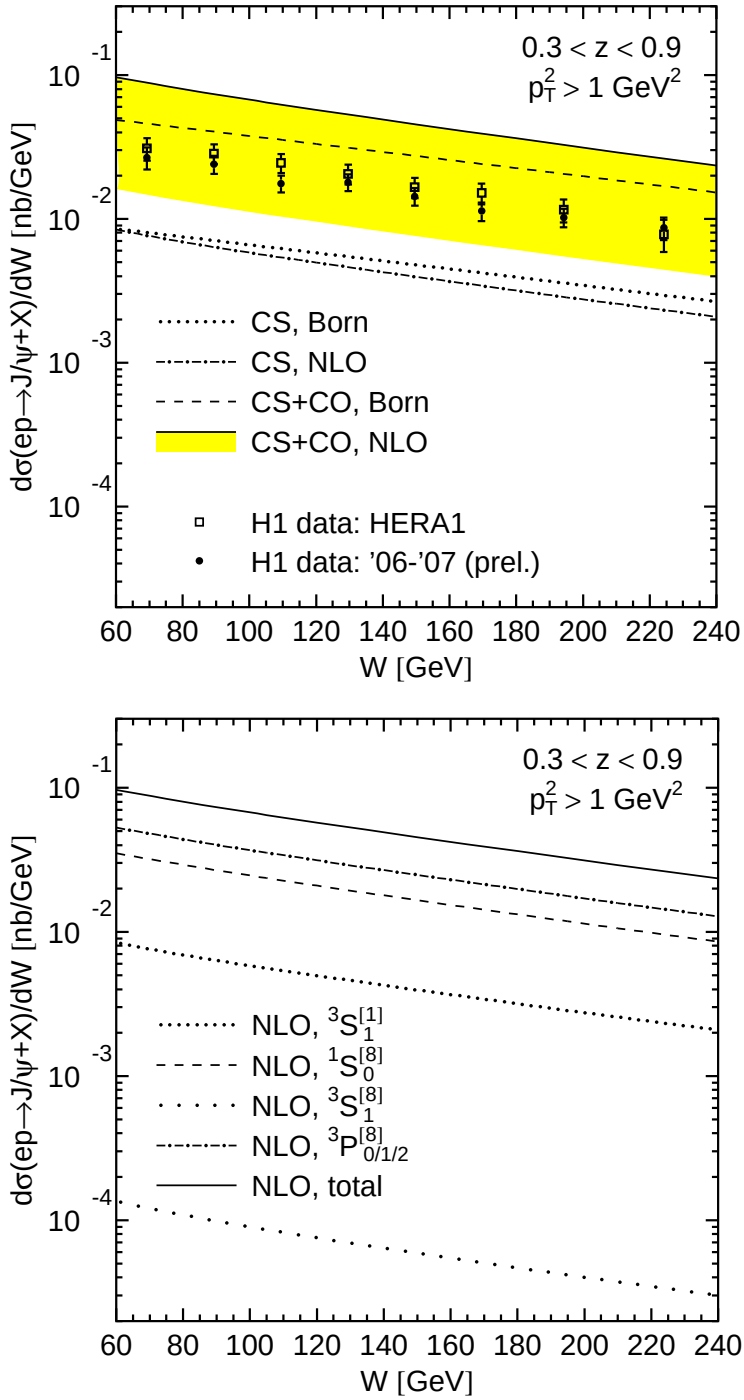

Figure 6.5.: The differential cross section $d\sigma(ep \to J/\psi + X)/dW$ of direct J/ψ photoproduction at HERA. Upper graph: Born and NLO predictions compared to H1 data, for the color singlet contributions only and for the sum of color singlet and color octet contributions. Lower graph: The contributions of the different intermediate states to the NLO prediction.

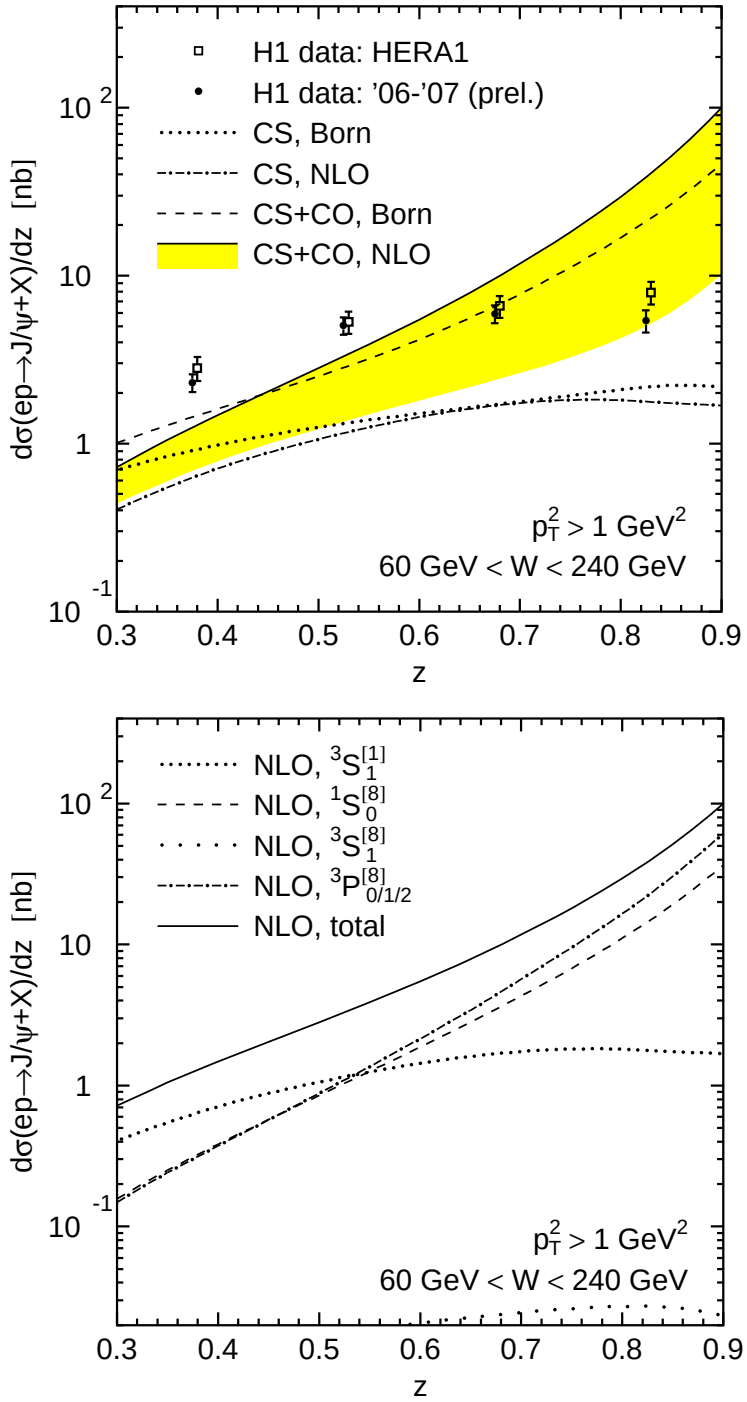

Figure 6.6.: The differential cross section $d\sigma(ep \to J/\psi + X)/dz$ of direct J/ψ photoproduction at HERA. Upper graph: Born and NLO predictions compared to H1 data, for the color singlet contributions only and for the sum of color singlet and color octet contributions. Lower graph: The contributions of the different intermediate states to the NLO prediction.

different set of parameters used, different factorization and renormalization scales and older PDFs. In fact, when we repeat our calculation for the color singlet states using Krämer's parameters, scales, PDFs and kinematic ranges, we obtain exact agreement with his results. Furthermore, recently another NLO color singlet model analysis for J/ψ photoproduction has been published [44], which shows color singlet model predictions well below ZEUS data.

The second conclusion is that in case of the $d\sigma(ep \to J/\psi + X)/dp_T^2$ and $d\sigma(ep \to J/\psi + X)/dW$ differential cross sections the sum of NLO color singlet and color octet contributions describes the data fairly well. The shape is very similar and the data points lie in the region we expect the NLO cross sections to be after we will have more accurate color octet long distance matrix elements. Unfortunately, in case of $d\sigma(ep \to J/\psi + X)/dz$ the sharp increase at high z is even sharper than already in the Born case. Nevertheless, also here the data points still lie within our NLO band. In the low z region, the data points even lie above our predictions. But below about $z = 0.45$ we expect significant contributions from resolved photoproduction processes with intermediate color octet states, which have not yet been considered in the present analysis. So we expect the cross section to rise in the low z region after including the resolved processes.

A third conclusion is that the contribution of intermediate ${}^3S_1^{[8]}$ states are phenomenologically not significant for photoproduction. In contrast to hadroproduction, the photoproduction cross section is insensitive to $\langle \mathcal{O}^{J/\psi}({}^3S_1^{[8]})\rangle$. Therefore the universality of $\langle \mathcal{O}^{J/\psi}({}^3S_1^{[8]})\rangle$ can not be tested by comparing Tevatron and HERA data. On the other hand, in case of $d\sigma(ep \to J/\psi + X)/dp_T^2$ and $d\sigma(ep \to J/\psi + X)/dz$, there is a slight difference in the slope of the ${}^1S_0^{[8]}$ and the ${}^3P_{0/1/2}^{[8]}$ contributions, and the data seems to prefer a stronger ${}^1S_0^{[8]}$ contribution. Unfortunately, the hadroproduction cross section is insensitive to the ratio of $\langle \mathcal{O}^{J/\psi}({}^3S_1^{[8]})\rangle$ and $\langle \mathcal{O}^{J/\psi}({}^3P_0^{[8]})\rangle$. Therefore the only quantity whose universality can actually be tested by comparing HERA and Tevatron data is the linear combination $M_r^{J/\psi}$ defined in (6.49).

7. Summary and outlook

Nonrelativistic QCD provides a rigorous factorization theorem for the production and decay of heavy quarkonia. A key feature is the inclusion of intermediate color octet, meaning color charged, states. These color octet states are needed for the description of the p_T distribution of the J/ψ hadroproduction cross section at the Tevatron. In order to establish NRQCD as the correct theory for hadroproduction, it is however necessary to show the significance of the color octet contributions in other high energy experiments as well, for example in the J/ψ photoproduction at HERA, and proof the universality of the long distance color octet matrix elements (MEs).

As for the state of knowledge before our work, for both photoproduction and hadroproduction, NLO calculations existed only for intermediate color singlet states. The relativistic corrections, meaning the contributions of the color octet states, were only known at leading order in α_s. It seemed that the color singlet model prediction described the HERA data fairly well, whereas the NRQCD prediction overshooted the data. Therefore it has been a desire for 13 years to know the NLO corrections to both photoproduction and hadroproduction, in order to decide more clearly whether the NRQCD factorization mechanism is realized in nature or not. We have now for the first time succeeded in calculating the full NLO corrections to direct J/ψ photoproduction including the color octet states.

We have solved a series of conceptual difficulties:

1. We found a way to evaluate the virtual corrections without having to deal with Coulomb divergences.

2. We have derived systematic formulas for an extension of the Passarino-Veltman reduction to the case of linear dependent propagator momenta, double propagator powers and an arbitrary number of Lorentz indices in the numerator.

3. We found a way to systematically evaluate the numerous different scalar Feynman integrals by applying the integration-by-parts reduction procedure, most frequently used in multi loop calculations.

4. We have systematically analyzed the non-standard infrared divergency structure in case of the P states and its cancellations.

Our calculation has passed a series of checks:

1. We could reproduce the Born results published in the literature.

2. We could analytically show the cancellation of all ultraviolet and all infrared divergences.

3. As for the evaluation of the virtual correction loop integrals, we have implemented two different reduction methods and could analytically proof that the results of both methods are equal.

4. We could check our analytic expressions for the real correction squared matrix elements by comparing them with the numerical results of MadOnia, a quarkonium version of MadGraph [43], which is an automatic program for numeric tree level calculations.

5. We could numerically show that our results are independent of the unphysical phase space slicing parameters, which is a test on our soft and collinear limits and the kinematics used.

6. We could reproduce Krämer's NLO results for the color singlet state [11] (when using his parameters, PDFs, scales and cuts).

The comparison of our results with HERA data shows that the color singlet contributions alone are not sufficient to describe HERA photoproduction. This result seems to contrast Krämer's conclusions, but is in agreement with another recent calculation of the color singlet contributions at NLO [44]. The sum of color singlet and color octet contributions, on the other hand, seems to describe the data much better. Unfortunately, the NRQCD prediction is still hampered by the large uncertainty associated with the values of the long distance matrix elements, which are extracted from fitting the hadroproduction predictions to Tevatron data.

In order to reduce this uncertainty it will be necessary to calculate the complete NLO predictions for J/ψ hadroproduction, so as to extract more precise values for the color octet MEs. This will be the subject of our future research. Thereby we will have to find more efficient ways to evaluate the real corrections, because in our current method huge amounts of computational ressources are needed for the numerical phase space integrations of the hard non-collinear region of the real corrections. We are going to follow two strategies: The first strategy is to implement a subtraction mechanism, extending the usual dipole subtraction scheme [31] to the case of heavy quarkonium production and our non-standard divergency structure. In a subtraction method we would need just about 10% of the integration precision needed in our phase space slicing method, so that the hadroproduction would be calculable at an acceptable time scale. The other strategy is to find an algorithm to simplify the expressions for the real correction squared matrix elements, or to use a completely different approach to compute the squared matrix elements, for example the helicity projection method.

We are also going to calculate the J/ψ polarization in both photoproduction and hadroproduction at NLO, because in both cases neither the leading order NRQCD prediction, nor the NLO color singlet model prediction is able to describe the J/ψ polarization at high p_T [44, 45].

A. Our tensor reduction

The application of the spin projectors in (2.4) till (2.7) leads to tensor integrals with linearly dependent propagator momenta, and in the case of P states also to double propagator powers due to the derivative with respect to the relative momentum $2q$ between the charm and the anticharm. A simple example integral would be

$$I_{\text{example}} = \frac{(2\pi\mu)^{4-D}}{i\pi^2} \int \frac{d^D Q \; Q^\mu Q^\nu}{Q^2 \left[(Q+\frac{P}{2})^2 - m_c^2\right] \left[(Q-\frac{P}{2})^2 - m_c^2\right]^2}. \tag{A.1}$$

A direct application of the Passarino-Veltman reduction formulas [24] is not possible, as we would have to call for example the integral (A.1) a D function, something like

$$I_{\text{example,PV}} = D^{\mu\nu}\left(\frac{P}{2}, -\frac{P}{2}, -\frac{P}{2}, 0, m_c, m_c, m_c\right). \tag{A.2}$$

This would lead to zero Gram determinants, by which we would have to divide in the course of the reduction procedure. For our calculation we have therefore generalized the Passarino-Veltman formulas to the case of propagators with linear dependent propagator momenta and double propagator powers. The basic idea behind this extensions is simply that we classify the integrals not according to the number of propagators, but according to the number of independent momenta appearing in them, so we would call the integral (A.1) a B function, to be precise,

$$I_{\text{example}} = B^{\mu\nu}\left(\frac{P}{2}, 0, m_c; -1, m_c, 2, 1\right) \tag{A.3}$$

in the notation we are going to introduce below. Our formulas allow for an arbitrary number of Lorentz indices in the numerators. They are general enough to reduce all tensor integrals appearing in our calculation to scalar ones.

We remark that the mentioned problem of vanishing Gram determinants is different from the one studied in [46]. In that paper the problem of numerical instabilities due to small Gram determinants is addressed and not the case of zero Gram determinants.

A.1. Definition of the tensor integrals and tensor decomposition

Let us start by defining the naming convention for our generalized tensor integrals as

$$A^{\mu_1\ldots\mu_p}(m_0; m_5, x, y) \equiv \frac{(2\pi\mu)^{4-D}}{i\pi^2} \int \frac{d^D Q \; Q^{\mu_1} \ldots Q^{\mu_P}}{\left[Q^2 - m_0^2\right]^y \left[Q^2 - m_5^2\right]^x} \tag{A.4}$$

$$
\begin{aligned}
&B^{\mu_1\ldots\mu_p}(p_1,m_0,m_1;a,m_5,x,y)\\
&\quad\equiv\ \frac{(2\pi\mu)^{4-D}}{i\pi^2}\int\frac{d^DQ\;Q^{\mu_1}\ldots Q^{\mu_P}}{\left[Q^2-m_0^2\right]^y\left[(Q+p_1)^2-m_1^2\right]\left[(Q+ap_1)^2-m_5^2\right]^x}
\end{aligned}
\tag{A.5}
$$

$$
\begin{aligned}
&C^{\mu_1\ldots\mu_p}(p_1,p_2,m_0,m_1,m_2;a,b,m_5,x,y)\\
&\quad\equiv\ \frac{(2\pi\mu)^{4-D}}{i\pi^2}\int\frac{d^DQ\;Q^{\mu_1}\ldots Q^{\mu_P}}{\left[Q^2-m_0^2\right]^y\left[(Q+p_1)^2-m_1^2\right]\left[(Q+p_2)^2-m_2^2\right]}\\
&\qquad\times\frac{1}{\left[(Q+ap_1+bp_2)^2-m_5^2\right]^x}
\end{aligned}
\tag{A.6}
$$

$$
\begin{aligned}
&D^{\mu_1\ldots\mu_p}(p_1,p_2,p_3,m_0,m_1,m_2,m_3;a,b,c,m_5,x,y)\\
&\quad\equiv\ \frac{(2\pi\mu)^{4-D}}{i\pi^2}\int\frac{d^DQ\;Q^{\mu_1}\ldots Q^{\mu_P}}{\left[Q^2-m_0^2\right]^y\left[(Q+p_1)^2-m_1^2\right]\left[(Q+p_2)^2-m_2^2\right]}\\
&\qquad\times\frac{1}{\left[(Q+p_3)^2-m_3^2\right]\left[(Q+ap_1+bp_2+cp_3)^2-m_5^2\right]^x},
\end{aligned}
\tag{A.7}
$$

where Q is the loop momentum, the p_i external momenta, m_i particle masses, μ_i Lorentz indices and a, b, c, x and y numbers. We impose the restrictions that

1. p_1, p_2 and p_3 must be linearly independent and not zero.
2. $x \geqq 0$ and $y \geqq 1$.
3. $a \neq 0$ in B functions, $b \neq 0$ in C functions, $c \neq 0$ in D functions.

These conditions are not very restrictive, so that we can identify each tensor integral appearing in our calculation (in some cases after a simple transformation of the loop momentum) as one of the integrals (A.4) till (A.7).

Once we have identified our tensor integrals, we perform a tensor decomposition, that means we rewrite the integrals as the sum of all possible Lorentz structures which can appear, multiplied by so called tensor coefficient functions, according to

$$
A^{\mu_1\ldots\mu_P}\equiv\begin{cases}0 & \text{if } P \text{ odd}\\ \left\{g^{P/2}\right\}^{\mu_1\ldots\mu_p}A_{P/2} & \text{if } P \text{ even}\end{cases}
\tag{A.8}
$$

$$
B^{\mu_1\ldots\mu_P}\equiv\sum_{n=0}^{P\,\mathrm{DIV}\,2}\left\{g^n\,p_1^{P-2n}\right\}^{\mu_1\ldots\mu_p}B_{n,P-2n}
\tag{A.9}
$$

$$
C^{\mu_1\ldots\mu_P}\equiv\sum_{n=0}^{P\,\mathrm{DIV}\,2}\sum_{m=0}^{P-2n}\left\{g^n\,p_1^m\,p_2^{P-2n-m}\right\}^{\mu_1\ldots\mu_p}C_{n,m,P-2n-m}
\tag{A.10}
$$

$$
D^{\mu_1\ldots\mu_P}\equiv\sum_{n=0}^{P\,\mathrm{DIV}\,2}\sum_{m=0}^{P-2n}\sum_{k=0}^{P-2n-m}\left\{g^n\,p_1^m\,p_2^k\,p_3^{P-2n-m-k}\right\}^{\mu_1\ldots\mu_p}D_{n,m,k,P-2n-m-k}\ ,
\tag{A.11}
$$

where P DIV 2 means the integer part of $\frac{P}{2}$, and $\{g^a\, p_1^b\, p_2^c\, p_3^d\}^{\mu_1\dots\mu_P}$ with $2a+b+c+d=P$ stands for the sum of all *different* terms which can be constructed by distributing the P Lorentz indices $\mu_1\dots\mu_P$ over the a g's, the b p_1's, the c p_2's and the d p_3's. This short notation becomes clearer if we consider the concrete example

$$\begin{aligned} B^{\mu\nu\rho\sigma} &= p_1^\mu p_1^\nu p_1^\rho p_1^\sigma\, B_{0,4} + \big(g^{\mu\nu} p_1^\rho p_1^\sigma + g^{\mu\rho} p_1^\nu p_1^\sigma + g^{\mu\sigma} p_1^\nu p_1^\rho + g^{\nu\rho} p_1^\mu p_1^\sigma + g^{\nu\sigma} p_1^\mu p_1^\rho \\ &\quad + g^{\rho\sigma} p_1^\mu p_1^\nu\big) B_{1,2} + \big(g^{\mu\nu} g^{\rho\sigma} + g^{\mu\rho} g^{\nu\sigma} + g^{\mu\sigma} g^{\nu\rho}\big)\, B_{2,0}. \end{aligned} \tag{A.12}$$

Now, the purpose of the tensor reduction is to express all tensor coefficient functions $A_{P/2}$, $B_{n,P-2n}$, $C_{n,m,P-2n-m}$ and $D_{n,m,k,P-2n-m-k}$ in terms of coefficient functions A_0, $B_{0,0}$, $C_{0,0,0}$ and $D_{0,0,0,0}$, which are scalar integrals. This is achieved by the successive application of reduction formulas, which will be derived in the following subsections.

A.2. Tensor reduction of the generalized A functions

We multiply the right hand sides of (A.4) and (A.8) with $g_{\mu_1\mu_2}$ and solve the resulting equation for $A_{P/2}$. If $y>1$, we obtain

$$A_{r+1} = \frac{1}{D+2r}\Big(A_r\big(m_0; m_5, x, y-1\big) + m_0^2 A_r\Big). \tag{A.13}$$

If $y=1$ and $x>0$, we obtain

$$A_{r+1} = \frac{1}{D+2r}\Big(A_r\big(m_0; m_5, x-1, 1\big) + m_5^2 A_r\Big). \tag{A.14}$$

If $y=1$ and $x=0$, we obtain

$$A_{r+1} = \frac{m_0^2}{D+2r} A_r. \tag{A.15}$$

In the cases, where we omitted explicit function arguments, the arguments are meant to be $(m_0; m_5, x, y)$.

A.3. Tensor reduction of the generalized B functions

We multiply the right hand sides of (A.5) and (A.9) in turn with $g_{\mu_1\mu_2}$ and p_{1,μ_1}. In the two resulting relations, we extract two equations by comparing the coefficients of the specific tensor structure

$$g^{\mu_3\mu_4}\dots g^{\mu_{2r+1}\mu_{2r+2}}\, p_1^{\mu_{2r+3}}\dots p_1^{\mu_P},$$

respectively

$$g^{\mu_2\mu_3}\dots g^{\mu_{2r}\mu_{2r+1}}\, p_1^{\mu_{2r+2}}\dots p_1^{\mu_P}.$$

Solving these equations for $B_{r+1,P-2r-2}$ and $B_{r,P-2r}$ results in

$$B_{r+1,s} = \frac{1}{D+2r+s-1}\Big(S^{B,0}_{r,s} - S^{B,1}_{r,s+1}\Big) \tag{A.16}$$

$$B_{r,s+1} = \frac{1}{p^2}\Big(S^{B,1}_{r,s} - s\,B_{r+1,s-1}\Big), \tag{A.17}$$

where

$$S^{B,0}_{i,j} \equiv B_{i,j}(\emptyset) + m_0^2 B_{i,j} \tag{A.18}$$

$$S^{B,1}_{i,j} \equiv \frac{1}{2}\Big(B_{i,j}(\not{1}) - B_{i,j}(\emptyset) - (p_1^2 - m_1^2 + m_0^2)B_{i,j}\Big). \tag{A.19}$$

Here, $B_{i,j}(\not{n})$ stands for the coefficient of the tensor structure $\{g^i\,p_1^j\}^{\mu_1\cdots\mu_{2i+j}}$ of the tensor integral $B^{\mu_1\cdots\mu_{2i+j}}$ with the power of the nth propagator (the one with mass m_n) decreased by one. In the following we present explicit formulas for the different cases which appear, starting with $B_{r,s}(\not{1})$. In the case $x=0$ and $s>0$,

$$B_{r,s}(\not{1}) = 0. \tag{A.20}$$

If $x=0$ and $s=0$,

$$B_{r,s}(\not{1}) = A_r\big(m_0;0,0,y\big). \tag{A.21}$$

If $x>0$,

$$B_{r,s}(\not{1}) = a^s B_{r,s}\big(ap_1,m_0,m_5;1,m_5,x-1,y\big). \tag{A.22}$$

As for $B_{r,s}(\emptyset)$, if $y>1$,

$$B_{r,s}(\emptyset) = B_{r,s}\big(p_1,m_0,m_1;a,m_5,x,y-1\big). \tag{A.23}$$

If $y=1$ and ($x=0$ or $a=1$),

$$B_{r,s}(\emptyset) = (-1)^s A_r\big(m_1;m_5,x,1\big). \tag{A.24}$$

If $y=1$ and $x>0$ and $a\neq 1$,

$$B_{r,s}(\emptyset) = \sum_{\alpha=0}^{s}\binom{s}{\alpha}(-1)^\alpha(a-1)^{s-\alpha}B_{r,s-\alpha}\big((a-1)p_1,m_1,m_5;1,m_5,x-1,1\big). \tag{A.25}$$

Whenever we have omitted explicit function arguments in this section, the arguments are meant to be $(p_1,m_0,m_1;a,m_5,x,y)$.

A.4. Tensor reduction of the generalized C functions

We multiply the right hand sides of (A.6) and (A.10) in turn with $g_{\mu_1\mu_2}$, p_{1,μ_1} and p_{2,μ_1}. In the three resulting relations, we extract three equations by comparing the coefficients of the specific tensor structure

$$g^{\mu_3\mu_4}\dots g^{\mu_{2r+1}\mu_{2r+2}}\,p_1^{\mu_{2r+3}}\dots p_1^{\mu_{2r+s+2}}\,p_2^{\mu_{2r+s+3}}\dots p_2^{\mu_P},$$

respectively

$$g^{\mu_2\mu_3}\dots g^{\mu_{2r}\mu_{2r+1}}\,p_1^{\mu_{2r+2}}\dots p_1^{\mu_{2r+s+1}}\,p_2^{\mu_{2r+s+2}}\dots p_2^{\mu_P}.$$

Solving these equations for $C_{r+1,s,P-2r-s-2}$, $C_{r,s+1,P-2r-s-1}$ and $C_{r,s,P-2r-s}$ results in

$$C_{r+1,s,t}=\frac{1}{D+2r+s+t-2}\Big(S^{C,0}_{r,s,t}-S^{C,1}_{r,s+1,t}-S^{C,2}_{r,s,t+1}\Big) \tag{A.26}$$

$$\begin{pmatrix} C_{r,s+1,t}\\ C_{r,s,t+1}\end{pmatrix}=\frac{1}{\begin{vmatrix} p_1^2 & p_1\cdot p_2\\ p_1\cdot p_2 & p_2^2\end{vmatrix}}\times\begin{pmatrix} p_2^2 & -p_1\cdot p_2\\ -p_1\cdot p_2 & p_1^2\end{pmatrix}\begin{pmatrix} S^{C,1}_{r,s,t}-s\,C_{r+1,s-1,t}\\ S^{C,2}_{r,s,t}-t\,C_{r+1,s,t-1}\end{pmatrix}, \tag{A.27}$$

where

$$S^{C,0}_{i,j,k} \equiv C_{i,j,k}(\emptyset)+m_0^2C_{i,j,k} \tag{A.28}$$

$$S^{C,1}_{i,j,k} \equiv \frac{1}{2}\Big(C_{i,j,k}(\not{1})-C_{i,j,k}(\emptyset)-(p_1^2-m_1^2+m_0^2)C_{i,j,k}\Big) \tag{A.29}$$

$$S^{C,2}_{i,j,k} \equiv \frac{1}{2}\Big(C_{i,j,k}(\not{2})-C_{i,j,k}(\emptyset)-(p_2^2-m_2^2+m_0^2)C_{i,j,k}\Big). \tag{A.30}$$

Here, $C_{i,j,k}(\not{n})$ stands for the coefficient of the tensor structure $\{g^i\,p_1^j\,p_2^k\}^{\mu_1\cdots\mu_{2i+j+k}}$ of the tensor integral $C^{\mu_1\cdots\mu_{2i+j+k}}$ with the power of the nth propagator (the one with mass m_n) decreased by one. In the following we present explicit formulas for the different cases which appear, starting with $C_{r,s,t}(\not{2})$. If $x=0$ and $t>0$,

$$C_{r,s,t}(\not{2})=0. \tag{A.31}$$

If $x=0$ and $t=0$,

$$C_{r,s,t}(\not{2})=B_{r,s}\big(p_1,m_0,m_1;0,0,0,y\big). \tag{A.32}$$

If $x>0$ and $a=0$,

$$C_{r,s,t}(\not{2})=b^t\,C_{r,s,t}\big(p_1,bp_2,m_0,m_1,m_5;0,1,m_5,x-1,y\big). \tag{A.33}$$

If $x > 0$ and $a \neq 0$,

$$C_{r,s,t}(\not{2}) = \sum_{m=0}^{s} \binom{s}{m} a^{s-m} b^t \times C_{r,m,s+t-m}\big(p_1, ap_1 + bp_2, m_0, m_1, m_5; 0, 1, m_5, x-1, y\big). \tag{A.34}$$

As for $C_{r,s,t}(\not{1})$, if ($x = 0$ or $a = 0$) and $s > 0$,

$$C_{r,s,t}(\not{1}) = 0. \tag{A.35}$$

If ($x = 0$ or $a = 0$) and $s = 0$,

$$C_{r,s,t}(\not{1}) = B_{r,t}\big(p_2, m_0, m_2; b, m_5, x, y\big). \tag{A.36}$$

If $x > 0$ and $a \neq 0$,

$$C_{r,s,t}(\not{1}) = \sum_{m=0}^{t} \binom{t}{m} a^s b^{t-m} \times C_{r,m,s+t-m}\big(p_2, ap_1 + bp_2, m_0, m_2, m_5; 0, 1, m_5, x-1, y\big). \tag{A.37}$$

Finally, we present the formulas for $C_{r,s,t}(\emptyset)$. If $y > 1$,

$$C_{r,s,t}(\emptyset) = C_{r,s,t}\big(p_1, p_2, m_0, m_1, m_2; a, b, m_5, x, y-1\big). \tag{A.38}$$

If $y = 1$ and ($x = 0$ or $a + b = 1$),

$$C_{r,s,t}(\emptyset) = \sum_{\alpha=0}^{s} \binom{s}{\alpha} (-1)^s B_{r,s+t-\alpha}\big(p_2 - p_1, m_1, m_2; b, m_5, x, 1\big). \tag{A.39}$$

If $y = 1$ and $x > 0$ and $a + b \neq 1$ and $a = 1$,

$$C_{r,s,t}(\emptyset) = \sum_{\alpha=0}^{s} \sum_{m=0}^{t} \binom{s}{\alpha} \binom{t}{m} (-1)^s b^{t-m} \times C_{r,s-\alpha+m,t-m}\big(p_2 - p_1, bp_2, m_1, m_2, m_5; 0, 1, m_5, x-1, 1\big). \tag{A.40}$$

And if $y = 1$ and $x > 0$ and $a + b \neq 1$ and $a \neq 1$,

$$C_{r,s,t}(\emptyset) = \sum_{\alpha=0}^{s+t} \sum_{m=0}^{s+t-\alpha} \sum_{w=\mathrm{Max}(0,\alpha-s+m)}^{\mathrm{Min}(m,t)} \binom{t}{w} \frac{s!}{\alpha!\,(m-w)!\,(s-\alpha-m+w)!} \times (-1)^{\alpha+m-w} (a-1)^{s-\alpha-m+w} b^{t-w} \times C_{r,m,s+t-\alpha-m}\big(p_2 - p_1, (a-1)p_1 + bp_2, m_1, m_2, m_5; 0, 1, m_5, x-1, 1\big). \tag{A.41}$$

Whereever we have omitted explicit function arguments in this section, the arguments are meant to be $(p_1, p_2, m_0, m_1, m_2; a, b, m_5, x, y)$.

A.5. Tensor reduction of the generalized D functions

We multiply the right hand sides of (A.7) and (A.11) in turn with $g_{\mu_1\mu_2}$, p_{1,μ_1} , p_{2,μ_1} and p_{3,μ_1}. In the four resulting relations, we extract four equations by comparing the coefficients of the specific tensor structure

$$g^{\mu_3\mu_4}\dots g^{\mu_{2r+1}\mu_{2r+2}}\,p_1^{\mu_{2r+3}}\dots p_1^{\mu_{2r+s+2}}\,p_2^{\mu_{2r+s+3}}\dots p_2^{\mu_{2r+s+t+2}}\,p_3^{\mu_{2r+s+t+3}}\dots p_3^{\mu_P},$$

respectively

$$g^{\mu_2\mu_3}\dots g^{\mu_{2r}\mu_{2r+1}}\,p_1^{\mu_{2r+2}}\dots p_1^{\mu_{2r+s+1}}\,p_2^{\mu_{2r+s+2}}\dots p_2^{\mu_{2r+s+t+1}}\,p_3^{\mu_{2r+s+t+2}}\dots p_3^{\mu_P}.$$

Solving these equations for $D_{r+1,s,t,P-2r-s-t-2}$, $D_{r,s+1,t,P-2r-s-t-1}$, $D_{r,s,t+1,P-2r-s-t-1}$ and $D_{r,s,t,P-2r-s-t}$ results in

$$\begin{aligned} D_{r+1,s,t,u} &= \frac{1}{D+2r+s+t+u-3} \\ &\quad\times\Big(S^{D,0}_{r,s,t,u}-S^{D,1}_{r,s+1,t,u}-S^{D,2}_{r,s,t+1,u}-S^{D,3}_{r,s,t,u+1}\Big) \end{aligned} \tag{A.42}$$

$$\begin{aligned} \begin{pmatrix} D_{r,s+1,t,u}\\ D_{r,s,t+1,u}\\ D_{r,s,t,u+1}\end{pmatrix} &= \frac{1}{\begin{vmatrix} p_1^2 & p_1\cdot p_2 & p_1\cdot p_3\\ p_1\cdot p_2 & p_2^2 & p_2\cdot p_3\\ p_1\cdot p_3 & p_2\cdot p_3 & p_3^2\end{vmatrix}} \\ &\times\begin{pmatrix} p_2^2\,p_3^2-(p_2\cdot p_3)^2 & p_1\cdot p_3\,p_2\cdot p_3-p_1\cdot p_2\,p_3^2 & p_1\cdot p_2\,p_2\cdot p_3-p_1\cdot p_3\,p_2^2\\ p_1\cdot p_3\,p_2\cdot p_3-p_1\cdot p_2\,p_3^2 & p_1^2\,p_3^2-(p_1\cdot p_3)^2 & p_1\cdot p_2\,p_1\cdot p_3-p_2\cdot p_3\,p_1^2\\ p_1\cdot p_2\,p_2\cdot p_3-p_1\cdot p_3\,p_2^2 & p_1\cdot p_2\,p_1\cdot p_3-p_2\cdot p_3\,p_1^2 & p_1^2p_2^2-(p_1\cdot p_2)^2\end{pmatrix} \\ &\times\begin{pmatrix} S^{D,1}_{r,s,t,u}-s\,D_{r+1,s-1,t,u}\\ S^{D,2}_{r,s,t,u}-t\,D_{r+1,s,t-1,u}\\ S^{D,3}_{r,s,t,u}-u\,D_{r+1,s,t,u-1}\end{pmatrix}, \end{aligned} \tag{A.43}$$

where

$$S^{D,0}_{i,j,k,l} \equiv D_{i,j,k,l}(\emptyset)+m_0^2D_{i,j,k,l} \tag{A.44}$$

$$S^{D,1}_{i,j,k,l} \equiv \frac{1}{2}\Big(D_{i,j,k,l}(\not{1})-D_{i,j,k,l}(\emptyset)-(p_1^2-m_1^2+m_0^2)D_{i,j,k,l}\Big) \tag{A.45}$$

$$S^{D,2}_{i,j,k,l} \equiv \frac{1}{2}\Big(D_{i,j,k,l}(\not{2})-D_{i,j,k,l}(\emptyset)-(p_2^2-m_2^2+m_0^2)D_{i,j,k,l}\Big) \tag{A.46}$$

$$S^{D,3}_{i,j,k,l} \equiv \frac{1}{2}\Big(D_{i,j,k,l}(\not{3})-D_{i,j,k,l}(\emptyset)-(p_3^2-m_3^2+m_0^2)D_{i,j,k,l}\Big). \tag{A.47}$$

Here, $D_{i,j,k,l}(\not{n})$ stands for the coefficient of the tensor structure $\{g^i\,p_1^j\,p_2^k\,p_3^l\}^{\mu_1\cdots\mu_{2i+j+k+l}}$ of the tensor integral $C^{\mu_1\cdots\mu_{2i+j+k+l}}$ with the power of the nth propagator (the one with mass m_n) decreased by one. In the following we present explicit formulas for the different cases which appear, starting with $D_{r,s,t,u}(\not{3})$. If $x=0$ and $u>0$,

$$D_{r,s,t,u}(\not{3})=0. \tag{A.48}$$

If $x = 0$ and $u = 0$,

$$D_{r,s,t,u}(\not{3}) = C_{r,s,t}(p_1, p_2, m_0, m_1, m_2; a, b, m_5, 0, y). \tag{A.49}$$

If $x > 0$ and $a = 0$ and $b = 0$,

$$D_{r,s,t,u}(\not{3}) = c^u D_{r,s,t,u}\big(p_1, p_2, cp_3, m_0, m_1, m_2, m_5; 0, 0, 1, m_5, x-1, y\big). \tag{A.50}$$

If $x > 0$ and $a \neq 0$ and $b = 0$,

$$\begin{aligned} D_{r,s,t,u}(\not{3}) &= \sum_{m=0}^{s} \binom{s}{m} a^{s-m} c^u \\ &\quad \times D_{r,m,t,s+u-m}\big(p_1, p_2, ap_1 + cp_3, m_0, m_1, m_2, m_5; 0, 0, 1, m_5, x-1, y\big). \end{aligned} \tag{A.51}$$

If $x > 0$ and $a = 0$ and $b \neq 0$,

$$\begin{aligned} D_{r,s,t,u}(\not{3}) &= \sum_{k=0}^{t} \binom{t}{k} b^{t-k} c^u \\ &\quad \times D_{r,s,k,t+u-k}\big(p_1, p_2, bp_2 + cp_3, m_0, m_1, m_2, m_5; 0, 0, 1, m_5, x-1, y\big). \end{aligned} \tag{A.52}$$

If $x > 0$ and $a \neq 0$ and $b \neq 0$,

$$\begin{aligned} D_{r,s,t,u}(\not{3}) &= \sum_{m=0}^{s} \sum_{k=0}^{t} \binom{s}{m} \binom{t}{k} a^{s-m} b^{t-k} c^u \\ &\quad \times D_{r,m,k,s+t+u-m-k}\big(p_1, p_2, ap_1 + bp_2 + cp_3, m_0, m_1, m_2, m_5; \\ &\qquad 0, 0, 1, m_5, x-1, y\big). \end{aligned} \tag{A.53}$$

As for $D_{r,s,t,u}(\not{2})$, if ($x = 0$ or $b = 0$) and $t > 0$,

$$D_{r,s,t,u}(\not{2}) = 0. \tag{A.54}$$

If ($x = 0$ or $b = 0$) and $t = 0$,

$$D_{r,s,t,u}(\not{2}) = C_{r,s,u}\big(p_1, p_3, m_0, m_1, m_3; a, c, m_5, x, y\big). \tag{A.55}$$

If $x > 0$ and $b \neq 0$ and $a = 0$,

$$\begin{aligned} D_{r,s,t,u}(\not{2}) &= \sum_{k=0}^{u} \binom{u}{k} b^t c^{u-k} \\ &\quad \times D_{r,s,k,t+u-k}\big(p_1, p_3, bp_2 + cp_3, m_0, m_1, m_3, m_5; 0, 0, 1, m_5, x-1, y). \end{aligned} \tag{A.56}$$

If $x > 0$ and $b \neq 0$ and $a \neq 0$,

$$\begin{aligned} D_{r,s,t,u}(\not{2}) &= \sum_{m=0}^{s} \sum_{k=0}^{u} \binom{s}{m} \binom{u}{k} a^{s-m} b^t c^{u-k} \\ &\quad \times D_{r,m,k,s+t+u-m-k}\big(p_1, p_3, ap_1 + bp_2 + cp_3, m_0, m_1, m_3, m_5; \\ &\qquad 0, 0, 1, m_5, x-1, y). \end{aligned} \tag{A.57}$$

As for $D_{r,s,t,u}(\not{1})$, if ($x = 0$ or $a = 0$) and $s > 0$,

$$D_{r,s,t,u}(\not{1}) = 0. \tag{A.58}$$

If ($x = 0$ or $a = 0$) and $s = 0$,

$$D_{r,s,t,u}(\not{1}) = C_{r,t,u}\big(p_2, p_3, m_0, m_2, m_3; b, c, m_5, x, y\big). \tag{A.59}$$

If $x > 0$ and $a \neq 0$ and $b = 0$,

$$\begin{aligned} D_{r,s,t,u}(\not{1}) &= \sum_{k=0}^{u} \binom{u}{k} a^s c^{u-k} \\ &\quad \times D_{r,t,k,s+u-k}\big(p_2, p_3, ap_1 + cp_3, m_0, m_2, m_3, m_5; 0, 0, 1, m_5, x-1, y\big). \end{aligned} \tag{A.60}$$

If $x > 0$ and $a = 0$ and $b \neq 0$,

$$\begin{aligned} D_{r,s,t,u}(\not{1}) &= \sum_{m=0}^{t} \sum_{k=0}^{u} \binom{t}{m} \binom{u}{k} a^s b^{t-m} c^{u-k} \\ &\quad \times D_{r,m,k,s+t+u-m-k}\big(p_2, p_3, ap_1 + bp_2 + cp_3, m_0, m_2, m_3, m_5; \\ &\qquad\qquad 0, 0, 1, m_5, x-1, y\big). \end{aligned} \tag{A.61}$$

Finally, for $D_{r,s,t,u}(\emptyset)$, if $y > 1$,

$$D_{r,s,t,u}(\emptyset) = D_{r,s,t,u}\big(p_1, p_2, p_3, m_0, m_1, m_2, m_3; a, b, c, m_5, x, y-1\big). \tag{A.62}$$

If $y = 1$ and ($x = 0$ or $a + b + c = 1$),

$$\begin{aligned} D_{r,s,t,u}(\emptyset) &= \sum_{\alpha=0}^{s+t+u} \sum_{m=0}^{s-\alpha} \frac{s!}{a!\, m!\, (s-\alpha-m)!} (-1)^s \\ &\quad \times C_{r,m+t,s+u-\alpha-m}\big(p_2 - p_1, p_3 - p_1, m_1, m_2, m_3; b, c, m_5, x, 1\big). \end{aligned} \tag{A.63}$$

If $y = 1$ and $x > 0$ and $a + b + c \neq 1$ and $a = 1$ and $b = 0$,

$$\begin{aligned} D_{r,s,t,u}(\emptyset) &= \sum_{\alpha=0}^{s+t+u} \sum_{m=t}^{s+t-\alpha} \sum_{k=\mathrm{Max}(0,s+t-\alpha-m)}^{s+t+u-\alpha-m} \binom{u}{\alpha+m+k-s-t} \\ &\quad \times \frac{s!}{\alpha!\, (m-t)!\, (s+t-\alpha-m)!} (-1)^s c^{s+t+u-\alpha-m-k} \\ &\quad \times D_{r,m,k,s+t+u-\alpha-m-k}\big(p_2 - p_1, p_3 - p_1, cp_3, m_1, m_2, m_3; \\ &\qquad\qquad m_5, 0, 0, 1, m_5, x-1, 1\big). \end{aligned} \tag{A.64}$$

If $y = 1$ and $x > 0$ and $a + b + c \neq 1$ and $a \neq 1$ and $b = 0$,

$$D_{r,s,t,u}(\emptyset) = \sum_{\alpha=0}^{s+t+u} \sum_{m=t}^{s+t+u-\alpha} \sum_{k=0}^{s+t+u-\alpha-m} \sum_{w=\mathrm{Max}(0,-s-t+\alpha+m+k)}^{\mathrm{Min}(k,u)} \binom{u}{w}$$
$$\times \frac{s!}{\alpha!\,(m-t)!\,(k-w)!\,(s+t-\alpha-m-k+w)!}$$
$$\times (-1)^{\alpha+m-t+k-w}(a-1)^{s+t-\alpha-m-k+w}c^{u-w}$$
$$\times D_{r,m,k,s+t+u-\alpha-m-k}\big(p_2 - p_1, p_3 - p_1, (a-1)p_1 + cp_3, m_1, m_2, m_3, m_5;$$
$$0, 0, 1, m_5, x-1, 1\big). \tag{A.65}$$

If $y = 1$ and $x > 0$ and $a + b + c \neq 1$ and $a = 1$ and $b \neq 0$,

$$D_{r,s,t,u}(\emptyset) = \sum_{\alpha=0}^{s+t+u} \sum_{m=0}^{s+t+u-\alpha} \sum_{k=0}^{s+t+u-\alpha-m} \sum_{z=\mathrm{Max}(0,\alpha+m-s,\alpha+m-s+k-u)}^{\mathrm{Min}(m,t,\alpha+m+k-s)} \binom{t}{z}$$
$$\times \binom{u}{\alpha+m-z+k-s} \frac{s!}{\alpha!\,(m-z)!\,(s-\alpha-m+z)!}(-1)^s b^{t-z} c^{s+u-\alpha-m-k+z}$$
$$\times D_{r,m,k,s+t+u-\alpha-m-k}\big(p_2 - p_1, p_3 - p_1, bp_2 + cp_3, m_1, m_2, m_3, m_5;$$
$$0, 0, 1, m_5, x-1, 1\big). \tag{A.66}$$

And if $y = 1$ and $x > 0$ and $a + b + c \neq 1$ and $a \neq 1$ and $b \neq 0$,

$$D_{r,s,t,u}(\emptyset) = \sum_{\alpha=0}^{s+t+u} \sum_{m=0}^{s+t+u-\alpha} \sum_{k=0}^{s+t+u-\alpha-m} \sum_{z=0}^{\mathrm{Min}(m,t)} \sum_{w=\mathrm{Max}(0,-s+\alpha+m-z+k)}^{\mathrm{Min}(k,u)} \binom{t}{z}\binom{u}{w}$$
$$\times \frac{s!}{\alpha!\,(m-z)!\,(k-w)!\,(s-\alpha-m+z-k+w)!}$$
$$\times (-1)^{\alpha+m-z+k-w}(a-1)^{s-\alpha-m+z-k+w}b^{t-z}c^{u-w}$$
$$\times D_{r,m,k,s+t+u-\alpha-m-k}\big(p_2 - p_1, p_3 - p_1, (a-1)p_1 + bp_2 + cp_3, m_1, m_2, m_3, m_5;$$
$$0, 0, 1, m_5, x-1, 1\big). \tag{A.67}$$

B. Use of integration-by-parts

The method of integration-by-parts was originally proposed in [47]. Its aim is to express a large number of scalar diagrams which belong to a certain topology to a small, distinct set of master integrals. *Topology* here means a class of Feynman integrals which only differ in propagator powers. The method is based on the properties

$$
\begin{aligned}
0 &= \frac{\partial}{\partial Q^\mu}\, Q_i^\mu f(Q_1,\ldots,Q_n,p_1,\ldots,p_m) \\
0 &= \frac{\partial}{\partial Q^\mu}\, p_i^\mu f(Q_1,\ldots,Q_n,p_1,\ldots,p_m)
\end{aligned}
\tag{B.1}
$$

of any dimensionally regularized Feynman integral f with loop momenta Q_i and external momenta p_i. If we apply (B.1) to a diagram with general propagator powers λ_i (which can even be negative), we obtain relations between different members of the corresponding topology. Particular linear combinations of these relations can then express integrals in terms of others with lower (or less negative) propagator powers.

Usually, integration by parts is used in multi loop calculations, as one loop integrals which appear in normal QCD calculations are already master integrals. In the case of our integrals with linearly dependent propagator momenta and double propagator powers, however, this method is very effective. The reason is that we now have each time several possibilities to express scalar products in the numerator, which appear as a result of the derivations in (B.1), in terms of the propagators. This increases the number of integration-by-parts relations drastically.

In the following we list the different topologies, for which we have implemented our integration-by-parts procedure. Every scalar integral appearing in our calculation can be expressed as one of the following functions. The notation is the one we use in our actual implementation. It is actually somewhat redundant, as in fact, there are only four different topologies, the rest of the topologies differs from these four only by permutation of the external momenta k_1, k_2 and $-k_3$.

$T_1(\lambda_1,\lambda_2,\lambda_3,\lambda_4,\lambda_5) \equiv$

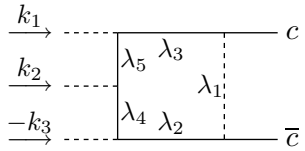

$$
\begin{aligned}
&= \frac{(2\pi\mu)^{4-D}}{i\pi^2}\int \frac{d^DQ}{\left[Q^2\right]^{\lambda_1}\left[(Q+\frac{P}{2})^2-m_c^2\right]^{\lambda_2}\left[(Q-\frac{P}{2})^2-m_c^2\right]^{\lambda_3}} \\
&\quad\times\frac{1}{\left[(Q+\frac{P}{2}+k_3)^2-m_c^2\right]^{\lambda_4}\left[(Q-\frac{P}{2}+k_1)^2-m_c^2\right]^{\lambda_5}}
\end{aligned}
\tag{B.2}
$$

$T_4(\lambda_1,\lambda_2,\lambda_3,\lambda_4,\lambda_5) \equiv$ 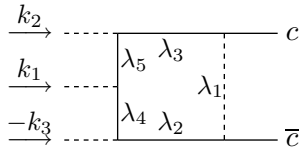

$$= \frac{(2\pi\mu)^{4-D}}{i\pi^2}\int \frac{d^DQ}{\left[Q^2\right]^{\lambda_1}\left[(Q+\frac{P}{2})^2-m_c^2\right]^{\lambda_2}\left[(Q-\frac{P}{2})^2-m_c^2\right]^{\lambda_3}} \times \frac{1}{\left[(Q+\frac{P}{2}+k_3)^2-m_c^2\right]^{\lambda_4}\left[(Q-\frac{P}{2}+k_2)^2-m_c^2\right]^{\lambda_5}} \tag{B.3}$$

$T_5(\lambda_1,\lambda_2,\lambda_3,\lambda_4,\lambda_5) \equiv$ 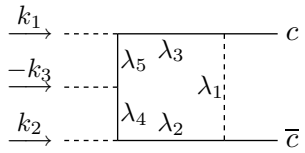

$$= \frac{(2\pi\mu)^{4-D}}{i\pi^2}\int \frac{d^DQ}{\left[Q^2\right]^{\lambda_1}\left[(Q+\frac{P}{2})^2-m_c^2\right]^{\lambda_2}\left[(Q-\frac{P}{2})^2-m_c^2\right]^{\lambda_3}} \times \frac{1}{\left[(Q+\frac{P}{2}-k_2)^2-m_c^2\right]^{\lambda_4}\left[(Q-\frac{P}{2}+k_1)^2-m_c^2\right]^{\lambda_5}} \tag{B.4}$$

$T_7(\lambda_1,\lambda_2,\lambda_3,\lambda_4,\lambda_5) \equiv$ 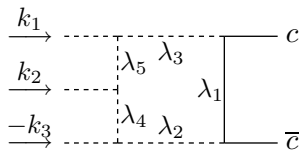

$$= \frac{(2\pi\mu)^{4-D}}{i\pi^2}\int \frac{d^DQ}{\left[Q^2-m_c^2\right]^{\lambda_1}\left[(Q+\frac{P}{2})^2\right]^{\lambda_2}\left[(Q-\frac{P}{2})^2\right]^{\lambda_3}\left[(Q+\frac{P}{2}+k_3)^2\right]^{\lambda_4}} \times \frac{1}{\left[(Q-\frac{P}{2}+k_1)^2\right]^{\lambda_5}} \tag{B.5}$$

$T_8(\lambda_1,\lambda_2,\lambda_3,\lambda_4,\lambda_5) \equiv$ 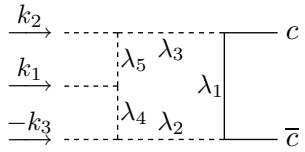

$$= \frac{(2\pi\mu)^{4-D}}{i\pi^2}\int \frac{d^DQ}{\left[Q^2-m_c^2\right]^{\lambda_1}\left[(Q+\frac{P}{2})^2\right]^{\lambda_2}\left[(Q-\frac{P}{2})^2\right]^{\lambda_3}\left[(Q+\frac{P}{2}+k_3)^2\right]^{\lambda_4}} \times \frac{1}{\left[(Q-\frac{P}{2}+k_2)^2\right]^{\lambda_5}} \tag{B.6}$$

$$T_9(\lambda_1,\lambda_2,\lambda_3,\lambda_4,\lambda_5) \equiv$$

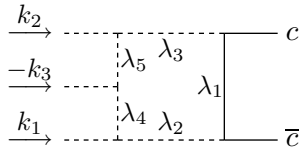

$$= \frac{(2\pi\mu)^{4-D}}{i\pi^2}\int \frac{d^DQ}{\left[Q^2-m_c^2\right]^{\lambda_1}\left[(Q+\frac{P}{2})^2\right]^{\lambda_2}\left[(Q-\frac{P}{2})^2\right]^{\lambda_3}\left[(Q+\frac{P}{2}-k_1)^2\right]^{\lambda_4}} \times \frac{1}{\left[(Q-\frac{P}{2}+k_2)^2\right]^{\lambda_5}} \tag{B.7}$$

$$T_2(\lambda_1,\lambda_2,\lambda_3,\lambda_4,\lambda_5) \equiv$$

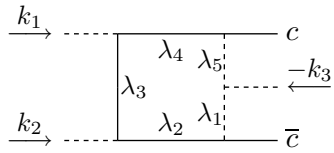

$$= \frac{(2\pi\mu)^{4-D}}{i\pi^2}\int \frac{d^DQ}{\left[Q^2\right]^{\lambda_1}\left[(Q+\frac{P}{2})^2-m_c^2\right]^{\lambda_2}\left[(Q+\frac{P}{2}-k_2)^2-m_c^2\right]^{\lambda_3}} \times \frac{1}{\left[(Q-\frac{P}{2}-k_3)^2-m_c^2\right]^{\lambda_4}\left[(Q-k_3)^2\right]^{\lambda_5}} \tag{B.8}$$

$$T_6(\lambda_1,\lambda_2,\lambda_3,\lambda_4,\lambda_5) \equiv$$

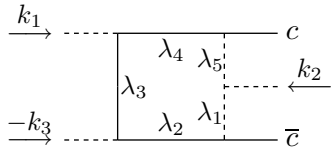

$$= \frac{(2\pi\mu)^{4-D}}{i\pi^2}\int \frac{d^DQ}{\left[Q^2\right]^{\lambda_1}\left[(Q+\frac{P}{2})^2-m_c^2\right]^{\lambda_2}\left[(Q+\frac{P}{2}+k_3)^2-m_c^2\right]^{\lambda_3}} \times \frac{1}{\left[(Q-\frac{P}{2}+k_2)^2-m_c^2\right]^{\lambda_4}\left[(Q+k_2)^2\right]^{\lambda_5}} \tag{B.9}$$

$$T_{12}(\lambda_1,\lambda_2,\lambda_3,\lambda_4,\lambda_5) \equiv$$

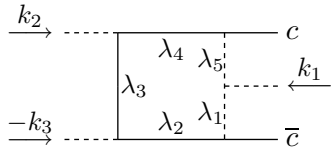

$$= \frac{(2\pi\mu)^{4-D}}{i\pi^2}\int \frac{d^DQ}{\left[Q^2\right]^{\lambda_1}\left[(Q+\frac{P}{2})^2-m_c^2\right]^{\lambda_2}\left[(Q+\frac{P}{2}+k_3)^2-m_c^2\right]^{\lambda_3}} \times \frac{1}{\left[(Q-\frac{P}{2}+k_1)^2-m_c^2\right]^{\lambda_4}\left[(Q+k_1)^2\right]^{\lambda_5}} \tag{B.10}$$

$$T_3(\lambda_1,\lambda_2,\lambda_3,\lambda_4,\lambda_5) \equiv$$

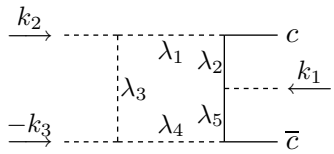

$$= \frac{(2\pi\mu)^{4-D}}{i\pi^2}\int \frac{d^DQ}{\left[Q^2\right]^{\lambda_1}\left[(Q+\frac{P}{2})^2-m_c^2\right]^{\lambda_2}\left[(Q+k_2)^2\right]^{\lambda_3}\left[(Q+P-k_1)^2\right]^{\lambda_4}} \times \frac{1}{\left[(Q+\frac{P}{2}-k_1)^2-m_c^2\right]^{\lambda_5}} \tag{B.11}$$

$$T_{10}(\lambda_1,\lambda_2,\lambda_3,\lambda_4,\lambda_5) \equiv$$

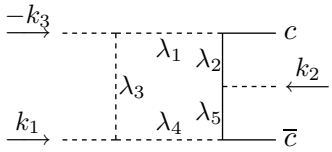

$$= \frac{(2\pi\mu)^{4-D}}{i\pi^2}\int \frac{d^DQ}{\left[Q^2\right]^{\lambda_1}\left[(Q+\frac{P}{2})^2-m_c^2\right]^{\lambda_2}\left[(Q-k_3)^2\right]^{\lambda_3}\left[(Q+P-k_2)^2\right]^{\lambda_4}} \times \frac{1}{\left[(Q+\frac{P}{2}-k_2)^2-m_c^2\right]^{\lambda_5}} \tag{B.12}$$

$$T_{11}(\lambda_1,\lambda_2,\lambda_3,\lambda_4,\lambda_5) \equiv$$

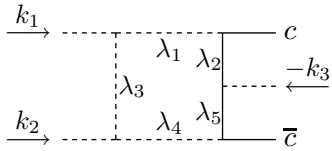

$$= \frac{(2\pi\mu)^{4-D}}{i\pi^2}\int \frac{d^DQ}{\left[Q^2\right]^{\lambda_1}\left[(Q+\frac{P}{2})^2-m_c^2\right]^{\lambda_2}\left[(Q+k_1)^2\right]^{\lambda_3}\left[(Q+P+k_3)^2\right]^{\lambda_4}} \times \frac{1}{\left[(Q+\frac{P}{2}+k_3)^2-m_c^2\right]^{\lambda_5}} \tag{B.13}$$

In our approach, we first derive all integration-by-parts relations for all topologies with FORM. Then we use these relations as input for the MAPLE based program AIR [48], which makes use of the Laporta algorithm [49], to derive expressions for every member of the topologies (in a given range of propagator momenta) explicitly in terms of the corresponding master integrals. Then we use a Mathematica script to simplify these expressions and expand them in ϵ. The resulting expressions are then included into the implementation of our automatic calculation.

For example in case of the topology T_1, all scalar diagrams are reduced to the master integrals

$$\begin{array}{llll} T_1(0,0,1,1,0), & T_1(0,0,1,1,1), & T_1(0,1,0,0,0), & T_1(0,1,0,0,1), \\ T_1(0,1,0,1,1), & T_1(0,1,1,0,1), & T_1(0,1,1,1,0), & T_1(0,1,1,1,1), \\ T_1(1,0,0,0,1), & T_1(1,0,0,1,0), & T_1(1,0,0,1,1), & T_1(1,0,1,0,1), \\ T_1(1,0,1,1,0), & T_1(1,0,1,1,1). & & \end{array}$$

Each of the master integrals of all topologies is easily identified with one (or a simple linear combination of two) of the 14 super master integrals listed in appendix C.

One feature of the integration-by-parts procedure is that after the reduction we can not distinguish between ultraviolet and infrared singularities any more. This can be seen for example from the fact that the reduced expressions contain terms like $T_1(1,0,0,1,0)/\epsilon$, where $T_1(1,0,0,1,0)$ is a scalar bubble diagram with an $\frac{1}{\epsilon}$ ultraviolet pole. Here, the resulting $\frac{1}{\epsilon^2}$ singularity must of course be infrared, but we cannot say anything about the nature of the resulting $\frac{1}{\epsilon}$ singularities. In order to distinguish between ultraviolet and infrared singularities we therefore extract the ultraviolet singularities from the scalar integrals before the application of the integration-by-parts reduction formulas.

C. The 14 super master integrals

At the end of the reduction procedure, the loop corrections are expressed in terms of 14 super master integrals: One tadpole, four bubbles, five triangles and four boxes. In this appendix we list their results. Please note that we neglect all imaginary parts, as only the real parts contribute to the squared amplitudes.

The tadpole diagram reads

$$\text{MasterA} \equiv \frac{(2\pi\mu)^{4-D}}{i\pi^2}\int \frac{d^DQ}{Q^2-m_c^2} = C_\epsilon m_c^2\left[\frac{1}{\epsilon}+1+\left(1+\frac{\pi^2}{12}\right)\epsilon\right]. \tag{C.1}$$

The bubble diagrams are

$$\begin{aligned}\text{MasterB1}(-k_3) &\equiv \frac{(2\pi\mu)^{4-D}}{i\pi^2}\int \frac{d^DQ}{\left[Q^2-m_c^2\right]\left[(Q+P+k_3)^2-m_c^2\right]}\\ &= C_\epsilon\left[\frac{1}{\epsilon}+2+\sqrt{\frac{s_1}{s}}\ln\left(\frac{\sqrt{s}-\sqrt{s_1}}{\sqrt{s}+\sqrt{s_1}}\right)\right]\end{aligned} \tag{C.2}$$

$$\begin{aligned}\text{MasterB2}(k_1) &\equiv \frac{(2\pi\mu)^{4-D}}{i\pi^2}\int \frac{d^DQ}{\left[Q^2-m_c^2\right](Q+\frac{P}{2}-k_1)^2}\\ &= C_\epsilon\left[\frac{1}{\epsilon}+2-\frac{t_1}{t_1+2m_c^2}\ln\left(-\frac{t_1}{2m_c^2}\right)+\frac{\pi^2}{12}\epsilon+\frac{t_1}{t_1+2m_c^2}\left(\ln^2\left(-\frac{t_1}{2m_c^2}\right)\right.\right.\\ &\quad -2\ln\left(-\frac{t_1}{2m_c^2}\right)-\ln\left(-\frac{t_1}{2m_c^2}\right)\ln\left(\left|1+\frac{t_1}{2m_c^2}\right|\right)-\text{Li}_2\left(-\frac{t_1}{2m_c^2}\right)+\frac{8m_c^2}{t_1}\\ &\quad \left.\left.+\frac{\pi^2}{6}+4\right)\epsilon\right]\end{aligned} \tag{C.3}$$

$$\begin{aligned}\text{MasterB3}(k_1) &\equiv \frac{(2\pi\mu)^{4-D}}{i\pi^2}\int \frac{d^DQ}{Q^2(Q+P-k_1)^2}\\ &= C_\epsilon\left[\frac{1}{\epsilon}+2-\ln\left(\frac{-t}{m_c^2}\right)+\left(\frac{1}{2}\ln^2\left(\frac{-t}{m_c^2}\right)-2\ln\left(\frac{-t}{m_c^2}\right)-\frac{\pi^2}{12}+4\right)\epsilon\right]\end{aligned} \tag{C.4}$$

$$\begin{aligned}\text{MasterB4} &\equiv \frac{(2\pi\mu)^{4-D}}{i\pi^2}\int \frac{d^DQ}{Q^2(Q+P)^2}\\ &= C_\epsilon\left[\frac{1}{\epsilon}+2-2\ln 2+\left(2\ln^2 2-4\ln 2-\frac{7}{12}\pi^2+4\right)\epsilon\right].\end{aligned} \tag{C.5}$$

The triangle diagrams read

$$\begin{aligned}
\text{MasterC1}(-k_3) &\equiv \frac{(2\pi\mu)^{4-D}}{i\pi^2}\int \frac{d^DQ}{\left[Q^2-m_c^2\right]\left[(Q+k_1)^2-m_c^2\right]\left[(Q+k_1+k_2)^2-m_c^2\right]} \\
&= -C_\epsilon\frac{1}{s}\left[\text{Li}_2\left(\frac{2\sqrt{s}}{\sqrt{s}+\sqrt{s_1}}\right)+\text{Li}_2\left(\frac{2\sqrt{s}}{\sqrt{s}-\sqrt{s_1}}\right)\right] \qquad \text{(C.6)}
\end{aligned}$$

$$\begin{aligned}
\text{MasterC2}(k_2) &\equiv \frac{(2\pi\mu)^{4-D}}{i\pi^2}\int \frac{d^DQ}{Q^2\left[(Q-\frac{P}{2}-k_3)^2-m_c^2\right]\left[(Q+\frac{P}{2}-k_1)^2-m_c^2\right]} \\
&= C_\epsilon\frac{2}{s_1-t_1}\left[\text{Li}_2\left(1+\frac{t_1}{2m_c^2}\right)-\text{Li}_2\left(1+\frac{s_1}{2m_c^2}\right)\right] \qquad \text{(C.7)}
\end{aligned}$$

$$\begin{aligned}
\text{MasterC3}(k_1) &\equiv \frac{(2\pi\mu)^{4-D}}{i\pi^2}\int \frac{d^DQ}{Q^2\left[(Q+\frac{P}{2})^2-m_c^2\right]\left[(Q+\frac{P}{2}-k_1)^2-m_c^2\right]} \\
&= C_\epsilon\frac{2}{t_1}\left[-\text{Li}_2\left(1+\frac{t_1}{2m_c^2}\right)+\frac{\pi^2}{6}\right] \qquad \text{(C.8)}
\end{aligned}$$

$$\begin{aligned}
\text{MasterC4}(-k_3) &\equiv \frac{(2\pi\mu)^{4-D}}{i\pi^2}\int \frac{d^DQ}{Q^2\left[(Q-\frac{P}{2})^2-m_c^2\right]\left[(Q+\frac{P}{2}+k_3)^2-m_c^2\right]} \\
&= C_\epsilon\frac{2}{s_1}\left[\text{Li}_2\left(1-\frac{s}{2m_c^2}\right)-\text{Li}_2\left(\frac{s_1+s}{s_1+\sqrt{ss_1}}\right)+\text{Li}_2\left(\frac{-4m_c^2}{s_1+\sqrt{ss_1}}\right)\right. \\
&= \left.-\text{Li}_2\left(\frac{s_1+s}{s_1-\sqrt{ss_1}}\right)+\text{Li}_2\left(\frac{-4m_c^2}{s_1-\sqrt{ss_1}}\right)+\frac{\pi^2}{12}\right] \qquad \text{(C.9)}
\end{aligned}$$

$$\begin{aligned}
\text{MasterC5}(k_1) &\equiv \frac{(2\pi\mu)^{4-D}}{i\pi^2}\int \frac{d^DQ}{Q^2\left[(Q-\frac{P}{2})^2-m_c^2\right](Q-P+k_1)^2} \\
&= C_\epsilon\frac{2}{t_1}\left[\frac{1}{2}\ln^2\left(\frac{-t}{2m_c^2}\right)+\text{Li}_2\left(1-\frac{2m_c^2}{t}\right)+\text{Li}_2\left(\frac{t}{4m_c^2}\right)\right. \\
&\quad \left.-\text{Li}_2\left(\frac{2(2m_c^2-t)}{-t}\right)+\frac{5}{12}\pi^2\right]. \qquad \text{(C.10)}
\end{aligned}$$

And the box diagrams are

$$\begin{aligned}
&\text{MasterD1}(-k_3,k_1) \\
&\equiv \frac{(2\pi\mu)^{4-D}}{i\pi^2}\int \frac{d^DQ}{Q^2\left[(Q-\frac{P}{2})^2-m_c^2\right]\left[(Q-\frac{P}{2}+k_1)^2-m_c^2\right]\left[(Q+\frac{P}{2}+k_3)^2-m_c^2\right]} \\
&= C_\epsilon\frac{4}{\sqrt{ts_1t_1}}\left[\text{Li}_2\left(\frac{\sqrt{s_1t}-\sqrt{st_1}}{\sqrt{s_1t}+\sqrt{s_1t_1}}\right)+\text{Li}_2\left(\frac{\sqrt{s_1t}-\sqrt{st_1}}{\sqrt{s_1t}-\sqrt{s_1t_1}}\right)\right. \\
&\quad \left.-\text{Li}_2\left(\frac{\sqrt{s_1t}+\sqrt{st_1}}{\sqrt{s_1t}+\sqrt{s_1t_1}}\right)-\text{Li}_2\left(\frac{\sqrt{s_1t}+\sqrt{st_1}}{\sqrt{s_1t}-\sqrt{s_1t_1}}\right)\right] \qquad \text{(C.11)}
\end{aligned}$$

$$
\begin{aligned}
&\text{MasterD2}(-k_3,k_1)\\
&\equiv \frac{(2\pi\mu)^{4-D}}{i\pi^2}\int \frac{d^DQ}{Q^2(Q-k_3)^2\left[(Q-\frac{P}{2}-k_3)^2-m_c^2\right]\left[(Q-\frac{P}{2}-k_3+k_1)^2-m_c^2\right]}\\
&= C_\epsilon\frac{2}{s_1t_1}\left[\frac{1}{\epsilon^2}+\frac{2}{\epsilon}\left(\ln\left(\frac{-u_1}{2m_c^2}\right)-\ln\left(\frac{-t_1}{2m_c^2}\right)-\ln\left(\frac{s_1}{2m_c^2}\right)\right)+2\ln^2\left(\frac{s_1}{2m_c^2}\right)\right.\\
&\quad +2\ln^2\left(\frac{-t_1}{2m_c^2}\right)-2\ln^2\left(\frac{-u_1}{2m_c^2}\right)+4\text{Li}_2\left(\frac{u_1-s_1}{t_1}\right)+4\text{Li}_2\left(\frac{u_1-t_1}{s_1}\right)\\
&\quad \left.-4\text{Li}_2\left(\frac{(u_1-t_1)(u_1-s_1)}{s_1t_1}\right)-\frac{9}{4}\pi^2\right] \qquad \text{(C.12)}
\end{aligned}
$$

$$
\begin{aligned}
&\text{MasterD3}(k_1,k_2)\\
&\equiv \frac{(2\pi\mu)^{4-D}}{i\pi^2}\int \frac{d^DQ}{\left[Q^2-m_c^2\right](Q-\frac{P}{2})^2(Q-\frac{P}{2}+k_2)^2(Q+\frac{P}{2}-k_1)^2}\\
&= C_\epsilon\frac{2}{tu_1}\left[\frac{3}{2}\frac{1}{\epsilon^2}-\frac{1}{\epsilon}\left(2\ln\left(\frac{-u_1}{2m_c^2}\right)-\ln\left(\frac{-t_1}{2m_c^2}\right)+\ln\left(\frac{-t}{m_c^2}\right)\right)\right.\\
&\quad \left.+2\ln\left(\frac{-u_1}{2m_c^2}\right)\ln\left(\frac{-t}{m_c^2}\right)-\ln^2\left(\frac{-t_1}{2m_c^2}\right)-2\text{Li}_2\left(1-\frac{t_1}{u_1}\right)-\frac{13}{24}\pi^2\right] \qquad \text{(C.13)}
\end{aligned}
$$

$$
\begin{aligned}
&\text{MasterD4}(k_2)\equiv \frac{(2\pi\mu)^{4-D}}{i\pi^2}\int \frac{d^DQ}{Q^2(Q+k_2)^2(Q+k_1+k_2)^2(Q+k_3)^2}\\
&= C_\epsilon\frac{2}{st}\left[\frac{1}{\epsilon^2}-\frac{1}{\epsilon}\ln\left(\frac{-st}{4m_c^2}\right)+\frac{1}{2}\ln^2\left(\frac{-st}{4m_c^2}\right)+\text{Li}_2\left(1-\frac{t}{4m_c^2}\right)\right.\\
&\quad \left.+\text{Li}_2\left(1-\frac{s}{4m_c^2}\right)-\frac{\pi^2}{4}\right]. \qquad \text{(C.14)}
\end{aligned}
$$

We have calculated the tadpole and the bubble diagrams ourselves and compared the results up to $\mathcal{O}(\epsilon^0)$ with [11]. The expressions for the triangle diagrams as well as of the box diagrams MasterD1, MasterD2 and MasterD3 are taken over from [11]. The expression for MasterD4 is taken over from [15, 50]. The triangle diagrams and the box diagram MasterD1 are finite, so that we could check their analytic expressions numerically using LoopTools [51].

MasterA, MasterB2, MasterB3 and MasterB4 have been expanded up to $\mathcal{O}(\epsilon)$, because, as a result of the integration-by-parts procedure, they will be multiplied with $\frac{1}{\epsilon}$ terms, as already mentioned at the end of appendix B. All other super master integrals are expanded only up to $\mathcal{O}(\epsilon^0)$.

The results of the super master integrals for different permutations of the external momenta k_1, k_2 and $-k_3$ can easily be derived by exchanging the Mandelstam invariants

according to

$$\begin{aligned}
&k_1 \leftrightarrow k_2\text{:} && \text{exchange } t \leftrightarrow u \text{ and } t_1 \leftrightarrow u_1 \\
&k_1 \leftrightarrow -k_3\text{:} && \text{exchange } s \leftrightarrow t \text{ and } s_1 \leftrightarrow t_1 \\
&k_2 \leftrightarrow -k_3\text{:} && \text{exchange } s \leftrightarrow u \text{ and } s_1 \leftrightarrow u_1.
\end{aligned}$$

In the case when the invariants are replaced in arguments of logarithms, these have to be analytically continued into the physical regions $s, s_1 > 0$ and $t, t_1, u, u_1 < 0$. Special care must be taken when exchanging the invariants within the arguments of squared logarithms. Here, the imaginary part of the logarithm must not be neglected, because it can lead to an extra term $-\pi^2$, as for example

$$\ln^2(t \pm i\epsilon) = \ln^2(-t) \pm 2i\pi \ln(-t) - \pi^2. \tag{C.15}$$

D. The Born squared matrix elements

In this appendix we list the explicit analytic expressions for all partonic Born squared matrix elements appearing in our calculation, summed (not averaged) over all color and polarization degrees of freedom of all incoming and outgoing particles. We present the results expanded up to the $\mathcal{O}(\epsilon^2)$, as they will be multiplied with $\frac{1}{\epsilon}$ and $\frac{1}{\epsilon^2}$ poles.

The results for the processes $\gamma + q \to c\bar{c}[n] + q$ are given by

$$\sum_{\text{col,pol}} |\mathcal{M}_{\text{Born}}(\gamma + q \to c\bar{c}[^3S_1^{[1]}] + q)|^2 = 0 \tag{D.1}$$

$$\sum_{\text{col,pol}} |\mathcal{M}_{\text{Born}}(\gamma + q \to c\bar{c}[^1S_0^{[8]}] + q)|^2 = -\frac{16 C_A C_F Q_c^2 e^2 g_s^4}{m_c t_1^2 t}(s^2 + u^2) \tag{D.2}$$

$$\begin{aligned}
&\sum_{\text{col,pol}} |\mathcal{M}_{\text{Born}}(\gamma + q \to c\bar{c}[^3S_1^{[8]}] + q)|^2 = \\
&- \frac{2 C_A C_F Q_q^2 e^2 g_s^4}{m_c^3 s u}(t_1^2 + 4t_1 u + 4u^2 - 2t_1 u_1 - 4u u_1 + 2u_1^2) \\
&+ \frac{4 C_A C_F Q_q^2 e^2 g_s^4}{m_c^3 s u}(t_1^2 + 2t_1 u + 2u^2 - t_1 u_1 - 2u u_1 + u_1^2)\epsilon \\
&- \frac{2 C_A C_F Q_q^2 e^2 g_s^4 t_1^2}{m_c^3 s u}\epsilon^2
\end{aligned} \tag{D.3}$$

$$\begin{aligned}
&\sum_{\text{col,pol}} |\mathcal{M}_{\text{Born}}(\gamma + q \to c\bar{c}[^3P_0^{[8]}] + q)|^2 = \\
&\quad - \frac{16 C_A C_F Q_c^2 e^2 g_s^4}{3 m_c^3 t t_1^4}(s^2 + u^2)(t_1 - 2u + 2u_1)^2 \\
&\quad + \frac{16 C_A C_F Q_c^2 e^2 g_s^4}{9 m_c^3 t t_1^4}(t_1^2 - 4t_1 u - 4u^2)(t_1 - 2u + 2u_1)^2\epsilon \\
&\quad + \frac{32 C_A C_F Q_c^2 e^2 g_s^4}{27 m_c^3 t t_1^4}(t_1^2 - 4t_1 u - 4u^2)(t_1 - 2u + 2u_1)^2\epsilon^2
\end{aligned} \tag{D.4}$$

$$\begin{aligned}
&\sum_{\text{col,pol}} |\mathcal{M}_{\text{Born}}(\gamma + q \to c\bar{c}[^3P_1^{[8]}] + q)|^2 = \\
&\quad - \frac{32 C_A C_F Q_c^2 e^2 g_s^4}{m_c^3 t_1^4}(t_1^3 + t_1^2(3u - u_1) + 2t_1 u u_1 + 2u^2(-u + u_1))
\end{aligned}$$

$$
\begin{aligned}
&+ \quad \frac{32 C_A C_F Q_c^2 e^2 g_s^4}{m_c^3 t_1^3}(3t_1^2 + 7t_1 u + 4u^2 - 3t_1 u_1)\epsilon \\
&- \quad \frac{64 C_A C_F Q_c^2 e^2 g_s^4 t}{m_c^3 t_1^2}\epsilon^2
\end{aligned} \tag{D.5}
$$

$$
\begin{aligned}
&\sum_{\text{col,pol}} |\mathcal{M}_{\text{Born}}(\gamma + q \to c\overline{c}[^3P_2^{[8]}] + q)|^2 = \\
&- \quad \frac{32 C_A C_F Q_c^2 e^2 g_s^4}{3 m_c^3 t^2 t_1^4}\big(t_1^5 + t_1^4(5u - 3u_1) + 2u^2(u-u_1)^3 - 2t_1 u(u-u_1)^2(2u+u_1) \\
&\quad + t_1^3(5u^2 - 12uu_1 + 9u_1^2) - t_1^2(5u^3 + 3u^2 u_1 - 15uu_1^2 + 7u_1^3)\big) \\
&+ \quad \frac{32 C_A C_F Q_c^2 e^2 g_s^4}{9 m_c^3 t^2 t_1^4}\big(4t_1^5 + t_1^4(8u - 6u_1) + 8u^2(u-u_1)^3 - 4t_1 u(u-u_1)^2(7u+2u_1) \\
&\quad + t_1^3(5u^2 - 48uu_1 + 45u_1^2) - t_1^2(35u^3 + 15u^2 u_1 - 93uu_1^2 + 43u_1^3)\big)\epsilon \\
&- \quad \frac{32 C_A C_F Q_c^2 e^2 g_s^4}{27 m_c^3 t^2 t_1^4}\big(t_1^5 - 16t_1 u(u-u_1)^3 - 16u^2(u-u_1)^3 + t_1^4(-7u + 3u_1) \\
&\quad + 2t_1^3(31u^2 - 60uu_1 + 27u_1^2) + 2t_1^2(35u^3 - 93u^2 u_1 + 87uu_1^2 - 29u_1^3)\big)\epsilon^2.
\end{aligned} \tag{D.6}
$$

We have calculated the following results for the processes $\gamma + g \to c\overline{c}[n] + g$ according to (3.18). We have taken the complete polarization sum (3.19) and subtracted the respective ghost contributions.

$$
\begin{aligned}
&\sum_{\text{col,pol}} |\mathcal{M}_{\text{Born}}(\gamma + g \to c\overline{c}[^3S_1^{[1]}] + g)|^2 = \\
&+ \quad \frac{256(C_A - 2C_F) C_F Q_c^2 e^2 g_s^4 m_c}{s_1^2 t_1^2 u_1^2}(s^2 s_1^2 + t^2 t_1^2 + u^2 u_1^2) \\
&- \quad \frac{64(C_A - 2C_F) C_F Q_c^2 e^2 g_s^4}{m_c s_1^2 t_1^2 u_1^2}\big(4t_1^4(u - u_1) + 8t_1^3(2u^2 - 3uu_1 + u_1^2) \\
&\quad + t_1^2(27u^3 - 46u^2 u_1 + 23uu_1^2 - 4u_1^3) + u^2(7u^3 - 13u^2 u_1 + 9uu_1^2 - 3u_1^3) \\
&\quad + t_1 u(22u^3 - 39u^2 u_1 + 20uu_1^2 - 3u_1^3)\big)\epsilon \\
&+ \quad \frac{512(C_A - 2C_F) C_F Q_c^2 e^2 g_s^4 m_c}{s_1^2 t_1^2 u_1^2}\big(t_1^4 + t_1^3(4u - 2u_1) + 2t_1 u(-2u + u_1)^2 \\
&\quad + t_1^2(8u^2 - 6uu_1 + u_1^2) + u^2(3u^2 - 4uu_1 + 2u_1^2)\big)\epsilon^2
\end{aligned} \tag{D.7}
$$

$$
\begin{aligned}
&\sum_{\text{col,pol}} |\mathcal{M}_{\text{Born}}(\gamma + g \to c\overline{c}[^1S_0^{[8]}] + g)|^2 = \\
&+ \quad \frac{32 C_A^2 C_F Q_c^2 e^2 g_s^4 su}{m_c t s_1^2 t_1^2 u_1^2}(s^4 + t^4 + u^4 + (u - u_1)^4) \\
&- \quad \frac{64 C_A^2 C_F e^2 g_s^4 Q_c^2 su}{m_c s_1^2 t t_1^2 u_1^2}\big(t_1^4 + t_1^3(4u - 2u_1) + 2t_1 u(-2u + u_1)^2
\end{aligned}
$$

$$+t_1^2(8u^2-6uu_1+u_1^2)+u^2(3u^2-4uu_1+2u_1^2)\big)\epsilon \tag{D.8}$$

$$\sum_{\text{col,pol}} |\mathcal{M}_{\text{Born}}(\gamma+g\to c\overline{c}[^3S_1^{[8]}]+g)|^2 =$$

$$\begin{aligned}
&+\ \frac{256(C_A^2-4)C_FQ_c^2e^2g_s^4m_c}{s_1^2t_1^2u_1^2}(s^2s_1^2+t^2t_1^2+u^2u_1^2)\\
&-\ \frac{64(C_A^2-4)C_FQ_c^2e^2g_s^4}{m_cs_1^2t_1^2u_1^2}\big(4t_1^4(u-u_1)+8t_1^3(2u^2-3uu_1+u_1^2)\\
&\quad +t_1^2(27u^3-46u^2u_1+23uu_1^2-4u_1^3)+u^2(7u^3-13u^2u_1+9uu_1^2-3u_1^3)\\
&\quad +t_1u(22u^3-39u^2u_1+20uu_1^2-3u_1^3)\big)\epsilon\\
&+\ \frac{512(C_A^2-4)C_FQ_c^2e^2g_s^4m_c}{s_1^2t_1^2u_1^2}\big(t_1^4+t_1^3(4u-2u_1)+2t_1u(-2u+u_1)^2\\
&\quad +t_1^2(8u^2-6uu_1+u_1^2)+u^2(3u^2-4uu_1+2u_1^2)\big)\epsilon^2
\end{aligned} \tag{D.9}$$

$$\sum_{\text{col,pol}} |\mathcal{M}_{\text{Born}}(\gamma+g\to c\overline{c}[^3P_0^{[8]}]+g)|^2 =$$

$$\begin{aligned}
&+\ \frac{64C_A^2C_FQ_c^2e^2g_s^4su}{3m_c^3s_1^4t^2t_1^4u_1^4}\big(t_1^9(2u-3u_1)^2+4u^4(u-u_1)^3u_1^2(-2u+u_1)^2+t_1^8(36u^3\\
&\quad -132u^2u_1+151uu_1^2-51u_1^3)+8t_1u^3(u-u_1)^3u_1(2u^3+3u^2u_1-4uu_1^2+u_1^3)\\
&\quad +2t_1^7(68u^4-292u^3u_1+448u^2u_1^2-293uu_1^3+73u_1^4)+2t_1^6(140u^5-680u^4u_1\\
&\quad +1304u^3u_1^2-1264u^2u_1^3+636uu_1^4-131u_1^5)+2t_1^5(170u^6-902u^5u_1\\
&\quad +2068u^4u_1^2-2685u^3u_1^3+2071u^2u_1^4-869uu_1^5+151u_1^6)+2t_1^4(122u^7\\
&\quad -674u^6u_1+1795u^5u_1^2-3005u^4u_1^3+3225u^3u_1^4-2089u^2u_1^5+737uu_1^6\\
&\quad -109u_1^7)+t_1^3(96u^8-496u^7u_1+1520u^6u_1^2-3380u^5u_1^3+4940u^4u_1^4\\
&\quad -4454u^3u_1^5+2398u^2u_1^6-714uu_1^7+91u_1^8)+t_1^2(16u^9-40u^8u_1+172u^7u_1^2\\
&\quad -748u^6u_1^3+1602u^5u_1^4-1894u^4u_1^5+1358u^3u_1^6-602u^2u_1^7+153uu_1^8-17u_1^9)\big)\\
&-\ \frac{64C_A^2C_FQ_c^2e^2g_s^4su}{9m_c^3s_1^4t^2t_1^4u_1^4}\big(t_1^9(2u-3u_1)^2+4u^4(u-u_1)^3u_1^2(-2u+u_1)^2+t_1^8(36u^3\\
&\quad -132u^2u_1+151uu_1^2-51u_1^3)-8t_1u^2(u-u_1)^3u_1(4u^4-36u^3u_1+55u^2u_1^2\\
&\quad -31uu_1^3+6u_1^4)+t_1^7(136u^4-572u^3u_1+881u^2u_1^2-604uu_1^3+167u_1^4)\\
&\quad +t_1^6(280u^5-1276u^4u_1+2449u^3u_1^2-2585u^2u_1^3+1491uu_1^4-349u_1^5)\\
&\quad +t_1^5(340u^6-1600u^5u_1+3683u^4u_1^2-5460u^3u_1^3+4967u^2u_1^4-2362uu_1^5\\
&\quad +440u_1^6)+t_1^4(244u^7-1168u^6u_1+3353u^5u_1^2-6859u^4u_1^3+8661u^3u_1^4\\
&\quad -6119u^2u_1^5+2212uu_1^6-320u_1^7)+t_1^3(96u^8-520u^7u_1+2252u^6u_1^2\\
&\quad -6218u^5u_1^3+9593u^4u_1^4-8378u^3u_1^5+4156u^2u_1^6-1104uu_1^7+124u_1^8)\\
&\quad +t_1^2(16u^9-160u^8u_1+1240u^7u_1^2-4132u^6u_1^3+6957u^5u_1^4-6601u^4u_1^5\\
&\quad +3692u^3u_1^6-1220u^2u_1^7+228uu_1^8-20u_1^9)\big)\epsilon
\end{aligned}$$

$$
\begin{aligned}
- \quad & \frac{128C_A^2C_FQ_c^2e^2g_s^4su}{27m_c^3s_1^4t^2t_1^4u_1^4}\big(t_1^9(2u-3u_1)^2+4u^4(u-u_1)^3u_1^2(-2u+u_1)^2+t_1^8(36u^3 \\
& -132u^2u_1+151uu_1^2-51u_1^3)-8t_1u^2(u-u_1)^3u_1(4u^4-36u^3u_1+55u^2u_1^2 \\
& -31uu_1^3+6u_1^4)+t_1^7(136u^4-572u^3u_1+881u^2u_1^2-604uu_1^3+167u_1^4) \\
& +t_1^6(280u^5-1276u^4u_1+2449u^3u_1^2-2585u^2u_1^3+1491uu_1^4-349u_1^5) \\
& +t_1^5(340u^6-1600u^5u_1+3683u^4u_1^2-5460u^3u_1^3+4967u^2u_1^4-2362uu_1^5 \\
& +440u_1^6)+t_1^4(244u^7-1168u^6u_1+3353u^5u_1^2-6859u^4u_1^3+8661u^3u_1^4 \\
& -6119u^2u_1^5+2212uu_1^6-320u_1^7)+t_1^3(96u^8-520u^7u_1+2252u^6u_1^2 \\
& -6218u^5u_1^3+9593u^4u_1^4-8378u^3u_1^5+4156u^2u_1^6-1104uu_1^7+124u_1^8) \\
& +t_1^2(16u^9-160u^8u_1+1240u^7u_1^2-4132u^6u_1^3+6957u^5u_1^4-6601u^4u_1^5 \\
& +3692u^3u_1^6-1220u^2u_1^7+228uu_1^8-20u_1^9)\big)\epsilon^2 \qquad \text{(D.10)}
\end{aligned}
$$

$$
\sum_{\text{col,pol}} |\mathcal{M}_{\text{Born}}(\gamma+g\to c\bar{c}[^3P_1^{[8]}]+g)|^2 =
$$

$$
\begin{aligned}
+ \quad & \frac{64C_A^2C_FQ_c^2e^2g_s^4}{m_c^3s_1^4t_1^4u_1^4}\big(2u^6(u-u_1)u_1^2(-2u+u_1)^2+t_1^8(2u^3-8u^2u_1+5uu_1^2-u_1^3) \\
& +2t_1^7(8u^4-36u^3u_1+35u^2u_1^2-14uu_1^3+2u_1^4)+t_1^6(52u^5-272u^4u_1+348u^3u_1^2 \\
& -202u^2u_1^3+56uu_1^4-6u_1^5)-2t_1u^4u_1(12u^5-50u^4u_1+74u^3u_1^2-48u^2u_1^3 \\
& +15uu_1^4-2u_1^5)+t_1^5(88u^6-556u^5u_1+872u^4u_1^2-646u^3u_1^3+252u^2u_1^4 \\
& -50uu_1^5+4u_1^6)+t_1^2u^2(8u^7-164u^6u_1+454u^5u_1^2-554u^4u_1^3+343u^3u_1^4 \\
& -117u^2u_1^5+22uu_1^6-2u_1^7)+2t_1^3u(20u^7-226u^6u_1+503u^5u_1^2-524u^4u_1^3 \\
& +292u^3u_1^4-91u^2u_1^5+15uu_1^6-u_1^7)+t_1^4(82u^7-660u^6u_1+1233u^5u_1^2 \\
& -1097u^4u_1^3+528u^3u_1^4-140u^2u_1^5+19uu_1^6-u_1^7)\big) \\
- \quad & \frac{64C_A^2C_FQ_c^2e^2g_s^4}{m_c^3s_1^4t_1^4u_1^4}\big(2u^6(u-u_1)u_1^2(-2u+u_1)^2+2t_1^8(u^3-8u^2u_1+5uu_1^2-u_1^3) \\
& +2t_1^7(8u^4-68u^3u_1+69u^2u_1^2-28uu_1^3+4u_1^4)+t_1^6(52u^5-496u^4u_1+667u^3u_1^2 \\
& -394u^2u_1^3+111uu_1^4-12u_1^5)-2t_1u^4u_1(28u^5-90u^4u_1+122u^3u_1^2-80u^2u_1^3 \\
& +27uu_1^4-4u_1^5)+t_1^5(88u^6-1004u^5u_1+1638u^4u_1^2-1223u^3u_1^3+482u^2u_1^4 \\
& -97uu_1^5+8u_1^6)+t_1^2u^2(8u^7-340u^6u_1+862u^5u_1^2-994u^4u_1^3+605u^3u_1^4 \\
& -205u^2u_1^5+37uu_1^6-3u_1^7)+t_1^3u(40u^7-868u^6u_1+1894u^5u_1^2-1912u^4u_1^3 \\
& +1046u^3u_1^4-319u^2u_1^5+50uu_1^6-3u_1^7)+t_1^4(82u^7-1212u^6u_1+2303u^5u_1^2 \\
& -2029u^4u_1^3+972u^3u_1^4-257u^2u_1^5+35uu_1^6-2u_1^7)\big)\epsilon \\
+ \quad & \frac{64C_A^2C_FQ_c^2e^2g_s^4}{m_c^3s_1^3t_1^3u_1^3}\big(t_1^6(8u^2-5uu_1+u_1^2)+t_1^5(48u^3-50u^2u_1+21uu_1^2-3u_1^3) \\
& +4u^4(6u^4-14u^3u_1+15u^2u_1^2-8uu_1^3+2u_1^4)+t_1^4(136u^4-184u^3u_1 \\
& +106u^2u_1^2-29uu_1^3+3u_1^4)+t_1u^2(112u^5-234u^4u_1+221u^3u_1^2-107u^2u_1^3 \\
& +26uu_1^4-2u_1^5)+t_1^2u(216u^5-399u^4u_1+327u^3u_1^2-138u^2u_1^3+28uu_1^4-2u_1^5)
\end{aligned}
$$

$$+t_1^3(224u^5-360u^4u_1+252u^3u_1^2-90u^2u_1^3+15uu_1^4-u_1^5)\big)\epsilon^2 \tag{D.11}$$

$$\sum_{\text{col,pol}} |\mathcal{M}_{\text{Born}}(\gamma+g\to c\overline{c}[^3P_2^{[8]}]+g)|^2 =$$

$$\begin{aligned}
&- \frac{64C_A^2C_FQ_c^2e^2g_s^4}{3m_c^3s_1^4t^2t_1^4u_1^4}\big(2u^6(u-u_1)^3u_1^2(-2u+u_1)^2+t_1^{10}(2u^3-3uu_1^2+3u_1^3)\\
&+2t_1^9(10u^4-6u^3u_1-14u^2u_1^2+24uu_1^3-9u_1^4)+2t_1u^4(u-u_1)^2u_1(52u^5\\
&-198u^4u_1+302u^3u_1^2-246u^2u_1^3+105uu_1^4-18u_1^5)+t_1^8(86u^5-76u^4u_1\\
&-105u^3u_1^2+259u^2u_1^3-185uu_1^4+45u_1^5)+2t_1^7(104u^6-78u^5u_1-171u^4u_1^2\\
&+375u^3u_1^3-343u^2u_1^4+161uu_1^5-30u_1^6)+t_1^6(310u^7+20u^6u_1-1263u^5u_1^2\\
&+1829u^4u_1^3-1412u^3u_1^4+788u^2u_1^5-281uu_1^6+45u_1^7)+2t_1^5(146u^8+322u^7u_1\\
&-1736u^6u_1^2+2303u^5u_1^3-1441u^4u_1^4+549u^3u_1^5-174u^2u_1^6+52uu_1^7-9u_1^8)\\
&+t_1^2u^2(8u^9+540u^8u_1-2890u^7u_1^2+6246u^6u_1^3-7309u^5u_1^4+5029u^4u_1^5\\
&-1969u^3u_1^6+337u^2u_1^7+18uu_1^8-10u_1^9)+2t_1^3u(28u^9+574u^8u_1-2805u^7u_1^2\\
&+5130u^6u_1^3-4828u^5u_1^4+2472u^4u_1^5-570u^3u_1^6-38u^2u_1^7+43uu_1^8-5u_1^9)\\
&+t_1^4(170u^9+1244u^8u_1-5803u^7u_1^2+8859u^6u_1^3-6482u^5u_1^4+2338u^4u_1^5\\
&-263u^3u_1^6-61u^2u_1^7+5uu_1^8+3u_1^9)\big)\\
&+ \frac{64C_A^2C_FQ_c^2e^2g_s^4}{9m_c^3s_1^4t^2t_1^4u_1^4}\big(14u^6(u-u_1)^3u_1^2(-2u+u_1)^2+2t_1^{10}(7u^3-12u^2u_1+9u_1^3)\\
&+2t_1^9(70u^4-162u^3u_1+73u^2u_1^2+93uu_1^3-54u_1^4)+2t_1u^4(u-u_1)^2u_1(268u^5\\
&-906u^4u_1+1154u^3u_1^2-822u^2u_1^3+339uu_1^4-60u_1^5)+t_1^8(602u^5-1564u^4u_1\\
&+1317u^3u_1^2+250u^2u_1^3-779uu_1^4+270u_1^5)+t_1^7(1456u^6-3588u^5u_1\\
&+4014u^4u_1^2-1833u^3u_1^3-794u^2u_1^4+1249uu_1^5-360u_1^6)+t_1^6(2170u^7\\
&-3676u^6u_1+3318u^5u_1^2-5095u^4u_1^3+4648u^3u_1^4-655u^2u_1^5-836uu_1^6\\
&+270u_1^7)+t_1^5(2044u^8+428u^7u_1-8386u^6u_1^2+2725u^5u_1^3+10762u^4u_1^4\\
&-10473u^3u_1^5+3090u^2u_1^6+14uu_1^7-108u_1^8)+t_1^2u^2(56u^9+2820u^8u_1\\
&-14134u^7u_1^2+26898u^6u_1^3-25711u^5u_1^4+12637u^4u_1^5-1996u^3u_1^6-1106u^2u_1^7\\
&+633uu_1^8-97u_1^9)+t_1^3u(392u^9+5828u^8u_1-26910u^7u_1^2+40824u^6u_1^3\\
&-24542u^5u_1^4-357u^4u_1^5+8622u^3u_1^6-4930u^2u_1^7+1178uu_1^8-97u_1^9)\\
&+t_1^4(1190u^9+5324u^8u_1-24577u^7u_1^2+26523u^6u_1^3-1262u^5u_1^4-15293u^4u_1^5\\
&+10948u^3u_1^6-3094u^2u_1^7+263uu_1^8+18u_1^9)\big)\epsilon\\
&- \frac{64C_A^2C_FQ_c^2e^2g_s^4}{27m_c^3s_1^4t^2t_1^4u_1^4}\big(8u^6(u-u_1)^3u_1^2(-2u+u_1)^2+t_1^{10}(8u^3-24u^2u_1-9uu_1^2\\
&+27u_1^3)+2t_1^9(40u^4-144u^3u_1+25u^2u_1^2+165uu_1^3-81u_1^4)\\
&+4t_1u^4(u-u_1)^2u_1(308u^5-966u^4u_1+1024u^3u_1^2-537u^2u_1^3+174uu_1^4\\
&-30u_1^5)+t_1^8(344u^5-760u^4u_1-231u^3u_1^2+1525u^2u_1^3-1259uu_1^4+405u_1^5)\\
&+2t_1^7(416u^6+744u^5u_1-4068u^4u_1^2+4425u^3u_1^3-2203u^2u_1^4+974uu_1^5
\end{aligned}$$

$$
\begin{aligned}
&-270u_1^6) + t_1^6(1240u^7 + 11744u^6u_1 - 42033u^5u_1^2 + 45065u^4u_1^3 - 18674u^3u_1^4 \\
&+3650u^2u_1^5 - 1361uu_1^6 + 405u_1^7) + 2t_1^5(584u^8 + 13432u^7u_1 - 50015u^6u_1^2 \\
&+63254u^5u_1^3 - 33433u^4u_1^4 + 5802u^3u_1^5 + 357u^2u_1^6 + 112uu_1^7 - 81u_1^8) \\
&+t_1^2u^2(32u^9 + 8040u^8u_1 - 38548u^7u_1^2 + 72744u^6u_1^3 - 69907u^5u_1^4 \\
&+35917u^4u_1^5 - 8509u^3u_1^6 - 281u^2u_1^7 + 606uu_1^8 - 94u_1^9) + 2t_1^3u(112u^9 \\
&+10984u^8u_1 - 48564u^7u_1^2 + 82125u^6u_1^3 - 67690u^5u_1^4 + 26574u^4u_1^5 \\
&-2223u^3u_1^6 - 1865u^2u_1^7 + 595uu_1^8 - 47u_1^9) + t_1^4(680u^9 + 32264u^8u_1 \\
&-130783u^7u_1^2 + 193761u^6u_1^3 - 131378u^5u_1^4 + 35968u^4u_1^5 + 1855u^3u_1^6 \\
&-2605u^2u_1^7 + 221uu_1^8 + 27u_1^9)\big)\epsilon^2
\end{aligned}
\tag{D.12}
$$

For the calculation of the hard collinear part of the real corrections due to the splitting of the initial photon, we also need the Born level squared matrix elements of the processes $q + g \to c\overline{c}[n] + q$ and $q + \overline{q} \to c\overline{c}[n] + g$. We present their results expanded only up to $\mathcal{O}(\epsilon)$, as they are multiplied only by $\frac{1}{\epsilon}$ poles, see (5.104).

$$
|\mathcal{M}_{\text{Born}}(q + g \to c\overline{c}[^3S_1^{[1]}] + q)|^2 = 0 \tag{D.13}
$$

$$
|\mathcal{M}_{\text{Born}}(q + g \to c\overline{c}[^1S_0^{[8]}] + q)|^2 = \frac{4(4 - C_A^2)C_F g_s^6}{m_c u u_1^2}(2t^2 + 2tu_1 + u_1^2) \tag{D.14}
$$

$$
\begin{aligned}
&|\mathcal{M}_{\text{Born}}(q + g \to c\overline{c}[^3S_1^{[8]}] + q)|^2 = \\
&+ \quad \frac{C_F g_s^6 u}{4m_c^5 st}(3t^2 + 2t_1^2 + t(-4t_1 + u_1)) \\
&+ \quad \frac{C_A C_F^2 g_s^6}{2m_c^5 st}(-t^3 + t^2t_1 + tt_1u_1 + t_1u_1^2) \\
&- \quad \frac{C_A^2 C_F g_s^6}{4m_c^5 stu_1^2}\big(8t^5 - 16t^4(t_1 - u_1) + 2t_1^2u_1^2(-t_1 + u_1) + t^3(12t_1^2 - 28t_1u_1 + 13u_1^2) \\
&\quad +tu_1(-4t_1^3 + 10t_1^2u_1 - 7t_1u_1^2 + u_1^3) + t^2(-4t_1^3 + 16t_1^2u_1 - 21t_1u_1^2 + 6u_1^3)\big)
\end{aligned}
\tag{D.15}
$$

$$
\begin{aligned}
&|\mathcal{M}_{\text{Born}}(q + g \to c\overline{c}[^3P_0^{[8]}] + q)|^2 = \\
&+ \quad \frac{4(4 - C_A^2)C_F g_s^6}{3m_c^3 uu_1^4}(2u - 3u_1)^2(2t^2 + 2tu_1 + u_1^2)
\end{aligned}
\tag{D.16}
$$

$$
\begin{aligned}
&|\mathcal{M}_{\text{Born}}(q + g \to c\overline{c}[^3P_1^{[8]}] + q)|^2 = \\
&+ \quad \frac{8(4 - C_A^2)C_F g_s^6}{m_c^3 u_1^4}(2t^2(-t + t_1) + 2tt_1u_1 + (3t - t_1)u_1^2 + u_1^3)
\end{aligned}
\tag{D.17}
$$

$$
\begin{aligned}
&|\mathcal{M}_{\rm Born}(q+g\to c\overline{c}[^3P_2^{[8]}]+q)|^2 = \\
&+\quad \frac{8(4-C_A^2)C_F g_s^6}{3m_c^3 u u_1^4}(2u^4-14u^3u_1+31u^2u_1^2-24uu_1^3+6u_1^4+2t_1^2(u^2-6uu_1 \\
&\quad +6u_1^2)+2t_1(2u^3-13u^2u_1+18uu_1^2-6u_1^3)) \qquad \text{(D.18)}
\end{aligned}
$$

The corresponding results for the processes $q+\overline{q}\to c\overline{c}[n]+g$ can be obtained from (D.13) till (D.18) simply by crossing the external particles accordingly. Just exchange $s\leftrightarrow u$ and $s_1\leftrightarrow u_1$ and add an overall factor (-1).

E. Explicit results for the soft #2 terms

In this appendix we list the explicit results of the $\mathcal{S}$ terms defined in (5.69), which build up the soft #2 terms. The expressions listed here are expanded up to $\mathcal{O}(\epsilon)$, because $\mathcal{S}$ will be multiplied by the $\frac{1}{\epsilon}$ pole in (5.68).

The results for the processes $\gamma + q \to c\bar{c}[n] + q + g$ are

$$\begin{aligned}
\mathcal{S}({}^3P_0^{[8]}) = & \frac{16(C_A^2-4)C_F Q_q Q_c e^2 g_s^4 s}{3 m_c s_1 t_1^2 u_1}\big(t_1^3 + 4u^2(u_1-u) + t_1^2(u+u_1) \\
& -2t_1(2u^2 - 4uu_1 + u_1^2)\big) \\
+ & \frac{16(4-C_A^2)C_F Q_q Q_c e^2 g_s^4}{9 m_c s_1 t_1^2 u_1}\big(t_1^3 + 8u^2(u-u_1) - 2t_1^2(u+u1) \\
& -4t_1(u^2 - 2uu_1 + 2u_1^2)\big)\,\epsilon
\end{aligned} \tag{E.1}$$

$$\begin{aligned}
\mathcal{S}({}^3P_1^{[8]}) = & \frac{16(4-C_A^2)C_F Q_q Q_c e^2 g_s^4}{m_c s_1 t_1^2 u_1}\big(t_1^3 + t_1^2(6u-4u_1) + t_1(11u^2 - 16uu_1 + 7u_1^2) \\
& +2(3u^3 - 7u^2u_1 + 6uu_1^2 - 2u_1^3)\big) \\
+ & \frac{32(C_A^2-4)C_F Q_q Q_c e^2 g_s^4}{m_c s_1 t_1^2 u_1}\big(t_1^3 + 4u^3 + t_1^2(5u-3u_1) - 8u^2u_1 + 6uu_1^2 - 2u_1^3 \\
& +2t_1(4u^2 - 5uu_1 + 2u_1^2)\big)\,\epsilon
\end{aligned} \tag{E.2}$$

$$\begin{aligned}
\mathcal{S}({}^3P_2^{[8]}) = & \frac{16(4-C_A^2)C_F Q_q Q_c e^2 g_s^4}{3 m_c s_1 t_1^2 u_1}\big(t_1^3 + 26u^3 + 2t_1^2(5u-4u_1) - 50u^2u_1 + 36uu_1^2 \\
& -12u_1^3 + t_1(29u^2 - 40uu_1 + 13u_1^2)\big) \\
+ & \frac{16(C_A^2-4)C_F Q_q Q_c e^2 g_s^4}{9 m_c s_1 t_1^2 u_1}\big(t_1^3 + 4t_1^2(4u-5u_1) + 4t_1(17u^2 - 25uu_1 + 7u_1^2) \\
& +4(20u^3 - 38u^2u_1 + 27uu_1^2 - 9u_1^3)\big)\epsilon.
\end{aligned} \tag{E.3}$$

The results for the processes $\gamma + g \to c\bar{c}[n] + g + g$ are given by

$$\begin{aligned}
\mathcal{S}({}^3P_0^{[8]}) = & \frac{-256 C_A^3 C_F Q_c^2 e^2 g_s^4 m_c s u}{3 s_1^4 t_1^3 u_1^4}\big(t_1^6(4u-6u_1) + 4u^4u_1(2u^2 - 3uu_1 + u_1^2) \\
& +t_1^5(28u^2 - 60uu_1 + 26u_1^2) + t_1^4(76u^3 - 208u^2u_1 + 177uu_1^2 - 55u_1^3) \\
& +2t_1^3(50u^4 - 162u^3u_1 + 205u^2u_1^2 - 131uu_1^3 + 33u_1^4) \\
& +t_1^2(64u^5 - 226u^4u_1 + 384u^3u_1^2 - 388u^2u_1^3 + 201uu_1^4 - 41u_1^5) \\
& +2t_1(8u^6 - 24u^5u_1 + 55u^4u_1^2 - 88u^3u_1^3 + 73u^2u_1^4 - 30uu_1^5 + 5u_1^6)\big)
\end{aligned}$$

$$
\begin{aligned}
+ \quad & \frac{512C_A^3C_FQ_c^2e^2g_s^4m_csu}{9s_1^4t_1^3u_1^4}\big(t_1^6(2u-3u_1)+t_1^5(14u^2-30uu_1+13u_1^2) \\
& +t_1^4(38u^3-104u^2u_1+96uu_1^2-35u_1^3) \\
& -2u^2u_1(4u^4-18u^3u_1+26u^2u_1^2-15uu_1^3+3u_1^4) \\
& +t_1^3(50u^4-159u^3u_1+232u^2u_1^2-179uu_1^3+51u_1^4) \\
& +t_1^2(32u^5-110u^4u_1+231u^3u_1^2-287u^2u_1^3+165uu_1^4-34u_1^5) \\
& +t_1(8u^6-36u^5u_1+112u^4u_1^2-184u^3u_1^3+145u^2u_1^4-54uu_1^5+8u_1^6)\big)\epsilon \qquad \text{(E.4)}
\end{aligned}
$$

$$
\begin{aligned}
\mathcal{S}({}^3P_1^{[8]}) = & \frac{-256C_A^3C_FQ_c^2e^2g_s^4m_c}{s_1^4t_1^3u_1^4}\big(2t_1^7(u^2-3uu_1+u_1^2) \\
& +t_1^6(16u^3-55u^2u_1+39uu_1^2-8u_1^3) \\
& -2u^4u_1(6u^4-17u^3u_1+19u^2u_1^2-10uu_1^3+2u_1^4) \\
& +t_1^5(52u^4-210u^3u_1+215u^2u_1^2-85uu_1^3+12u_1^4) \\
& +t_1^4(88u^5-428u^4u_1+561u^3u_1^2-314u^2u_1^3+81uu_1^4-8u_1^5) \\
& +t_1^3(82u^6-496u^5u_1+794u^4u_1^2-562u^3u_1^3+197u^2u_1^4-33uu_1^5+2u_1^6) \\
& +t_1^2u(40u^6-321u^5u_1+616u^4u_1^2-525u^3u_1^3+227u^2u_1^4-49uu_1^5+4u_1^6) \\
& +t_1u^2(8u^6-104u^5u_1+239u^4u_1^2-238u^3u_1^3+121u^2u_1^4-32uu_1^5+4u_1^6)\big) \\
+ \quad & \frac{256C_A^3C_FQ_c^2e^2g_s^4m_c}{s_1^4t_1^3u_1^4}\big(2t_1^7(u^2-6uu_1+2u_1^2) \\
& +t_1^6(16u^3-101u^2u_1+77uu_1^2-16u_1^3) \\
& -2u^4u_1(14u^4-37u^3u_1+39u^2u_1^2-20uu_1^3+4u_1^4) \\
& +t_1^5(52u^4-364u^3u_1+405u^2u_1^2-165uu_1^3+24u_1^4) \\
& +t_1^4(88u^5-722u^4u_1+1019u^3u_1^2-582u^2u_1^3+153uu_1^4-16u_1^5) \\
& +t_1^3(82u^6-840u^5u_1+1422u^4u_1^2-1006u^3u_1^3+349u^2u_1^4-59uu_1^5+4u_1^6) \\
& +t_1^2u(40u^6-565u^5u_1+1120u^4u_1^2-933u^3u_1^3+387u^2u_1^4-79uu_1^5+6u_1^6) \\
& +t_1u^2(8u^6-200u^5u_1+459u^4u_1^2-438u^3u_1^3+211u^2u_1^4-52uu_1^5+6u_1^6)\big)\epsilon
\end{aligned}
$$

(E.5)

$$
\begin{aligned}
\mathcal{S}({}^3P_2^{[8]}) = & \frac{256C_A^3C_FQ_c^2e^2g_s^4m_c}{3s_1^4t_1^3u_1^4}\big(2t_1^7(u^2+3uu_1-3u_1^2) \\
& +t_1^6(16u^3+33u^2u_1-65uu_1^2+24u_1^3) \\
& +t_1^5(52u^4+82u^3u_1-251u^2u_1^2+169uu_1^3-36u_1^4) \\
& +2u^4u_1(26u^4-63u^3u_1+61u^2u_1^2-30uu_1^3+6u_1^4) \\
& +t_1^4(88u^5+148u^4u_1-533u^3u_1^2+464u^2u_1^3-171uu_1^4+24u_1^5) \\
& +t_1^3(82u^6+232u^5u_1-746u^4u_1^2+698u^3u_1^3-309u^2u_1^4+65uu_1^5-6u_1^6) \\
& +t_1u^2(8u^6+184u^5u_1-449u^4u_1^2+418u^3u_1^3-203u^2u_1^4+48uu_1^5-4u_1^6) \\
& +t_1^2u(40u^6+271u^5u_1-728u^4u_1^2+675u^3u_1^3-311u^2u_1^4+65uu_1^5-4u_1^6)\big)
\end{aligned}
$$

$$
\begin{aligned}
+ \quad & \frac{-256C_A^3C_FQ_c^2e^2g_s^4m_c}{9s_1^4t_1^3u_1^4}\big(2t_1^7(7u^2+12uu_1-18u_1^2) \\
& +t_1^6(112u^3+93u^2u_1-341uu_1^2+144u_1^3) \\
& +t_1^5(364u^4+124u^3u_1-1145u^2u_1^2+889uu_1^3-216u_1^4) \\
& +2u^4u_1(134u^4-297u^3u_1+259u^2u_1^2-120uu_1^3+24u_1^4) \\
& +t_1^4(616u^5+238u^4u_1-2195u^3u_1^2+2066u^2u_1^3-849uu_1^4+144u_1^5) \\
& +t_1^3(574u^6+772u^5u_1-3122u^4u_1^2+2678u^3u_1^3-1125u^2u_1^4+275uu_1^5-36u_1^6) \\
& +t_1u^2(56u^6+952u^5u_1-2159u^4u_1^2+1678u^3u_1^3-611u^2u_1^4+84uu_1^5+2u_1^6) \\
& +t_1^2u(280u^6+1273u^5u_1-3332u^4u_1^2+2517u^3u_1^3-827u^2u_1^4+95uu_1^5+2u_1^6)\big)\epsilon.
\end{aligned}
\tag{E.6}
$$

Bibliography

[1] C. Amsler *et al.* [Particle Data Group], Phys. Lett. B **667**, 1 (2008).

[2] R. Barbieri, R. Gatto and E. Remiddi, Phys. Lett. B **61**, 465 (1976).

[3] W. E. Caswell and G. P. Lepage, Phys. Lett. B **167**, 437 (1986).

[4] G. T. Bodwin, E. Braaten and G. P. Lepage, Phys. Rev. D **51**, 1125 (1995) [Erratum-ibid. D **55**, 5853 (1997)].

[5] P. L. Cho and A. K. Leibovich, Phys. Rev. D **53**, 150 (1996); P. L. Cho and A. K. Leibovich, Phys. Rev. D **53**, 6203 (1996).

[6] M. Krämer, Prog. Part. Nucl. Phys. **47**, 141 (2001).

[7] R. Baier and R. Rückl, Phys. Lett. B **102**, 364 (1981); R. Baier and R. Rückl, Z. Phys. C **19**, 251 (1983).

[8] J. Campbell, F. Maltoni and F. Tramontano, Phys. Rev. Lett. **98**, 252002 (2007).

[9] E. L. Berger and D. L. Jones, Phys. Rev. D **23**, 1521 (1981).

[10] P. Ko, J. Lee and H. S. Song, Phys. Rev. D **54**, 4312 (1996) [Erratum-ibid. D **60**, 119902 (1999)].

[11] M. Krämer, Nucl. Phys. B **459**, 3 (1996).

[12] N. Brambilla *et al.* [Quarkonium Working Group], arXiv:hep-ph/0412158 (2005).

[13] M. Cacciari and M. Krämer, Phys. Rev. Lett. **76**, 4128 (1996).

[14] A. Petrelli, M. Cacciari, M. Greco, F. Maltoni and M. L. Mangano, Nucl. Phys. B **514**, 245 (1998).

[15] M. Klasen, B. A. Kniehl, L. N. Mihaila and M. Steinhauser, Nucl. Phys. B **713**, 487 (2005).

[16] E. J. Williams, Proc. R. Soc. London A **139**, 163 (1933); C. F. v. Weizsäcker, Z. Phys. **88**, 612 (1934).

[17] G. 't Hooft and M. J. G. Veltman, Nucl. Phys. B **44**, 189 (1972).

[18] P. Breitenlohner and D. Maison, Commun. Math. Phys. **52**, 11 (1977).

[19] J. G. Körner, G. Schuler, G. Kramer and B. Lampe, Phys. Lett. B **164**, 136 (1985).

[20] R. Cutler and D. W. Sivers, Phys. Rev. D **17**, 196 (1978).

[21] T. Hahn, Comput. Phys. Commun. **140**, 418 (2001).

[22] R. Mertig, M. Böhm and A. Denner, Comput. Phys. Commun. **64**, 345 (1991).

[23] J. A. M. Vermaseren, Report No. NIKHEF-00-032, arXiv:math-ph/0010025 (2000).

[24] G. Passarino and M. J. G. Veltman, Nucl. Phys. B **160**, 151 (1979).

[25] B. Gong and J. X. Wang, Phys. Rev. Lett. **100**, 232001 (2008).

[26] Y. J. Zhang, Y. J. Gao and K. T. Chao, Phys. Rev. Lett. **96**, 092001 (2006); Y. J. Zhang and K. T. Chao, Phys. Rev. Lett. **98**, 092003 (2007).

[27] A. Pineda and J. Soto, Phys. Rev. D **58**, 114011 (1998).

[28] A. V. Manohar, Phys. Rev. D **56**, 230 (1997).

[29] E. Braaten and Y. Q. Chen, Phys. Rev. D **55**, 2693 (1997).

[30] B. W. Harris and J. F. Owens, Phys. Rev. D **65**, 094032 (2002).

[31] S. Catani and M. H. Seymour, Nucl. Phys. B **485**, 291 (1997) [Erratum-ibid. B **510**, 503 (1998)]; S. Catani, S. Dittmaier, M. H. Seymour and Z. Trocsanyi, Nucl. Phys. B **627**, 189 (2002).

[32] G. Altarelli and G. Parisi, Nucl. Phys. B **126**, 298 (1977).

[33] E. Byckling and K. Kajantie, "Particle kinematics," Wiley London, New York, 1973.

[34] G. P. Lepage, J. Comput. Phys. **27**, 192 (1978).

[35] C. Adloff *et al.* [H1 Collaboration], Eur. Phys. J. C **25**, 25 (2002).

[36] M. Steder, presented at IWHQ07, Autumn 2007, H1prelim-07-172.

[37] J. Pumplin, D. R. Stump, J. Huston, H. L. Lai, P. M. Nadolsky and W. K. Tung, JHEP **0207**, 012 (2002).

[38] B. A. Kniehl and G. Kramer, Eur. Phys. J. C **6**, 493 (1999).

[39] F. Abe *et al.* [CDF Collaboration], Phys. Rev. Lett. **79**, 578 (1997).

[40] B. Cano-Coloma and M. A. Sanchis-Lozano, Nucl. Phys. B **508**, 753 (1997).

[41] B. A. Kniehl and C. P. Palisoc, Eur. Phys. J. C **48**, 451 (2006).

[42] D. E. Acosta *et al.* [CDF Collaboration], Phys. Rev. D **71**, 032001 (2005).

[43] F. Maltoni and T. Stelzer, JHEP **0302**, 027 (2003).

[44] P. Artoisenet, J. M. Campbell, F. Maltoni and F. Tramontano, Phys. Rev. Lett. **102**, 142001 (2009).

[45] A. Abulencia *et al.* [CDF Collaboration], Phys. Rev. Lett. **99**, 132001 (2007).

[46] A. Denner and S. Dittmaier, Nucl. Phys. B **734**, 62 (2006).

[47] K. G. Chetyrkin and F. V. Tkachov, Nucl. Phys. B **192**, 159 (1981).

[48] C. Anastasiou and A. Lazopoulos, JHEP **0407**, 046 (2004).

[49] S. Laporta, Int. J. Mod. Phys. A **15**, 5087 (2000).

[50] S. Papadopoulos, A. P. Contogouris and J. Ralston, Phys. Rev. D **25**, 2218 (1982).

[51] T. Hahn and M. Perez-Victoria, Comput. Phys. Commun. **118**, 153 (1999)

Acknowledgments

I would like to thank Prof. Kniehl for assigning this very interesting and challenging project to me and for his continuous support throughout the time. I would like to thank Prof. Bartels and Prof. Kramer for being the second referees of my dissertation and disputation. I would like to thank Vladimir Bytev, Martin Hentschinski, Mariam Khan, Luminita Mihaila, Joan Soto, Michael Steder, Vitaly Velizhanin, Jos Vermaseren and Stefan Weinzierl for useful discussions, advice and inspiration at different stages of the project. I would like to thank all members of our institute, especially Mohammad, for making my time as a Ph.D. student such a pleasent one.

Ich bedanke mich bei meinen Eltern, die mich stets vorbehaltslos und auf selbstlose Weise materiell und immateriell unterstützt haben. Ich hoffe, diese Promotion erfüllt sie mit Stolz.

และที่สำคัญขอกล่าวขอบคุณคู่ชีวิตของผม ที่อุตส่าห์มาอยู่ต่างประเทศ เพื่อที่ผมจะมีโอกาสที่จะศึกษาปริญญาเอกให้สำเร็จ ที่ให้ความรัก ความเข้าใจ และกำลังใจตลอดมา